Supporting Information

Directing group-assisted *para*-selective C–H alkynylation of unbiased arenes enabled by rhodium catalysis

Uttam Dutta,[a]# Gaurav Prakash,[a]# Kirti Devi,[a] Kongkona Borah,[a] Xinglong Zhang,*[b] Debabrata Maiti*[a]

[a] Dr. U. Dutta, G. Prakash, K. Devi, K. Borah, Prof. Dr. D. Maiti
Department of Chemistry, Indian Institute of Technology Bombay
Powai, Mumbai-400076 (India)
[b] Institute of High Performance Computing, Agency for Science, Technology and Research (A*STAR), 1 Fusionopolis Way, #16−16 Connexis, Singapore-138632
E-mail: zhang_xinglong@ihpc.a-star.edu.sg (XZ), dmaiti@iitb.ac.in (DM)
# These authors contributed equally.

List of Contents

1. General Consideration:

a. Reagents Information. Unless otherwise stated, all the reactions were carried out in screw cap reaction tubes. All the solvents were bought from Aldrich/Alfa Aesar (India)/TCI (India)/Merck in a sure-seal bottle and were used as received. Chloro(1,5-cyclooctadiene)rhodium(I) dimer, $[Rh(COD)Cl]_2$ was bought from TCI (India). Cupric chromite ($Cu_2Cr_2O_5$) was obtained from Sigma Aldrich, silver sulphate (Ag_2SO_4) was obtained from Merck. All the benzyl chlorides and bromides were bought from Aldrich/Alfa Aesar and (India)/TCI (India)/Spectrochem. For column chromatography, silica gel (100–200 mesh) from SRL Co. was used. A gradient elution using pet ether and ethyl acetate was performed based on Merck aluminium TLC sheets (silica gel 60F254).

b. Analytical information. All isolated compounds were characterized by ^1H NMR, ^{13}C NMR spectroscopy. NMR spectra were recorded either on a Bruker 500 or 400 MHz instrument. All ^1H NMR experiments are reported in units, parts per million (ppm), and were measured relative to the signals for residual chloroform (7.26 ppm) in the deuterated solvent, unless otherwise stated. All ^{13}C NMR spectra were reported in ppm relative to $CDCl_3$ (77.20 ppm), All coupling constants were reported in Hertz (Hz) and all were obtained with ^1H decoupling. High-resolution mass spectra (HRMS) were recorded on a micro-mass ESI TOF (time of flight) mass spectrometer.

2. Optimization details for rhodium-catalyzed *para*-C–H alkynylation

Yield and selectivity were determined by HPLC of crude reaction mixture using acetophenone as internal standard:

Table S1. Optimization of solvent

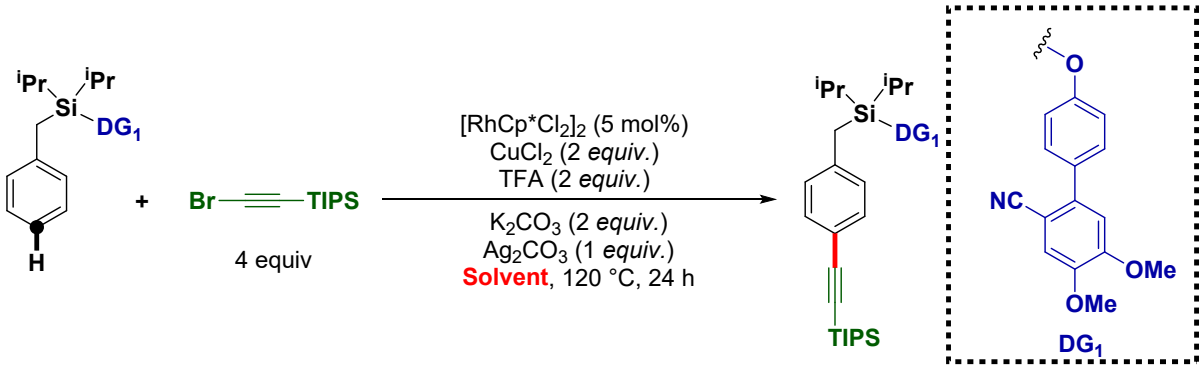

Sr. No.	Solvent	Yield (%) (*p:others*)
1	**DCE**	**20 (15:1)**
2	DCM	15 (14:1)
3	$CHCl_3$	18 (14:1)
4	CCl_4	10 (10:1)
5	HFIP	n.d.
6	TFE	trace
7	dioxane	n.d.
8	Toluene	trace
9	TFT	10 (10:1)
10	MeOH	n.d.

Table S2. Optimization of Rh–catalyst

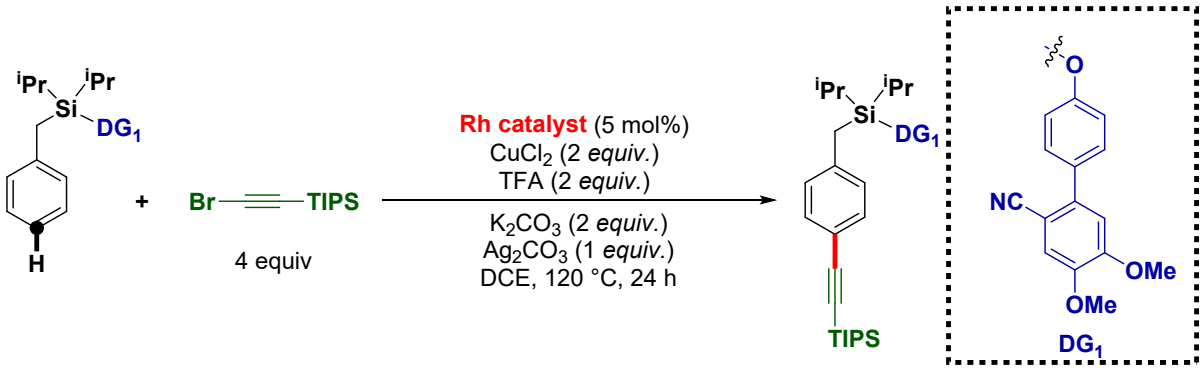

Entry	Rh-Catalyst	Yield (%) (*p:others*)
1	$[RhCp^*Cl_2]_2$	20 (15:1)
2	**$[Rh(COD)Cl]_2$**	**25 (15:1)**
3	$Rh(OAc)_2$	n.d.

4	$Rh(PPh_3)_3Cl$	n.d.
5	[Rh(COD)(*S*)-BINAP]BF_4	trace
6	Without Rh-catalyst	n.d.

Table S3. Optimization of silver salt

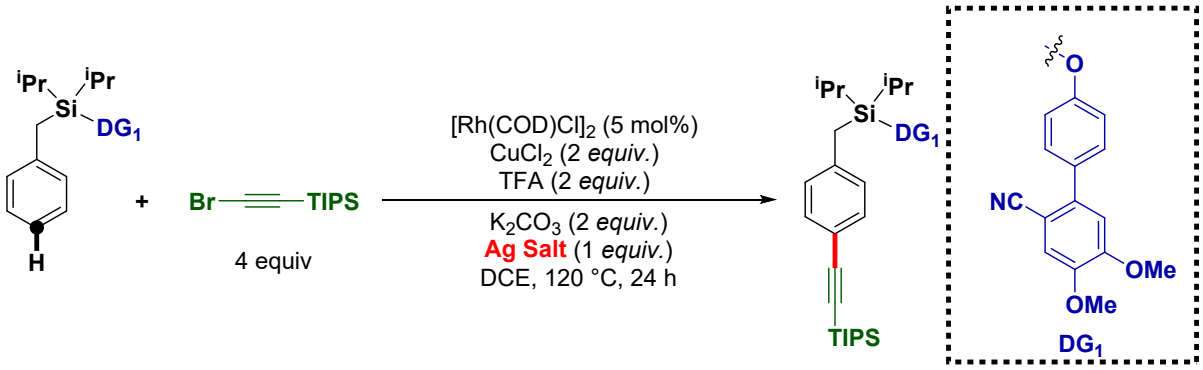

Entry	Ag-salt	Yield (%) (*p:others*)
1	No Ag-Salt	trace
2	AgOAc	15 (15:1)
3	Ag_2CO_3	25 (15:1)
4	AgTFA	trace
5	AgI	n.d.
6	**Ag_2SO_4**	**30 (15:1)**
7	Ag_2O	26 (15:1)
8	$AgSbF_6$	n.d.

Table S4. Optimization of Cu-salt

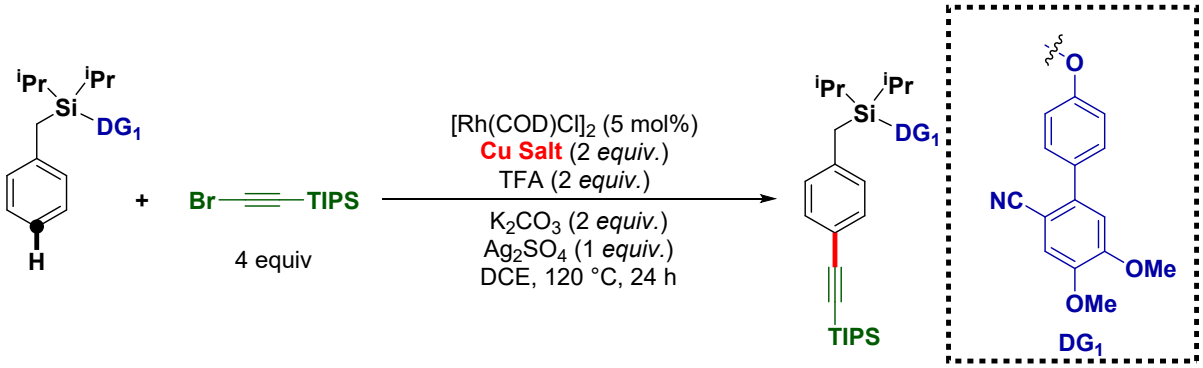

Sr. No.	Cu-salt	Yield (%) (*p:others*)
1	No Cu salt	20 (15:1)
2	$CuCl_2$	30 (15:1)
3	CuCl	25 (14:1)
4	$Cu(TFA)_2$	trace
5	$Cu(OAc)_2.H_2O$	24 (15:1)
6	Cu_2O	trace
7	$Cu(OTf)_2$	trace
8	**$Cu_2Cr_2O_5$**	**51 (15:1)**
9	CuO	45 (14:1)
10	CuF_2	26 (10:1)
11	$CuSO_4$	43 (10:1)

Table S5. Optimization of ligand

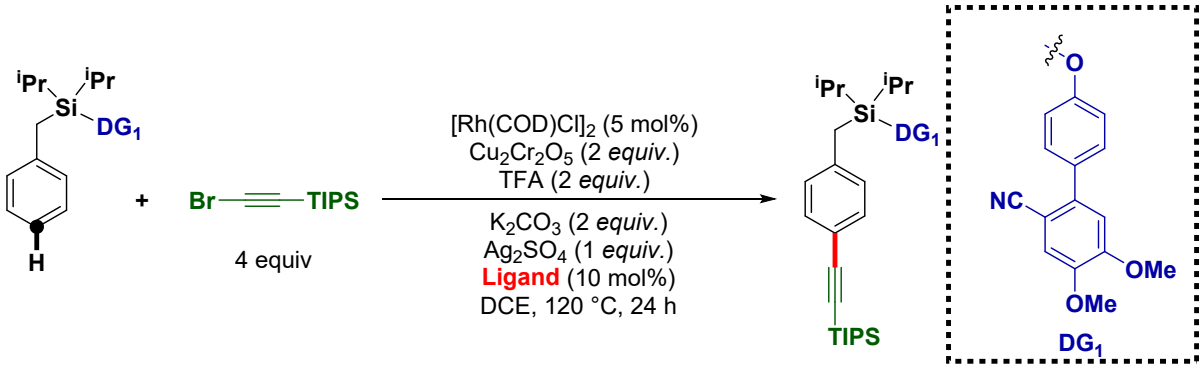

Sr. No.	Nitrogen based ligand	Yield (%) (*p:others*)
1	**No Ligand**	**51 (15:1)**
2	Pyridine	n.d.
3	DMAP	n.d.
4	Quinoline	trace
5	2,2'-Bipyridine	n.d.

Sr. No.	Phosphine Based Ligand	Yield (%) (*p:others*)
1	**No Ligand**	**51 (15:1)**
2	PPh_3	15
3	SPhos	15
4	XPhos	40
5	RuPhos	30

Table S6. Optimization of acid-additive

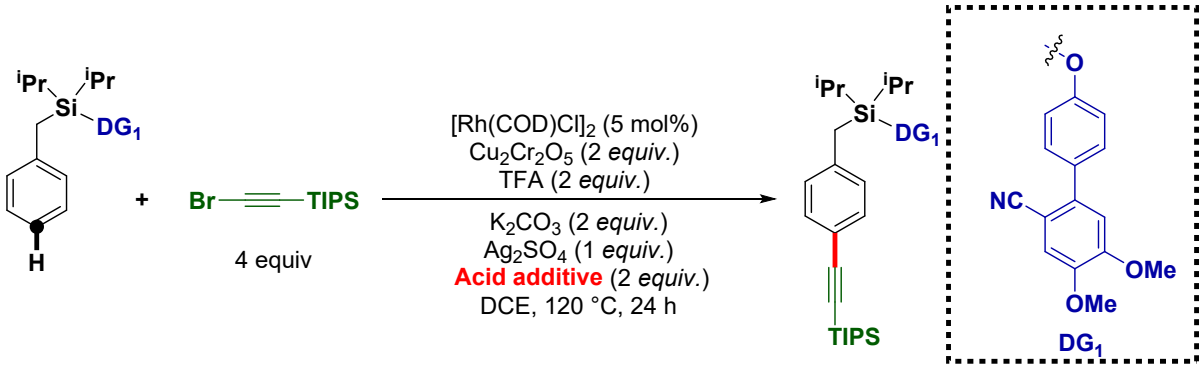

Sr. No.	Additives	Yield (%) (*p:others*)
1	No acid	trace
2	TFA	51 (15:1)
3	Acetic acid	26(10:1)
4	Pivalic acid	30 (12:1)
5	**Adamantane-1-carboxylic acid**	**62 (15:1)**
6	Formic acid	trace
7	Cyclohexyl-1-carboxylic acid	n.d.

Table S7. Optimization of base-additive

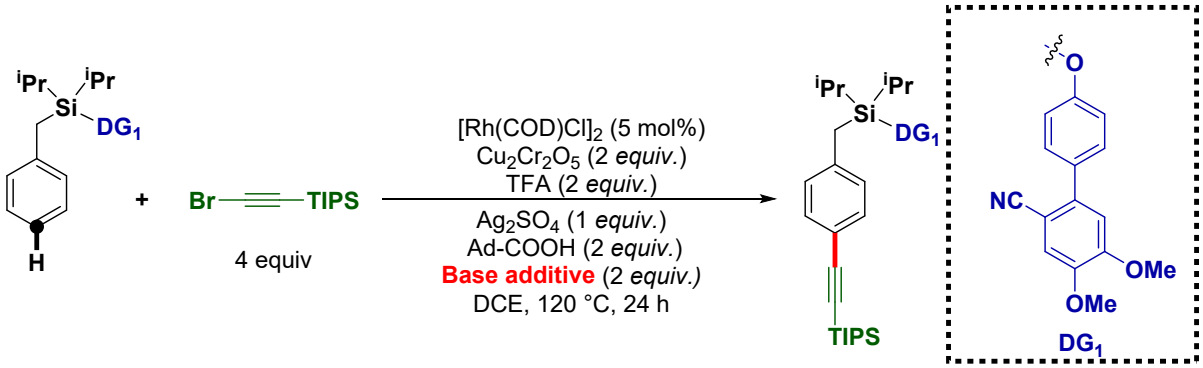

Sr. No.	Additives	Yield (%) (*p:others*)

1	No base	30 (>15:1)
2	K_2CO_3	62 (15:1)
3	$KHCO_3$	trace
4	$NaHCO_3$	50 (>15:1)
5	Li_2CO_3	trace
6	**Na_2CO_3**	**76 (>15:1)**
7	Cs_2CO_3	10 (12:1)
8	Na_3PO_4	n.d.

Table S8. Optimization of temperature

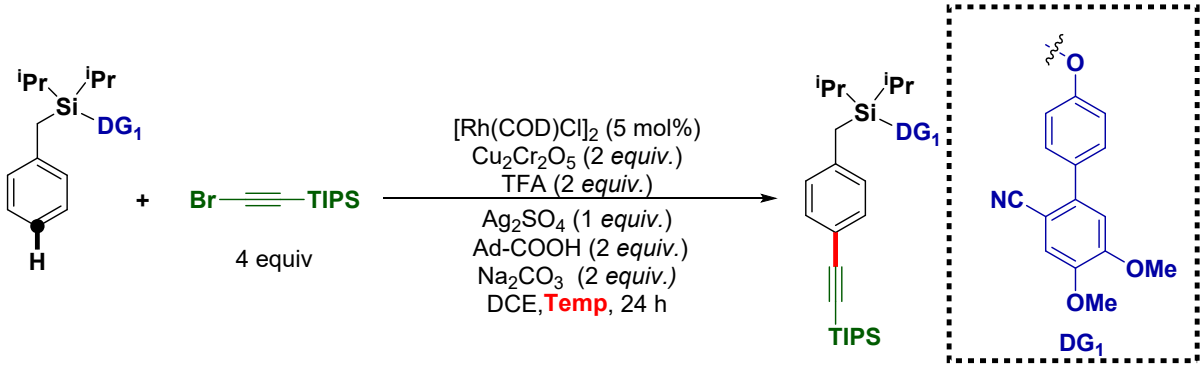

Sr. No.	Temperature (°C)	Yield (%) (*p:others*)
1	80	15 (12:1)
2	90	50 (12:1)
3	100	60 (12:1)
4	110	70 (>15:1)
5	**120**	**76 (>15:1)**
6	130	71 (>15:1)

Table S8. Optimization of alkyne amount

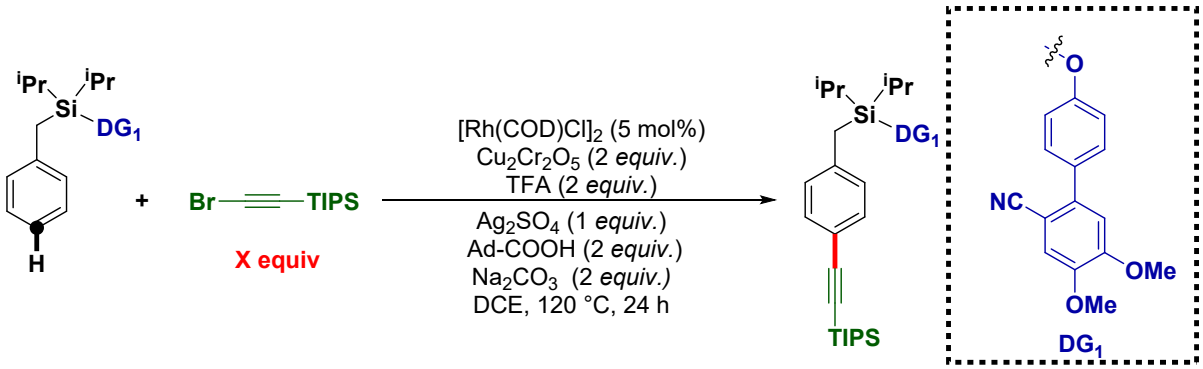

Sr. No.	Alkyne amount (*equiv.*)	Yield (%) (*p:others*)
1	1	30 (>15:1)
2	2	35 (>15:1)
3	2.5	60 (>15:1)
4	**3**	**76 (>15:1)**
5	4	76 (>15:1)
6	5	62 (>15:1)

Table S9. Trial for green oxidant oxygen gas as the co-oxidant

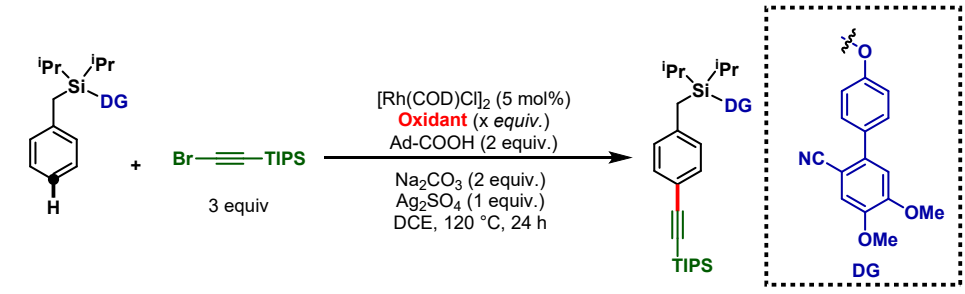

Sr. No.	Cu-salt	Yield (%) (*p:others*)
1	**$Cu_2Cr_2O_5$ (1 *equiv.*)**	**76% (>15:1)**

3	$Cu_2Cr_2O_5$ (20 mol%) + O_2	41% (>15:1)
4	$Cu_2Cr_2O_5$ (30 mol%) + O_2	52% (>15:1)

3. General procedures for the preparation of substrates and coupling partners

a. Synthesis of directing group and substrates[1]

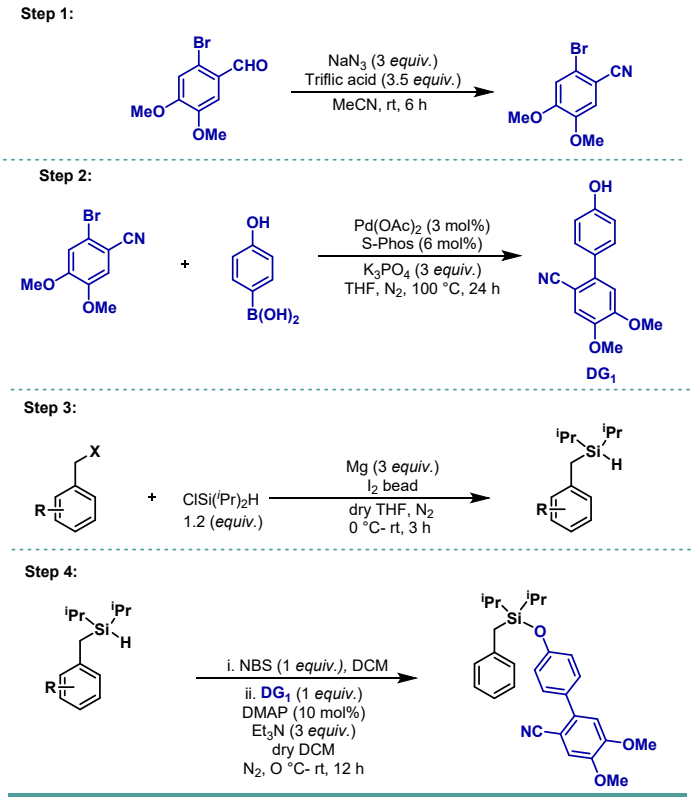

Scheme S1. Synthesis of directing group and substrates

Step-1: In an oven dried round bottom flask (250 mL), charged with stir-bar, aldehyde substrate (A) (20 mmol) and NaN_3 (3 *equiv.*) were taken. MeCN (60 mL) was added to it and stirred at room temperature for 15 mins. 3.5 equiv. of triflic acid was added to the mixture in portion with a plastic dropper. After the addition the reaction was allowed to stir at room temperature for 6 hours. Upon completion the reaction was diluted with ethyl acetate and the organic solvent was evaporated under reduced pressure. The solid residue was dissolved in ethyl acetate and washed with saturated

$NaHCO_3$ solution (3 times). The organic fraction was then dried over anhydrous Na_2SO_4 and purified through column chromatography. Quantitative conversion; white solid.

Step-2: 2 In an oven dried reaction tube, charged with stir-bar, $Pd(OAc)_2$ (3 mol%), S-phos (6 mol%), aryl bromide (3 mmol), 4-hydroxyphenyl boronic acid (3.5 mmol) and K_3PO_4 (3 *equiv.*) were added. The reaction tubes were capped with Teflon cap and purged with N_2 using schlenk line set up. THF was added to the reaction mixture (5 mL) and submerged in a preheated 100 °C oil bath and allowed for vigorous stirring for 24 hours. After 24 hours, reaction mixture was allowed to cool and diluted with EtOAc and extracted with brine solution. The organic layer was dried over Na_2SO_4 and concentrated by evaporation. Concentrated organic part was purified by column chromatography. Pale yellow crystalline compound was isolated in 75% yields using ethyl acetate and pet-ether mixture (20:80) as an eluent.

Step 3: 2 In a clean, oven-dried screw cap reaction tube, charged with magnetic stir–bar, activated magnesium turnings (15 mmol, 3 *equiv.*) and I_2 (one bead) were taken. The reaction tube was evacuated and back filled with nitrogen three times. Dry THF (15 mL) was added to it followed by di-isopropylchlorosilane (6 mmol, 1.2 *equiv.*) in drop wise fashion and stirred at room temperature for 15 mins. A solution of benzyl chloride/bromide (5 mmol) in dry THF (10 mL) was added to the solution drop wise over a period of 15 minutes under ice cold condition. The mixture was vigorously stirred for 3 hours. Upon completion, the reaction mixture was quenched and washed with brine solution (3X10 mL). Aqueous part was washed thrice with ethyl acetate (3 × 20 mL). The combined organic layer was then dried over anhydrous Na_2SO_4. The compound was purified using chromatography [silica gel (100-200 mesh size)] and petroleum-ether as the eluent. Benzyldiisopropylsilane was collected and used for next step.

Step 4: 2 To an ice cold suspension of *N*-bromosuccinimide (5.0 mmol, 1.0 *equiv.*) in 10 mL dry DCM, benzyldiisopropylsilane (5.0 mmol, 1.0 *equiv.*) was added drop wise under N_2 atmosphere. The reaction was kept on stirring for 3 hours at room temperature. In an another clean round bottomed flask, charged with magnetic stir–bar, 4'-hydroxy-4, 5-dimethoxybiphenyl-2-carbonitrile (5 mmol, 1.0 *equiv.*) and 4-dimethylaminopyridine (10 mol%) were taken. The set up was evacuated and refilled with N_2. 5 mL dry DCM was added to the mixture followed by triethylamine (15 mmol, 3.0 *equiv.*) in a drop wise fashion. The entire solution was kept for stirring at room temperature until 4'-hydroxy-4,5-dimethoxybiphenyl-2-carbonitrile gets dissolved

completely. The aforementioned solution of benzylbromodiisopropylsilane was added drop wise under the ice-cold condition. The reaction mixture was then stirred overnight at room temperature. Upon completion, the mixture was quenched with water (20 mL) and extracted with ethyl acetate thrice (3 × 30 mL). The organic layer was combined and dried over anhydrous Na_2SO_4. The final substrate was purified through column chromatography using silica gel (100-200 mesh size) and petroleum-ether/ethyl acetate (90/10, v/v) as the eluent. Isolated compound turned white solid upon drying. Yield: 73%

(b) General procedure E for synthesis of alkynyl bromide[2]

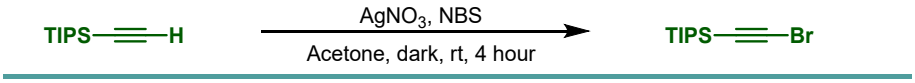

Scheme S2. Synthesis of alkynylating coupling partner (alkynyl bromide)

In a round bottom flask, wrapped with alumina foil to a solution of alkyne (5 mmol) in acetone (25 mL) *N*-bromo succinimide (5.5 mmol) and silver nitrate (0.5 mmol) were added at room temperature. The solution was stirred for 4 hours at room temperature in darkness. The reaction was quenched with cold water (5 mL) and extracted with pet ether (10 × 3). The combined organic layers were dried with Na_2SO_4 and concentrated to get desired alkynyl bromide.

(c) General procedure for rhodium-catalyzed *para*-C–H alkynylation of arenes with protected bromoacetylene

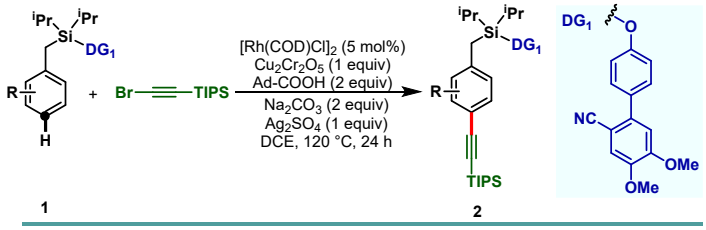

Scheme S3. General procedure for rhodium-catalyzed *para*-C–H alkynylation of arenes with protected bromoacetylene.

In an oven-dried screw cap reaction tube charged with a magnetic stir-bar silyl-ether scaffold (0.2 mmol), $[Rh(COD)Cl]_2$ (5 mol%, 0.01 mmol), $Cu_2Cr_2O_5$ (1 *equiv.*, 0.2 mmol), Ad-COOH (2 *equiv.*, 0.4 mmol), Na_2CO_3 (2 *equiv.*, 0.4 mmol), Ag_2SO_4 (1 equiv, 0.2 mmol) were taken. After that 2 mL DCE was added followed by bromo acetylene (3 *equiv.*) was added with a microlitre pipette under

aerobic condition. The tube was tightly capped and placed in a preheated oil bath at 120 ºC and the reaction mixture was stirred for 24 h. After completion of the reaction, the reaction mixture was then cooled to room temperature and filtered through a celite pad with ethyl acetate. The filtrate was washed with warm sat. $NaHCO_3$ solution and then the organic layers are collected and concentrated and the desired *para*-alkynylated compounds were purified using column chromatography using silica gel and ethyl acetate/petroleum ether as the eluent.

(d) General procedure for different post synthetic application (scheme 4)[3-12]

Procedure for directing group removal of directing group using TBAF[3]**:** In a clean, oven-dried screw cap reaction tube with previously placed magnetic stir–bar, compound 2a (0.5 mmol) was dissolved in 10 mL of THF, a solution of 1M TBAF (1.0 mL, 2.0 *equiv.*,) in THF was added drop wise at RT. The solution was stirred for 3 hours at room temperature. After completion of reaction, solvent was evaporated to dryness, and the residue was purified by using column chromatography using silica gel and petroleum ether as the eluent.

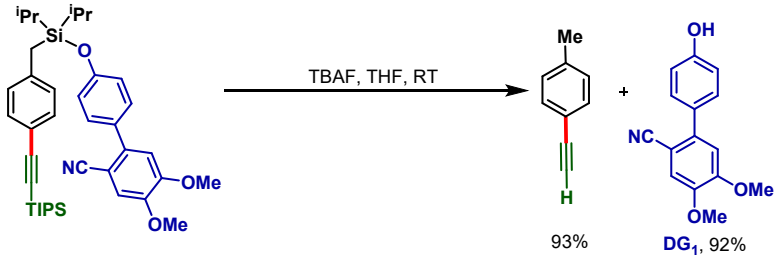

Scheme S4. Removal of directing group using TBAF.

Procedure for directing group removal of directing group using PTSA[3]
In a clean, oven-dried screw cap reaction tube with previously placed magnetic stir–bar, compound 2a (0.2 mmol) and *p*-toluenesulfonic acid (10 mol%) were dissolved in 3 mL of EtOH and 1 mL H_2O (EtOH/H_2O: 3/1). The solution was stirred at 110 °C for 16 hours. After being stirred, reaction mixture was removed from oil-bath and kept at room temperature. Ethanol was removed under reduced pressure and aqueous part was extracted by EtOAc. Organic part was evaporated to dryness and the residue was purified by column chromatography silica gel.

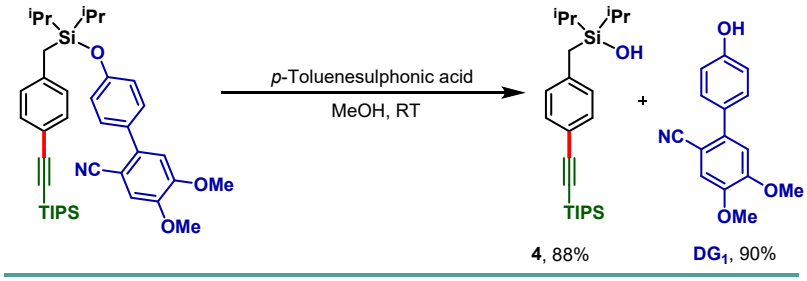

Scheme S5. Removal of directing group using PTSA.

Silanol directed *ortho*-C–H olefination of *para*-alkynylated product[4]

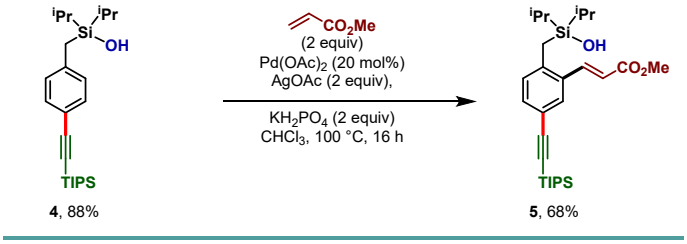

Scheme S6. Silanol directed *ortho*-C–H olefination of *para*-alkynylated product.

Procedure: A 20 mL oven-dried pressure tube was charged with benzyldiisopropylsilanol 2 (0.3 mmol), olefin (0.6 mmol), KH_2PO_4 (0.6 mmol), $Pd(OAc)_2$ (0.06 mmol), AgOAc (0.6 mmol) and $CHCl_3$ (3 mL). The reaction tube was then sealed, heated to 100 °C, and stirred for 16 hours. The reaction mixture was cooled to room temperature, diluted with ethyl acetate (5 mL), filtered through a pad of celite, and the filterate was then concentrated under vacuum. The crude product was purified by flash chromatography on silica gel (gradient eluent of EtOAc in Hexanes) to yield the product.

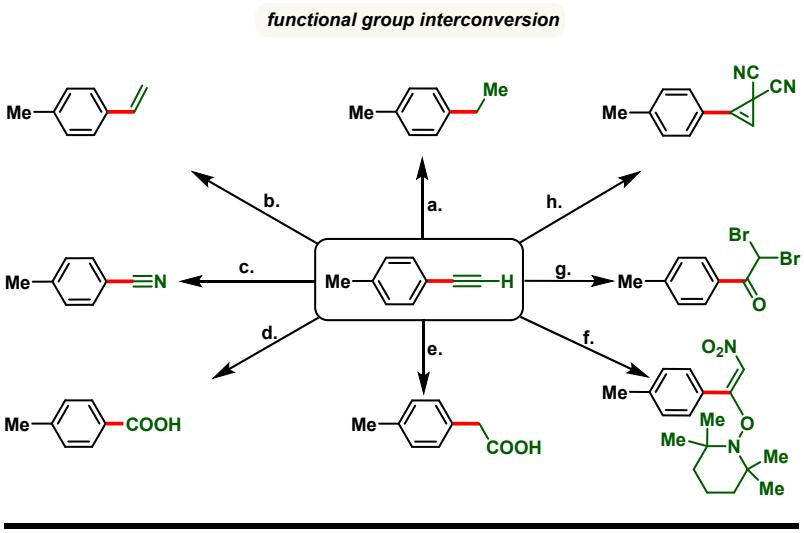

Scheme S7. post-synthetic modification of *para*-alkynylated arenes.

a. Reduction of alkyne to alkane Procedure: To a mixture of alkyne in methanol, 5 mol% Pd on charcoal was added and H_2 gas was pumped into the reaction mixture at 1 atm pressure. Further, after completion of reaction, reaction mixture was filtered and washed with methanol and purified on silica using column chromatography using silica gel (100–200 mesh) and petroleum ether as eluent.

b. Reduction of alkyne to alkene[5]: Reaction tube was charged with a magnetic bead and desired alkyne (0.2 mmol), Zinc (1.0 mmol), $NiBr_2$ (10 mol%), THF (0.5 mL), and HCO_2H (1.0 mmol). The reaction was then sealed and transferred to a preheated oil bath at 80 ^oC, and its contents were stirred rapidly for 16 h. After that it was allowed to cool, the crude reaction mixture was filtered through a celite plug and worked up using DCM and water. The reaction mixture was purified through column chromatography chromatography using silica gel (100–200 mesh) and petroleum ether as eluent.

c. Conversion of Ethynyl toluene to *para* tolunitrile Procedure[6]: Reaction tube was charged with magnetic bar and ethynyl toluene (0.5 mmol), ^{t}BuONO (1.0 mmol) and 2-picoline-*N*-oxide (1.0 mmol) under N_2 atmosphere. Then, THF was added (2 ml) to the reaction mixture. The reaction tube was placed in preheated oil bath at 70 ^oC and allowed to stir for 12 h. After completion of the reaction, it was allowed to cool and solvent was evaporated under reduced pressure and crude reaction mixture was purified using column chromatography using silica gel (100–200 mesh) and petroleum ether as eluent.

d. Conversion of Ethynyl toluene to 4-methyl benzoic acid Procedure[7]: To a mixture of Ethynyl toluene (0.5 mmol) in dioxane (5 mL), Oxone (2 *equiv.*) and TFA (2 *equiv.*) were added. The mixture was then heated to reflux for 10 h and then cooled to r.t. H_2O (10 mL) was added and the mixture was extracted with EtOAc (2 × 20 mL). The combined organic layers were treated with sat. $NaHCO_3$ solution and the aqueous layer was poured onto crushed ice and treated with 2 M HCl; a colorless solid precipitated out. The precipitate was filtered off and dried in vacuo to give 4-methyl benzoic acid. It was purified using column chromatography through silica gel(100-200mesh) and EtOAc–Petroleum ether as eluent (02:98).

e. Conversion of Ethynyl toluene to 4-methyl phenyl acetic acid Procedure[8]: In an oven dried reaction tube alkyne (0.5 mmol) and dry THF were added followed by drop wise addition of nBuLi (2.5 M in hexane, 1.2 *equiv.*) at −78 °C under nitrogen. It was stirred at same temperature for 1 h. Then, 4,4,5,5-tetramethyl-2-(1-methylethoxy)-1,3,2-dioxaborolane (^{i}PrOBpin, 2 *equiv.*) was added and allowed to stir at the same temperature for another 2 h. Then the reaction mixture was quenched with 4.0 M HCl in dioxane (1.5 *equiv.*) and allowed to warm at room temperature for additional 1 h with stirring. The solvent was evaporated under reduced pressure. It was filtered and washed with diethyl ether and used for next step without purification. Then in the solution of alkynyl boronate in acetone (5 ml) was added oxone (1.5 *equiv.*) in H_2O (5 ml). The reaction mixture was kept for stirring at 50 ^oC for 6 h. After that it was extracted with EtOAc (10 ml × 3). The organic layers were dried over Na_2SO_4 and concentrated under reduced pressure. The resulting crude compound was purified by silica gel column chromatography to provide 4-methyl phenyl acetic acid.

f. Conversion of Ethynyl toluene to (E)-2,2,6,6-tetramethyl-1-((2-nitro-1-(p-tolyl)vinyl)oxy)piperidine[9]: An oven-dried screw cap reaction tube was charged with a magnetic stir-bar, TEMPO (0.375 mmol) and corresponding alkyne (0.25 mmol). Solid reagents were weighed first followed by liquid reagents. Addition of 1.5 mL of THF was followed by the addition requisite amount of *tert*-butyl nitrite (0.5 mmol). The reaction mixture was stirred vigorously on a preheated oil bath at 70 °C for 12-24 h depending on the substrate. After completion of the reaction the mixture was diluted with EtOAc (2 mL) and evaporated under vacuum. The crude mixture was purified by column chromatography using silica gel (100-200 mesh size) and petroleum ether/ethyl acetate as the eluent.

g. Conversion of Ethynyl toluene to 2,2-dibromo-1-(*p*-tolyl)ethan-1-one 4 Procedure[10]: 4-ethynyl toluene (0.5 mmol), KBr (2 *equiv.*), oxone (2 *equiv.*) and acetonitrile 2 ml were added in a clean oven dried reaction tube and stirred at room temperature. Then water 1 ml was added dropwise, Then, reaction tube was heated at 50 °C for 1 h. Reaction was allowed to cool and extracted with EtOAc. The combined organic layers were washed with brine and dried over Na_2SO_4 and concentrated under reduced pressure. The crude reaction mixture was purified by column chromatography (silica gel 100–200 mesh, petroleum-ether) to get the final product.

h. Conversion of Ethynyl toluene to 1-isocyano-2-(*p*-tolyl)cycloprop-2-ene-1-carbonitrile[11]: $PhI(OAc)_2$ (1.1 mmol), K_2CO_3 (1.1 mmol), malononitrile (0.6 mmol) and ethynyl toluene (0.5 mmol) were dissolved in DCE (2.0 mL) in a 25 mL flask. The mixture was stirred at 80 °C for 1 h (monitored by TLC). Then the reaction mixture was cooled to room temperature, poured into water and extracted with DCM (3 × 10 mL). The combined organic phase was washed with water (3 × 10 mL). Reaction mixture was concentrated under reduced pressure, and the residue was purified by flash silica gel column chromatography (EtOAc–petroleum ether = 5:95).

Failed alkyne coupling partners:

Substrate with different selectivity:

Relatively bulky *meta*-substituents such *meta*-Me, *meta*-Cl and *meta*-CF_3 scaffolds delivered majorly the *meta*-alkynylated compounds. We reasoned that the bulkiness of these substituents prevents the accessibility of the *para*-C–H bond and therefore the sterically less hindered *meta*-C–H bond was activated.

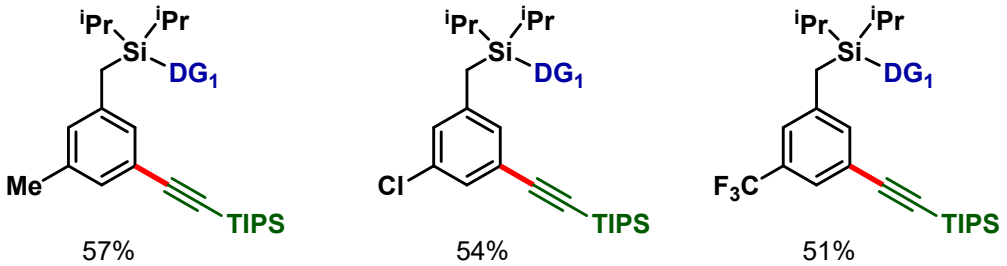

4. Characterization data

1. 4'-((diisopropyl(4-((triisopropylsilyl)ethynyl)benzyl)silyl)oxy)-4,5-dimethoxy-[1,1'-biphenyl]-2-carbonitrile (2a)

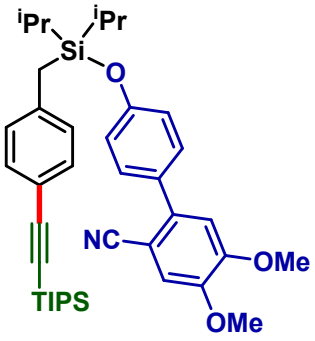

Column material: 100-200 mesh silica

Eluent: pet ether: ethyl acetate (96:04)

Yield: 76 %

Physical appearance: Dark yellow liquid

^{1}H NMR (500 MHz, $CDCl_3$) δ 7.40 (dd, *J* = 8.5, 4.3 Hz, 2H), 7.36 – 7.31 (m, 2H), 7.13 (s, 1H), 7.07 (d, *J* = 8.1 Hz, 2H), 6.94 – 6.82 (m, 3H), 3.96 (s, 3H), 3.93 (s, 3H), 2.40 (s, 1H), 1.27 – 1.17 (m, 2H), 1.12 (s, 21H), 1.07 – 1.03 (m, 12H).

^{13}CNMR (126 MHz, $CDCl_3$) δ 156.08, 152.69, 148.15, 140.16, 139.53, 132.20, 130.07, 130.03, 128.83, 120.15, 119.71, 119.46, 115.18, 112.50, 107.63, 102.32, 89.54, 56.43, 56.31, 18.85, 18.45, 17.61, 17.58, 13.10, 11.52, 11.40.

IR (thin film, cm^{-1}): 760, 841, 878, 923, 997, 1031, 1078, 1137, 1174, 1214, 1244, 1274, 1353, 1388, 1463, 1519, 1613, 1685, 2150, 2220, 2865, 2944, 3028

HR-MS (ESI-QTOF): $[M+Na]^+$ calculated for $C_{39}H_{53}NNaO_3Si_2$ m/z 662.3456 and found m/z 662.3454

2. 4'-((diisopropyl(2-methyl-4-((triisopropylsilyl)ethynyl)benzyl)silyl)oxy)-4,5-dimethoxy-[1,1'-biphenyl]-2-carbonitrile (2b)

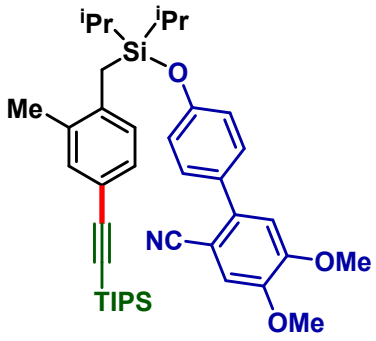

Column material: 100-200 mesh silica

Eluent: pet ether: ethyl acetate (96:04)

Yield: 79%

Physical appearance: Dark yellow liquid

^{1}H NMR (500 MHz, $CDCl_3$) δ 7.35 (d, *J* = 8.6 Hz, 2H), 7.23 (s, 1H), 7.21 (d, *J* = 7.9 Hz, 1H), 7.13 (s, 1H), 7.08 (d, 1H), 6.88 (s, 1H), 6.75 (d, *J* = 8.6 Hz, 2H), 3.95 (s, 3H), 3.92 (s, 3H), 2.36 (s, 2H), 2.27 (s, 3H), 1.30 – 1.23 (m, *J* = 14.7, 7.5 Hz, 2H), 1.11 (s, 21H), 1.07 (d, *J* = 7.4 Hz, 6H), 1.03 (d, *J* = 7.4 Hz, 6H).

^{13}C NMR (126 MHz, $CDCl_3$): δ 155.92, 152.67, 148.13, 140.22, 138.53, 135.68, 133.97, 131.37, 130.00, 129.70, 129.27, 119.97, 119.77, 119.48, 115.16, 112.49, 107.87, 102.30, 89.11, 56.45, 56.32, 20.44, 18.88, 18.49, 17.74, 17.56, 13.48, 11.55.

IR (thin film, cm^{-1}): 754, 839, 882, 917, 997, 1029, 1072, 1137, 1174, 1214, 1241, 1264, 1353, 1388, 1463, 1502, 1603, 1685, 2148, 2220, 2866, 2943, 3018

HR-MS (ESI-QTOF): $[M+Na]^+$ calculated for $C_{40}H_{55}NNaO_3Si_2$ m/z 676.3613 and found m/z 676.3606

3. 4'-(((2-chloro-4-((triisopropylsilyl)ethynyl)benzyl)diisopropylsilyl)oxy)-4,5-dimethoxy-[1,1'-biphenyl]-2-carbonitrile (2c)

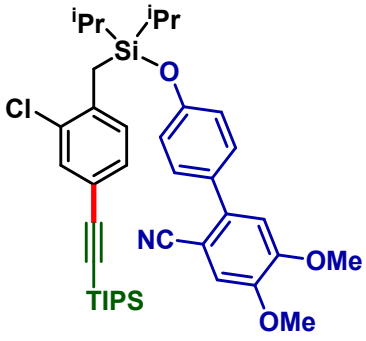

Column material: 100-200 mesh silica

Eluent: pet ether: ethyl acetate (96:04)

Yield: 70%

Physical appearance: Dark yellow liquid

^{1}H NMR (500 MHz, $CDCl_3$) δ 7.43 (d, J = 1.6 Hz, 1H), 7.40 (d, J = 8.7 Hz, 3H), 7.23 (dd, J = 8.0, 1.7 Hz, 1H), 7.15 (s, 1H), 7.13 – 7.12 (m, 1H), 6.90 (s, 1H), 6.88 (d, 2H), 3.96 (s, 3H), 3.93 (s, 3H), 2.55 (s, 2H), 1.33 – 1.23 (m, 2H), 1.11 (d, J = 1.6 Hz, 21H), 1.06 (d, J = 4.3 Hz, 6H), 1.05 (d, J = 4.3 Hz, 6H).

^{13}C NMR (126 MHz, $CDCl_3$) δ 155.92, 152.67, 148.13, 140.22, 138.53, 135.68, 133.97, 131.37, 130.00, 129.70, 129.27, 119.97, 119.77, 119.48, 115.16, 112.49, 107.87, 102.30, 89.11, 56.45, 56.32, 20.44, 18.88, 18.49, 17.74, 17.56, 13.48, 11.55.

IR (thin film, cm^{-1}): 679, 760, 797, 839, 882, 917, 996, 1031, 1070, 1138, 1173, 1217, 1242, 1265, 1353, 1387, 1463, 1502, 1603, 1746, 2157, 2220, 2866, 2943

HR-MS (ESI-QTOF): $[M+Na]^+$ calculated for $C_{39}H_{52}ClNNaO_3Si_2$ m/z 696.3066 and found m/z 696.3063

4. 4'-(((2-fluoro-4-((triisopropylsilyl)ethynyl)benzyl)diisopropylsilyl)oxy)-4,5-dimethoxy-[1,1'-biphenyl]-2-carbonitrile (2d)

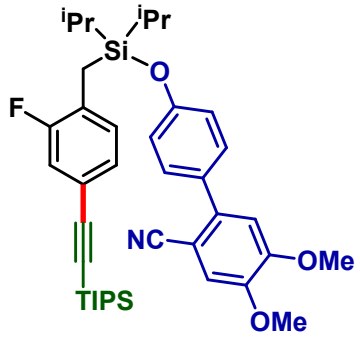

Column material: 100-200 mesh silica

Eluent: pet ether: ethyl acetate (96:04)

Yield: 68%

Physical appearance: Dark yellow liquid

^{1}H NMR (400 MHz, $CDCl_3$) δ 7.40 (d, *J* = 8.7 Hz, 2H), 7.16 – 7.06 (m, *J* = 8.2 Hz, 4H), 6.88 – 6.85 (m, 3H), 3.96 (s, 3H), 3.93 (s, 3H), 2.37 (d, *J* = 1.3 Hz, 2H), 1.29 – 1.19 (m, *J* = 19.6, 7.5 Hz, 2H), 1.11 (s, 21H), 1.06 (d, *J* = 1.3 Hz, 6H), 1.04 (d, *J* = 1.3 Hz, 6H).

^{13}C NMR (400 MHz, $CDCL_3$) δ 155.98, 152.68, 148.15, 140.18, 133.07, 131.49, 130.95,

130.90, 127.98, 127.95, 127.27, 127.10, 121.34, 120.10, 120.01, 119.49, 118.86, 118.62, 115.16, 112.49, 106.25, 102.31, 90.73, 56.46, 56.33, 18.84, 17.49, 17.44, 13.35, 11.48.

IR (thin film, cm^{-1}): 675, 765, 798, 839, 882, 918, 957, 997, 1030, 1078, 1138, 1174, 1217, 1266, 1353, 1388, 1463, 1503, 1560, 1603, 2153, 2220, 2867, 2944

HR-MS (ESI-QTOF): $[M+Na]^+$ calculated for $C_{39}H_{52}FNNaO_3Si_2$ m/z 680.3362 and found m/z 680.3359

5. 4'-(((3-fluoro-4-((triisopropylsilyl)ethynyl)benzyl)diisopropylsilyl)oxy)-4,5-dimethoxy-[1,1'-biphenyl]-2-carbonitrile (2e)

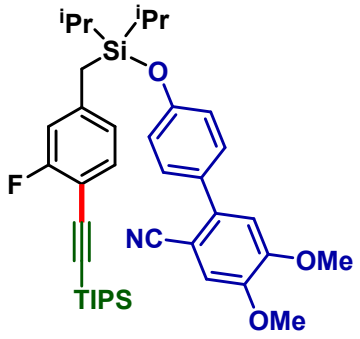

Column material: 100-200 mesh silica

Eluent: pet ether: ethyl acetate (96:04)

Yield: 65%

Physical appearance: Yellow liquid

^{1}H NMR (400 MHz, $CDCl_3$) δ 7.41 (d, *J* = 8.6 Hz, 2H), 7.29 (t, *J* = 7.8 Hz, 1H), 7.13 (s, 1H), 6.90 (d, *J* = 5.1 Hz, 2H), 6.88 (s, 1H), 6.84 (dd, *J* = 7.9, 1.6 Hz, 1H), 6.78 (d, *J* = 10.5 Hz, 1H), 3.96 (s, 3H), 3.93 (s, 3H), 2.38 (s, 2H), 1.28 – 1.19 (m, 2H), 1.12 (s, 21H), 1.05 (dd, *J* = 7.4, 1.7 Hz, 12H).

^{13}C NMR (101 MHz, $CDCl_3$) δ 155.91, 152.70, 148.17, 142.36, 142.28, 140.13, 133.65, 131.67, 130.14, 129.97, 124.56, 120.12, 119.47, 115.93, 115.72, 115.15, 112.53, 102.31, 100.35, 56.45, 56.32, 18.81, 17.61, 17.56, 13.14, 11.46.

IR (thin film, cm^{-1}): 669, 736, 814, 840, 884, 917, 997, 1268, 1352, 1463, 1503,1604, 1695, 2160, 220, 2327, 2866, 2935,

HR-MS (ESI-QTOF): $[M+H]^+$ calculated for $C_{39}H_{53}FNO_3Si_2$ m/z 658.3543 and found m/z 658.3467.

6. 4'-((diisopropyl(2-(trifluoromethyl)-4-((triisopropylsilyl)ethynyl)benzyl)silyl)oxy)-4,5-dimethoxy-[1,1'-biphenyl]-2-carbonitrile (2f)

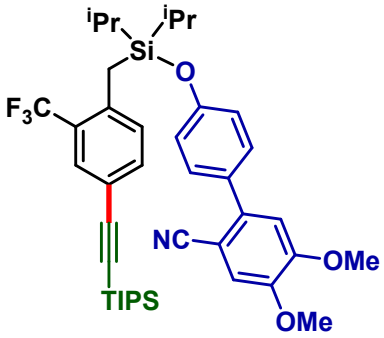

Column material: 100-200 mesh silica

Eluent: pet ether: ethyl acetate (96:04)

Yield: 69%

Physical appearance: Dark yellow liquid

^{1}H NMR (500 MHz, $CDCl_3$) δ 7.68 (d, J = 1.1 Hz, 1H), 7.48 (d, J = 8.0 Hz, 1H), 7.41 (d, J = 8.5 Hz, 2H), 7.33 (d, J = 8.0 Hz, 1H), 7.13 (s, 1H), 6.93 – 6.86 (m, J = 8.4 Hz, 3H), 3.96 (s, 3H), 3.93 (s, 3H), 2.57 (s, 2H), 1.31 – 1.25 (m, J = 13.6, 6.1 Hz, 2H), 1.12 (s, 21H), 1.04 (d, J = 7.5 Hz, 6H), 0.98 (d, J = 7.5 Hz, 6H).

^{13}C NMR (126 MHz, $CDCl_3$) δ 155.91, 152.73, 148.22, 140.12, 138.91, 134.84, 131.63, 130.17, 130.00, 129.96, 120.29, 120.06, 119.47, 115.21, 112.52, 105.91, 102.37, 91.58, 56.48, 56.35, 38.81, 36.50 18.96, 18.86, 18.68, 17.61, 17.39, 13.48, 11.61, 11.49.

IR (thin film, cm^{-1}): 672, 753, 802, 840, 882, 904, 997, 1031, 1052, 1121, 1139, 1173, 1216, 1242, 1266, 1320, 1353, 1388, 1412, 1463, 1503, 1603, 1747, 2159, 2220, 2867, 2944

HR-MS (ESI-QTOF): $[M+Na]^+$ calculated for $C_{40}H_{52}F_3NNaO_3Si_2$ m/z 730.3330 and found m/z 730.3328

7. 4'-((diisopropyl(2-methoxy-4-((triisopropylsilyl)ethynyl)benzyl)silyl)oxy)-4,5-dimethoxy-[1,1'-biphenyl]-2-carbonitrile (2g)

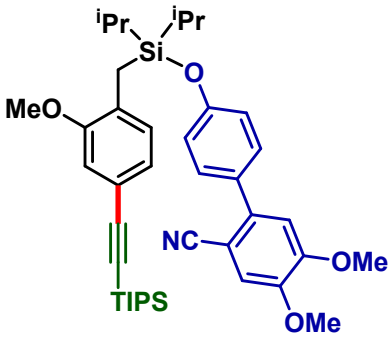

Column material: 100-200 mesh silica

Eluent: pet ether: ethyl acetate (96:04)

Yield: 74%

Physical appearance: Dark yellow liquid

^{1}H NMR (500 MHz, $CDCl_3$): δ 7.38 (d, *J* = 8.7 Hz, 2H), 7.13 (s, 1H), 7.01 (d, *J* = 7.7 Hz, 1H), 6.97 (d, *J* = 7.7, 1H), 6.90 (s, 1H), 6.86 (d, *J* = 8.7 Hz, 2H), 6.84 (s, 1H), 3.95 (s, 3H), 3.93 (s, 3H), 3.75 (s, 3H), 2.39 (s, 2H), 1.23 – 1.17 (m, 4H), 1.11 (s, 21H), 1.05 (d, *J* = 1.8 Hz, 6H), 1.03 (d, *J* = 1.8 Hz, 6H).

^{13}C NMR (126 MHz, $CDCl_3$) δ 156.32, 156.27, 152.67, 148.10, 140.32, 131.13, 130.01, 129.92, 128.90, 124.79, 120.64, 120.15, 119.54, 115.17, 113.27, 112.50, 107.84, 102.30, 89.16, 56.45, 56.32, 55.12, 18.88, 17.54, 17.51, 15.23, 13.52, 11.55.

IR (thin film, cm^{-1}): 667, 754, 806, 839, 883, 918, 945, 996, 1039, 1087, 1138, 1173, 1215, 1242, 1265, 1353, 1388, 1464, 1502, 1561, 1604, 2152, 2220, 2866, 2942

HR-MS (ESI-QTOF): $[M+Na]^+$ calculated for $C_{40}H_{55}NNaO_4Si_2$ m/z 692.3562 and found m/z 692.3561

8. 4'-(((2-isopropoxy-4-((triisopropylsilyl)ethynyl)benzyl)diisopropylsilyl)oxy)-4,5-dimethoxy-[1,1'-biphenyl]-2-carbonitrile (2h)

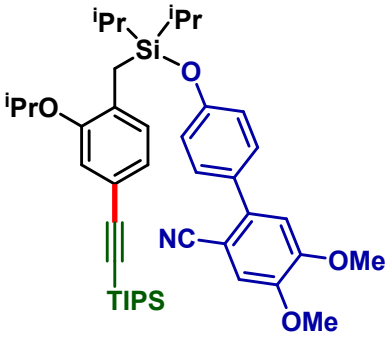

Column material: 100-200 mesh silica

Eluent: pet ether: ethyl acetate (96:04)

Yield: 70%

Physical appearance: Dark yellow liquid

^{1}H NMR (500 MHz, $CDCl_3$): δ 7.38 (d, *J* = 8.6 Hz, 2H), 7.13 (s, 1H), 7.02 (d, *J* = 7.7 Hz, 1H), 6.94 (d, *J* = 7.7, 1H), 6.90 (s, 1H), 6.88 – 6.85 (m, 3H), 4.59 – 4.52 (m, 1H), 3.95 (s, 3H), 3.93 (s, 3H), 2.39 (s, 2H), 1.33 (d, *J* = 6.0 Hz, 6H), 1.28 – 1.20 (m, 6H), 1.11 (s, 21H), 1.05 (d, *J* = 1.4 Hz, 6H), 1.03 (d, *J* = 1.4 Hz, 6H).

^{13}C NMR (126 MHz, $CDCl_3$): δ 156.34, 154.58, 152.68, 148.11, 140.33, 131.16, 130.31, 129.95, 129.68, 124.41, 120.44, 120.19, 119.54, 115.52, 115.19, 112.53, 108.05, 102.31, 88.94, 69.99, 56.47, 56.34, 22.32, 18.90, 17.65, 17.61, 14.90, 13.46, 11.58.

IR (thin film, cm^{-1}): 676, 758, 807, 840, 882, 918, 996, 1030, 1115, 1137, 1174, 1216, 1264, 1353, 1387, 1410,1463, 1502, 1560, 1603, 2148, 2220, 2866, 2942

HR-MS (ESI-QTOF): $[M+Na]^+$ calculated for $C_{42}H_{59}NNaO_4Si_2$ m/z 720.3875 and found m/z 720.3876

9. 4'-(((2-(fluoromethoxy)-4-((triisopropylsilyl)ethynyl)benzyl)diisopropylsilyl)oxy)-4,5-dimethoxy-[1,1'-biphenyl]-2-carbonitrile (2i)

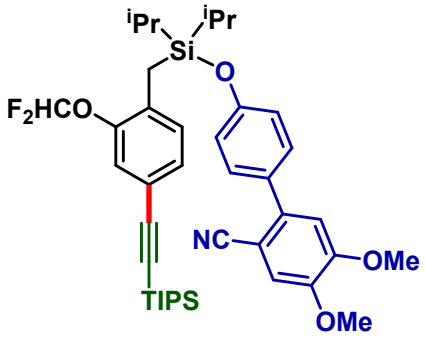

Column material: 100-200 mesh silica

Eluent: pet ether: ethyl acetate (96:04)

Yield: 75%

Physical appearance: Dark yellow liquid

^{1}H NMR (500 MHz, $CDCl_3$) δ 7.38 (d, *J* = 8.5 Hz, 2H), 7.19 (dd, *J* = 7.9, 1.3 Hz, 1H), 7.14 (d, *J* = 8.0 Hz, 2H), 7.09 (s, 1H), 6.89 (s, 1H), 6.83 (d, *J* = 8.5 Hz, 2H), 6.46 (t, *J* = 74.0 Hz, 1H), 3.95 (s, 3H), 3.93 (s, 3H), 2.42 (s, 2H), 1.28 – 1.22 (m, 2H), 1.11 (s, 21H), 1.07 (d, 6H), 1.05 (d, 6H).

^{13}C NMR (126 MHz, $CDCl_3$) δ 155.96, 152.71, 148.82, 148.18, 140.20, 131.68, 131.49, 131.01, 130.07, 130.03, 129.16, 121.27, 120.04, 119.95, 119.51, 116.53, 115.17, 112.51, 106.25, 102.35, 90.93, 56.47, 56.34, 18.86, 18.49, 17.55, 17.45, 15.06, 13.43, 11.50, 11.44.

IR (thin film, cm^{-1}): 677, 762, 792, 839, 882, 918, 997, 1041, 1124, 1173, 1216, 1264, 1353, 1387, 1463, 1503, 1560, 1604, 1685, 2153, 2220, 2867, 2944

HR-MS (ESI-QTOF): $[M+Na]^+$ calculated for $C_{40}H_{53}F_2NNaO_4Si_2$ m/z 728.3373 and found m/z 728.3373

10. 4'-((diisopropyl(2-(trifluoromethoxy)-4-((triisopropylsilyl)ethynyl)benzyl)silyl)oxy)-4,5-dimethoxy-[1,1'-biphenyl]-2-carbonitrile (2j)

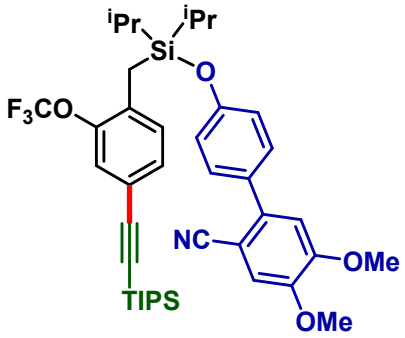

Column material: 100-200 mesh silica

Eluent: pet ether: ethyl acetate (96:04)

Yield: 73%

Physical appearance: Dark yellow liquid

^{1}H NMR (400 MHz, $CDCl_3$) δ 7.39 (d, 2H), 7.28 – 7.27 (m, 1H), 7.24 (d, *J* = 1.6 Hz, 1H), 7.17 (d, *J* = 7.9 Hz, 1H), 7.13 (s, 1H), 6.90 (s, 1H), 6.86 (d, 2H), 3.96 (s, 3H), 3.93 (s, 3H), 2.42 (s, 2H), 1.27 – 1.24 (m, 2H), 1.10 (s, 21H), 1.04 (d, *J* = 7.3 Hz, 12H).

^{13}C NMR (126 MHz, $CDCl_3$) δ 155.90, 152.68, 148.15, 140.14, 132.78, 131.52, 131.17, 130.44, 130.08, 123.71, 121.35, 119.99, 115.15, 112.47, 102.31, 91.27, 56.44, 56.31, 18.82, 18.47, 17.45, 17.37, 15.11, 13.39, 11.46, 11.41.

^{13}C NMR (126 MHz, $CDCl_3$) δ 155.90, 152.68, 149.91, 148.15, 146.58, 140.14, 132.78, 131.52, 131.17, 130.44, 130.08, 123.70, 121.35, 119.99, 115.15, 112.47, 105.88, 102.31, 91.27, 56.44, 56.31, 18.82, 18.47, 17.45, 17.37, 15.11, 13.39, 11.46, 11.41.

IR (thin film, cm^{-1}): 680, 760, 795, 849, 883, 925, 993, 1114, 1157, 1217, 1242, 1266, 1353, 1388, 1463, 1503, 1687, 2160, 2220, 2877, 2945

HR-MS (ESI-QTOF): $[M+Na]^+$ calculated for $C_{40}H_{52}F_3NNaO_4Si_2$ m/z 746.3279 and found 746.3282.

11. 4'-((diisopropyl(2-((trifluoromethyl)thio)-4-((triisopropylsilyl)ethynyl)benzyl)silyl)oxy)-4,5-dimethoxy-[1,1'-biphenyl]-2-carbonitrile (2k)

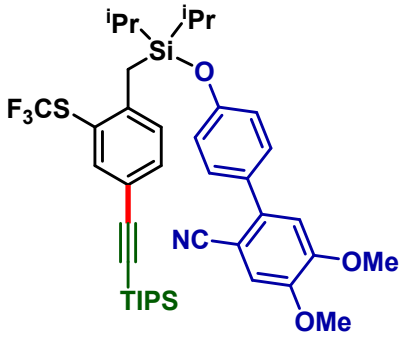

Column material: 100-200 mesh silica

Eluent: pet ether: ethyl acetate (96:04)

Yield: 78%

Physical appearance: Dark yellow liquid

^{1}H NMR (500 MHz, $CDCl_3$) δ 7.74 (s, 1H), 7.44 (dd, *J* = 8.0, 1.8 Hz, 1H), 7.37 (d, 2H), 7.28 (d, *J* = 8.1 Hz, 1H), 7.13 (s, 1H), 6.88 (s, 1H), 6.79 (d, *J* = 8.7 Hz, 2H), 3.95 (s, 3H), 3.93 (s, 3H), 2.77 (s, 2H), 1.30 – 1.23 (m, 2H), 1.12 (s, 21H), 1.06 (d, *J* = 7.5 Hz, 6H), 1.04 (d, *J* = 7.4 Hz, 6H).

^{13}C NMR (126 MHz, $CDCl_3$) δ 155.76, 152.72, 148.21, 146.03, 141.61, 140.11, 134.71, 131.62, 130.46, 130.12, 123.38, 121.41, 119.87, 119.47, 115.19, 112.51, 105.69, 102.35, 91.69, 56.48, 56.34, 20.26, 18.86, 17.75, 17.56, 13.58, 11.50.

IR (thin film, cm^{-1}): 680, 760, 795, 839, 882, 918, 997, 1114, 1157, 1217, 1242, 1266, 1353, 1388, 1463, 1503, 1603, 2158, 2220, 2867, 2945.096

HR-MS (ESI-QTOF): $[M+Na]^+$ calculated for $C_{40}H_{52}F_3NNaO_3SSi_2$ m/z 762.3051 and found m/z 762.3047

12. 4'-(((2,6-dimethyl-4-((triisopropylsilyl)ethynyl)benzyl)diisopropylsilyl)oxy)-4,5-dimethoxy-[1,1'-biphenyl]-2-carbonitrile (2l)

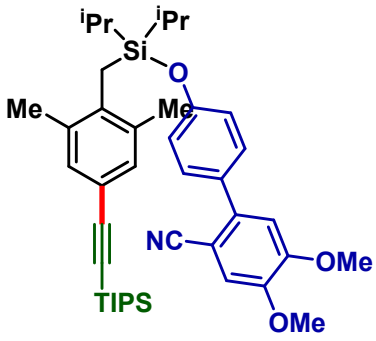

Column material: 100-200 mesh silica

Eluent: pet ether: ethyl acetate (96:04)

Yield: 71%

Physical appearance: Dark yellow liquid

^{1}H NMR (400 MHz, $CDCl_3$) δ 7.35 (d, *J* = 8.6 Hz, 2H), 7.12 (s, 1H), 7.11 (s, 2H), 6.88 (s, 1H), 6.78 (d, *J* = 8.6 Hz, 2H), 3.95 (s, 3H), 3.93 (s, 3H), 2.39 (s, 2H), 2.30 (s, 6H), 1.27 – 1.20 (m, 4H), 1.11 (s, 21H), 1.07 (d, *J* = 7.4 Hz, 6H), 0.97 (d, *J* = 7.3 Hz, 6H).

^{13}C NMR (101 MHz, $CDCl_3$) δ 155.93, 152.70, 148.15, 140.22, 137.95, 135.65, 131.71, 131.35, 130.00, 119.90, 119.27, 115.20, 112.50, 108.05, 102.32, 88.76, 56.46, 56.33, 21.35, 18.90, 17.67, 17.44, 16.36, 14.26, 11.58.

IR (thin film, cm^{-1}): 666, 755, 789, 839, 882, 917, 1027, 1071, 1137, 1174, 1217, 1242, 1266, 1353, 1388, 1463, 1503, 1560, 1603, 1686, 2147, 2220, 2866, 2943

HR-MS (ESI-QTOF): $[M+H]^+$ calculated for $C_{41}H_{58}NO_3Si_2$ m/z 668.3950 and found m/z 668.3943

13. 4'-(((2,6-dichloro-4-((triisopropylsilyl)ethynyl)benzyl)diisopropylsilyl)oxy)-4,5-dimethoxy-[1,1'-biphenyl]-2-carbonitrile (2m)

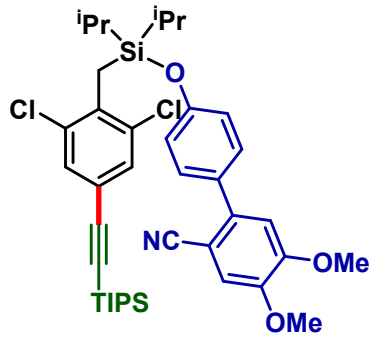

Column material: 100-200 mesh silica

Eluent: pet ether: ethyl acetate (96:04)

Yield: 72%

Physical appearance: Dark yellow liquid

^{1}H NMR (500 MHz, $CDCl_3$) δ 7.36 (d, 2H), 7.34 (s, 2H), 7.12 (s, 1H), 6.88 (s, 1H), 6.85 (d, *J* = 8.6 Hz, 2H), 3.95 (s, 3H), 3.92 (s, 3H), 2.74 (s, 2H), 1.41 – 1.32 (m, 2H), 1.11 – 1.05 (m, 33H).

^{13}C NMR (126 MHz, $CDCl_3$) δ 155.86, 152.69, 148.12, 140.26, 137.65, 134.14, 131.31, 129.90, 121.66, 120.06, 119.92, 119.47, 115.20, 112.49, 104.44, 102.31, 92.62, 56.45, 56.33, 18.81, 18.42, 17.60, 17.50, 14.43, 11.43.

IR (thin film, cm^{-1}): 668, 748, 801, 839, 882, 921, 997, 1030, 1070, 1137, 1174, 1214, 1242, 1267, 1353, 1389, 1454, 1503, 1604, 2148, 2220, 2866, 2944

HR-MS (ESI-QTOF): $[M+H]^+$ calculated for $C_{39}H_{52}Cl_2NO_3Si_2$ m/z 708.2857 and found m/z 708.2856

14. 4'-(((2-chloro-6-fluoro-4-((triisopropylsilyl)ethynyl)benzyl)diisopropylsilyl)oxy)-4,5-dimethoxy-[1,1'-biphenyl]-2-carbonitrile (2n)

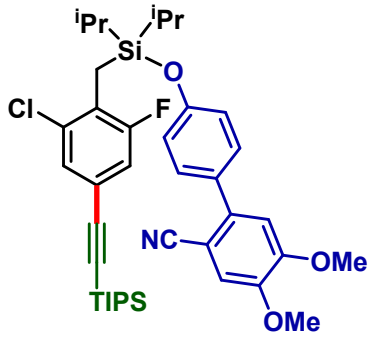

Column material: 100-200 mesh silica

Eluent: pet ether: ethyl acetate (96:04)

Yield: 74%

Physical appearance: Dark yellow liquid

^{1}H NMR (500 MHz, $CDCl_3$) δ 7.37 (d, *J* = 8.6 Hz, 2H), 7.25 (s, 1H), 7.12 (s, 1H), 7.02 (d, *J* = 9.8, 1.4 Hz, 1H), 6.88 (s, 1H), 6.85 (d, *J* = 8.6 Hz, 2H), 3.95 (s, 3H), 3.92 (s, 3H), 2.52 (d, *J* = 2.8 Hz, 2H), 1.33 – 1.28 (m, 2H), 1.10 (s, 21H), 1.07 (m, 12H).

^{13}C NMR (126 MHz, $CDCl_3$) δ 155.88, 152.69, 148.13, 140.26, 134.14, 133.57, 131.36, 129.97, 128.78, 127.50, 121.50, 119.95, 119.52, 117.16, 116.96, 115.19, 112.51, 104.81, 102.32, 92.36, 56.47, 56.34, 18.94, 18.83, 18.73, 17.50, 17.41, 14.01, 11.45.

IR (thin film, cm^{-1}): 666, 754, 802, 839, 882, 921, 996, 1032, 1137, 1173, 1217, 1267,

1353, 1401, 1465, 1503, 1547, 1604, 2158, 2220, 2867, 2926

HR-MS (ESI-QTOF): $[M+K]^+$ calculated for $C_{39}H_{51}ClFKNO_3Si_2$ m/z 730.2712 and found m/z 730.2709

15. 4'-(((2-fluoro-6-methoxy-4-((triisopropylsilyl)ethynyl)benzyl)diisopropylsilyl)oxy)-4,5-dimethoxy-[1,1'-biphenyl]-2-carbonitrile (2o)

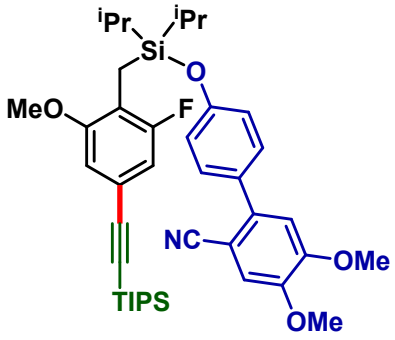

Column material: 100-200 mesh silica

Eluent: pet ether: ethyl acetate (96:04)

Yield: 77%

Physical appearance: Dark yellow liquid

^{1}H NMR (400 MHz, $CDCl_3$) δ 7.36 (d, *J* = 8.6 Hz, 2H), 7.12 (s, 1H), 6.89 (s, 1H), 6.84 (d, *J* = 8.6 Hz, 2H), 6.79 (d, *J* = 9.6, 1H), 6.64 (s, 1H), 3.94 (s, 3H), 3.92 (s, 3H), 3.73 (s, 3H), 2.35 (d, *J* = 1.8 Hz, 2H), 1.23 – 1.19 (m, 2H), 1.11 (s, 21H), 1.07 (d, *J* = 7.0 Hz, 12H).

^{13}C NMR (126 MHz, $CDCl_3$) δ 161.22, 159.30, 157.57, 157.49, 156.19, 152.64, 148.06, 140.32, 131.03, 129.79, 120.51, 120.41, 119.95, 119.49, 116.98, 116.83, 115.15, 112.48, 111.93, 111.73, 109.28, 109.26, 106.66, 106.63, 102.25, 90.27, 56.39, 56.26, 55.65, 18.81, 18.43, 17.39, 17.37, 13.81, 11.46, 11.39.

IR (thin film, cm^{-1}): 678, 768, 798, 839, 882, 914, 957, 997, 1030, 1088, 1138, 1174, 1219, 1282, 1343, 1388, 1463, 1503, 1560, 1603, 2154, 2222, 2867, 2944

HR-MS (ESI-QTOF): $[M+Na]^+$ calculated for $C_{40}H_{54}FNaNO_4Si_2$ m/z 710.3468 and found m/z 710.3472.

16. 4'-(((2,6-difluoro-4-((triisopropylsilyl)ethynyl)benzyl)diisopropylsilyl)oxy)-4,5-dimethoxy-[1,1'-biphenyl]-2-carbonitrile (2p)

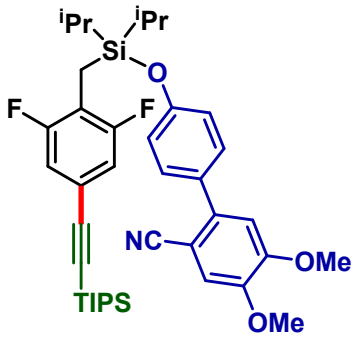

Column material: 100-200 mesh silica

Eluent: pet ether: ethyl acetate (96:04)

Yield: 69%

Physical appearance: Dark yellow liquid

^{1}H NMR (500 MHz, $CDCl_3$) δ 7.38 (d, *J* = 8.6 Hz, 2H), 7.12 (s, 1H), 6.94 (d, *J* = 7.4 Hz, 2H), 6.89 (s, 1H), 6.86 (d, *J* = 8.6 Hz, 2H), 3.95 (s, 3H), 3.93 (s, 3H), 2.34 (s, 2H), 1.29 – 1.23 (m, 3H), 1.10 (s, 21H), 1.07 (d, *J* = 7.4 Hz, 6H).

^{13}C NMR (126 MHz, $CDCl_3$) δ 161.45, 161.37, 159.50, 159.42, 155.89, 152.69, 148.14, 140.24, 131.43, 130.01, 120.01, 119.52, 115.19, 114.87, 114.65, 112.52, 102.31, 92.10, 56.47, 56.34, 18.83, 17.37, 17.33, 13.65, 11.45.

IR (thin film, cm^{-1}): 673, 759, 806, 839, 882, 919, 990, 1031, 1070, 1138, 1173, 1217, 1242, 1265, 1353, 1388, 1418, 1463, 1503, 1563, 1603, 2159, 2220, 2866, 2944

HR-MS (ESI-QTOF): $[M+Na]^+$ calculated for $C_{39}H_{51}F_2NNaO_3Si_2$ m/z 698.3268 and found m/z 698.3265

17. 4'-(((5-fluoro-2-methyl-4-((triisopropylsilyl)ethynyl)benzyl)diisopropylsilyl)oxy)-4,5-dimethoxy-[1,1'-biphenyl]-2-carbonitrile (2q)

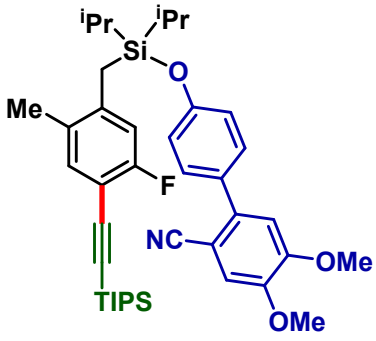

Column material: 100-200 mesh silica

Eluent: pet ether: ethyl acetate (95:05)

Yield: 70%

Physical appearance: Dark yellow liquid

^{1}H NMR (500 MHz, $CDCl_3$) δ 7.36 (d, *J* = 8.6 Hz, 2H), 7.17 (d, *J* = 7.4 Hz, 1H), 7.12 (s, 1H), 6.89 (s, 1H), 6.81 (d, *J* = 10.5 Hz, 1H), 6.77 (d, *J* = 8.6 Hz, 2H), 3.95 (s, 3H), 3.93 (s, 3H), 2.33 (s, 2H), 2.22 (s, 3H), 1.30 – 1.23 (m, *J* = 14.9, 7.4 Hz, 3H), 1.11 (s, 21H), 1.07 (d, *J* = 7.5 Hz, 6H), 1.03 (d, *J* = 7.4 Hz, 6H).

^{13}C NMR (126 MHz, $CDCl_3$) δ 162.55, 160.57, 155.77, 152.70, 148.17, 140.90, 140.84, 140.18, 135.08, 131.57, 131.24, 131.21, 130.09, 119.95, 119.50, 115.96, 115.79, 115.16, 112.53, 108.01, 107.88, 102.32, 100.63, 95.17, 56.47, 56.34, 19.67, 18.85, 17.72, 17.54, 13.51, 11.49.

IR (thin film, cm^{-1}): 756, 833, 882, 920, 996, 1071, 1170, 1199, 1236, 1321, 1384, 1436, 1462, 1600, 1631, 1701, 2150, 2220, 2866, 2943.

HR-MS (ESI-QTOF): $[M+Na]^+$ calculated for $C_{40}H_{54}FNNaO_3Si_2$ m/z 694.3518 and found m/z 694.3523

18. 4'-(((2,5-difluoro-4-((triisopropylsilyl)ethynyl)benzyl)diisopropylsilyl)oxy)-4,5-dimethoxy-[1,1'-biphenyl]-2-carbonitrile (2r)

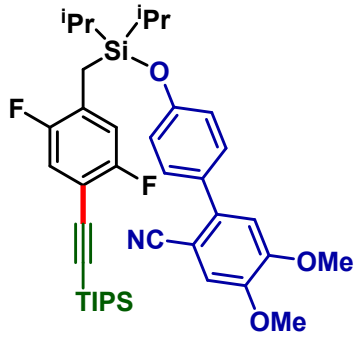

Column material: 100-200 mesh silica

Eluent: pet ether: ethyl acetate (95:05)

Yield: 69%

Physical appearance: Dark yellow liquid

^{1}H NMR (400 MHz, $CDCl_3$) δ 7.41 (d, *J* = 8.5 Hz, 2H), 7.13 (s, 1H), 7.06 (dd, *J* = 9.5, 5.9 Hz, 1H), 6.94 – 6.82 (m, 3H), 6.76 (s, 1H), 3.96 (s, 3H), 3.93 (s, 3H), 2.35 (d, *J* = 1.8 Hz, 2H), 1.32 – 1.21 (m, 2H), 1.12 (s, 21H), 1.07 (d, *J* = 3.5 Hz, 6H), 1.06 (d, *J* = 3.8 Hz, 6H).

^{13}C NMR (126 MHz, $CDCl_3$) δ 160.22, 158.25, 156.69, 155.80, 154.80, 154.78, 152.72, 148.20, 140.12, 131.74, 130.15, 120.13, 120.06, 119.56, 119.54, 119.44, 119.35, 119.33, 117.36, 117.32,

117.17, 117.13, 115.19, 112.57, 102.34, 99.21, 99.19, 96.88, 96.86, 77.46, 76.95, 56.46, 56.32, 18.78, 18.47, 17.46, 17.41, 13.38, 11.42.

IR (thin film, cm^{-1}) 777, 854, 897, 942, 918, 1075, 1204, 1325, 1379, 1431, 1471, 1607, 1634, 1711, 2157, 2217, 2874, 2951.

HR-MS (ESI-QTOF) $[M+Na]^+$ calculated for $C_{39}H_{51}F_2NNaO_3Si_2$ m/z 698.3268 and found m/z 698.3265

19. 4'-(((2-chloro-5-fluoro-4-((triisopropylsilyl)ethynyl)benzyl)diisopropylsilyl)oxy)-4,5-dimethoxy-[1,1'-biphenyl]-2-carbonitrile (2s)

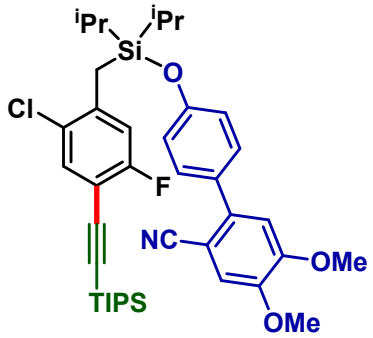

Column material: 100-200 mesh silica

Eluent: pet ether:ethyl acetate (95:05)

Yield: 77%

Physical appearance: Dark yellow liquid

^{1}H NMR (400 MHz, $CDCl_3$) δ 7.40 (t, *J* = 7.0 Hz, 3H), 7.13 (s, 1H), 6.89 (d, *J* = 8.1 Hz, 4H), 3.96 (s, 3H), 3.93 (s, 3H), 2.52 (s, 2H), 1.40 – 1.24 (m, 2H), 1.11 (s, 21H), 1.07 (d, *J* = 2.6 Hz, 6H), 1.05 (d, *J* = 2.2 Hz, 6H).

^{13}C NMR (101 MHz, $CDCl_3$) δ 162.71, 160.21, 155.77, 152.71, 148.19, 140.43, 140.35, 140.11, 133.89, 133.87, 131.70, 130.15, 127.84, 127.81, 120.09, 120.02, 119.44, 117.25, 117.02, 115.18, 112.55, 110.05, 109.87, 102.33, 98.85, 97.22, 97.19, 77.52, 76.88, 56.46, 56.32, 18.78, 18.48, 17.58, 17.45, 13.62, 11.43, 11.41.

IR (thin film, cm^{-1}) 778, 868, 957, 1054, 1214, 1397, 1415, 1454, 1617, 1714, 2163, 2214, 2867, 2987.

HR-MS (ESI-QTOF) $[M+K]^+$ calculated for $C_{39}H_{51}ClFKNO_3Si_2$ m/z 730.2712 and found m/z 730.2709

20. 4'-((diisopropyl(phenyl(4-((triisopropylsilyl)ethynyl)phenyl)methyl)silyl)oxy)-4,5-dimethoxy-[1,1'-biphenyl]-2-carbonitrile (2t)

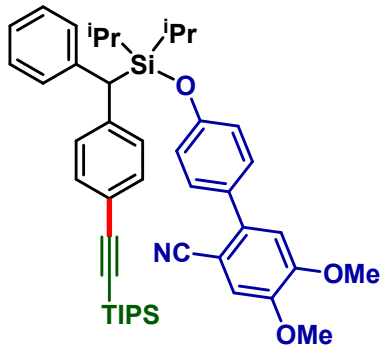

Column material: 100-200 mesh silica

Eluent: pet ether:ethyl acetate (96:04)

Yield: 72%

Physical appearance: Dark yellow liquid

^{1}H NMR (500 MHz, $CDCl_3$) δ 7.47 – 7.38 (m, 8H), 7.26 (dd, *J* = 8.9, 6.3 Hz, 2H), 7.14 (s, 1H), 6.90 (s, 1H), 6.87 (d, *J* = 8.6 Hz, 2H), 3.96 (s, 3H), 3.93 (s, 3H), 3.78 (s, 1H), 1.29 – 1.24 (m, 2H), 1.11 (s, 21H), 0.95 – 0.89 (m, 12H).

^{13}C NMR (126 MHz, $CDCl_3$) δ 155.98, 152.71, 148.19, 142.89, 141.68, 140.16, 132.38, 131.57, 130.11, 129.56, 129.48, 128.75, 125.99, 120.95, 120.04, 119.50, 115.18, 112.51, 107.44, 102.34, 90.19, 56.47, 56.35, 42.87, 19.18, 18.87, 18.49, 18.16, 18.10, 17.87, 17.81, 13.88, 13.81, 11.52, 11.43.

IR (thin film, cm^{-1}): 677, 750, 808, 837, 882, 919, 996, 1018, 1071, 1104, 1138, 1174, 1217, 1242, 1263, 1353, 1388, 1463, 1502, 1603, 2154, 2220, 2866, 2943

HR-MS (ESI-QTOF): $[M+Na]^+$ calculated for $C_{45}H_{57}NNaO_3Si_2$ m/z 738.3769 and found m/z 738.3767

21. 4'-((((4-chlorophenyl)(4-((triisopropylsilyl)ethynyl)phenyl)methyl)diisopropylsilyl)oxy)-4,5-dimethoxy-[1,1'-biphenyl]-2-carbonitrile (2u)

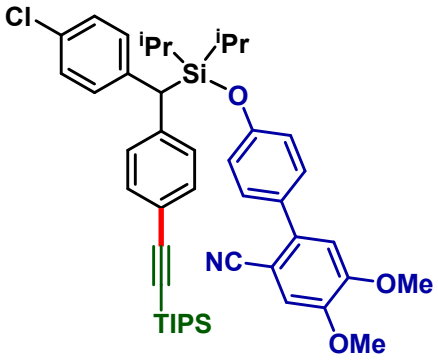

Column material: 100-200 mesh silica

Eluent: pet ether: ethyl acetate (96:04)

Yield: 60%

Physical appearance: Dark yellow liquid

^{1}H NMR (500 MHz, $CDCl_3$) δ 7.42 – 7.37 (m, 8H), 7.23 (d, *J* = 8.5 Hz, 2H), 7.14 (s, 1H), 6.90 (s, 1H), 6.87 (d, *J* = 8.6 Hz, 2H), 3.96 (s, 3H), 3.93 (s, 3H), 3.75 (s, 1H), 1.28 – 1.23 (m, 2H), 1.11 (s, 21H), 0.96 – 0.89 (m, 12H).

^{13}C NMR (126 MHz, $CDCl_3$) δ 155.80, 152.74, 148.24, 142.34, 140.42, 140.08, 132.50, 131.82, 131.77, 130.81, 130.19, 129.39, 128.82, 121.25, 119.97, 119.48, 115.19, 112.52, 107.25, 102.38, 90.50, 56.48, 56.36, 42.15, 18.87, 18.14, 17.83, 13.84, 13.82, 11.52.

IR (thin film, cm^{-1}): 677, 751, 832, 882, 918, 1014, 1092, 1137, 1174, 1216, 1241, 1262, 1353, 1388, 1463, 1502, 1603, 2154, 2220, 2866, 2943

HR-MS (ESI-QTOF): $[M+K]^+$ calculated for $C_{45}H_{56}ClKNO_3Si_2$ m/z 788.3119 and found m/z 788.3115.

22. 1-ethynyl-4-methylbenzene (3)

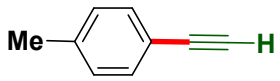

Column material: 100-200 mesh silica
Eluent: pet ether
Yield: 93%
Physical appearance: Colourless oil
^{1}H NMR (400 MHz, $CDCl_3$) δ 7.43 (d, J = 8.0 Hz, 2H), 7.16 (d, J = 7.9 Hz, 2H), 3.07 (s, 1H), 2.38 (s, 3H).
^{13}C NMR (101 MHz, $CDCl_3$) δ 139.06, 132.15, 129.20, 119.17, 83.98, 76.65, 21.60.
GC-MS (m/z): 106.06

23. methyl (E)-3-(2-((hydroxydiisopropylsilyl)methyl)-5 ((triisopropylsilyl)ethynyl)phenyl)acrylate(5)

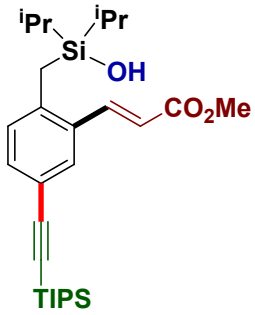

Column material: 100-200 mesh silica

Eluent: pet ether:EtOAc (95:05)
Yield: 68%
Physical appearance: Yellow liquid
^{1}H NMR (500 MHz, $CDCl_3$) δ 8.00 (d, *J* = 15.8 Hz, 1H), 7.63 (s, 1H), 7.34 (d, *J* = 8.0, 1.7 Hz, 1H), 7.09 (d, *J* = 8.0 Hz, 1H), 6.36 (d, *J* = 15.8 Hz, 1H), 3.80 (s, 3H), 2.35 (s, 2H), 1.12 (s, 21H), 1.03 – 0.97 (m, 14H).
^{13}C NMR (126 MHz, $CDCl_3$) δ 167.52, 142.59, 140.66, 133.30, 132.21, 130.16, 120.19, 119.02, 106.50, 90.33, 51.78, 19.90, 18.69, 18.66, 17.25, 17.17, 12.92, 11.33.
HR-MS (ESI-QTOF): $[M+K]^+$ calculated for $C_{28}H_{46}ClKNO_3Si_2$ m/z 486.2985 and found m/z 486.2989.

24. 1-ethyl-4-methylbenzene (6)

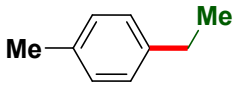

Column material: 100-200 mesh silica
Eluent: pet ether
Yield: 95%
Physical appearance: Pale yellow liquid
^{1}H NMR (400 MHz, $CDCl_3$) δ 7.27 (s, 4H), 2.79 (q, *J* = 7.6 Hz, 2H), 2.50 (s, 3H), 1.41 (t, *J* = 7.6 Hz, 3H).
^{13}C NMR (101 MHz, $CDCl_3$) δ 141.36, 135.12, 129.17, 127.91, 28.63, 21.12, 15.95.
GC-MS (m/z): 120.09

25. 1-methyl-4-vinylbenzene (7)

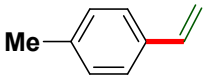

Column material: 100-200 mesh silica
Eluent: pet ether
Yield: 68%
Physical appearance: Colourless oil
^{1}H NMR (400 MHz, $CDCl_3$) δ 7.42 (d, *J* = 8.0 Hz, 2H), 7.23 (d, *J* = 7.9 Hz, 2H), 6.80 (dd, *J* = 17.6, 10.9 Hz, 1H), 5.81 (d, *J* = 17.6 Hz, 1H), 5.29 (d, *J* = 10.9 Hz, 1H), 2.44 (s, 3H).
^{13}C NMR (101 MHz, $CDCl_3$) δ 137.69, 136.84, 134.95, 129.33, 126.24, 112.84, 21.30.
GC-MS (m/z): 118.0

26. 4-methylbenzonitrile (8)

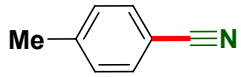

Column material: 100-200 mesh silica
Eluent: pet ether:EtOAc (98:02)
Yield: 65%
Physical appearance: Yellowish liquid
^{1}H NMR (400 MHz, $CDCl_3$) δ 7.48 (d, *J* = 7.9 Hz, 2H), 7.23 (d, *J* = 7.9 Hz, 2H), 2.38 (s, 3H)
^{13}C NMR (101 MHz, $CDCl_3$) δ 143.75, 131.99, 129.86, 119.15, 109.23, 21.80.
GC-MS (m/z): 117.06

27. 4-methylbenzoic acid (9)

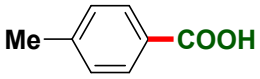

Column material: 100-200 mesh silica

Eluent: pet ether:EtOAc (90:10)
Yield: 89%
Physical appearance: White solid
MP: 274 °C.
^{1}H NMR (400 MHz, $CDCl_3$) δ 7.48 (d, *J* = 8.0 Hz, 2H), 7.30 (d, *J* = 7.9 Hz, 2H), 2.46 (s, 3H)
^{13}C NMR (101 MHz, $CDCl_3$) δ 170.08, 145.00, 130.85, 130.13, 129.12, 21.65.
GC-MS (m/z): 136.05

28. 2-(*p*-tolyl)acetic acid (10)

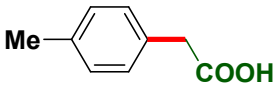

Column material: 100-200 mesh silica
Eluent: pet ether:EtOAc (90:10)
Yield: 70%
Physical appearance: White solid
^{1}H NMR (400 MHz, $CDCl_3$) δ 7.22 – 7.10 (m, 4H), 3.61 (s, 2H), 2.34 (s, 3H).
^{13}C NMR (101 MHz, $CDCl_3$) δ 178.76, 137.10, 130.34, 129.46, 129.37, 40.78, 21.19.
GC-MS (m/z): 150.06

29. (E)-2,2,6,6-tetramethyl-1-((2-nitro-1-(*p*-tolyl)vinyl)oxy)piperidine (11)

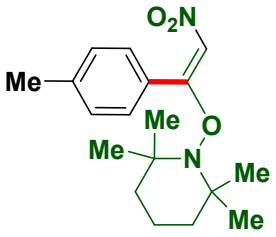

Column material: 100-200 mesh silica
Eluent: pet ether:EtOAc (99:01)
Yield: 85%
Physical appearance: Yellow solid
M. P.: 100-101 ºC
^{1}H NMR (500 MHz, $CDCl_3$) δ 7.84 (s, 1H), 7.38 (d, *J* = 8.1 Hz, 2H), 7.29 (d, *J* = 7.9 Hz, 2H), 2.45 (s, 3H), 1.69 – 1.60 (m, 6H), 1.24 (s, 6H), 1.22 (s, 6H).
^{13}C NMR (126 MHz, $CDCl_3$) δ 171.93, 141.07, 129.04, 128.79, 128.21, 123.23, 61.51, 39.60, 32.04, 21.62, 20.72, 16.73.
HRMS (ESI) calcd. for $C_{18}H_{27}N_2O_3$: 319.2022, found: 319.2034

30. 2,2-dibromo-1-(*p*-tolyl)ethan-1-one (12)

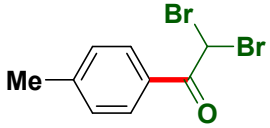

Column material: 100-200 mesh silica
Eluent: pet ether:EtOAc (95:05)
Yield: 93%
Physical appearance: pale yellow solid
MP: 98^{o}C
^{1}H NMR (500 MHz, $CDCl_3$) δ 8.01 (d, *J* = 8.3 Hz, 2H), 7.33 (d, *J* = 8.1 Hz, 2H), 6.72 (s, 1H), 2.47 (s, 3H).
^{13}C NMR (126 MHz, $CDCl_3$) δ 185.67, 145.75, 129.84, 129.67, 128.20, 39.86, 21.85.
GC-MS (m/z): 289.9

31. 2,2-dibromo-1-(*p*-tolyl)ethan-1-one (13)

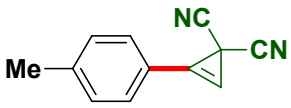

Column material: 100-200 mesh silica
Eluent: pet ether:EtOAc (95:05)
Yield: 95%

Physical appearance: colourless oil
^{1}H NMR (400 MHz, $CDCl_3$) δ 7.61 (d, *J* = 7.9 Hz, 2H), 7.38 (d, *J* = 7.9 Hz, 2H), 6.99 (s, 1H), 2.46 (s, 3H).
^{13}C NMR (126 MHz, $CDCl_3$) δ 143.99, 130.60, 130.42, 117.46, 116.35, 111.83, 91.16, 21.87, 3.62.
GC-MS (m/z): 180.06

5. Kinetic experiments:

As the *para*-scaffold and alkynyl bromide are involved in this reaction, we can assume the rate of the reaction is dependent only on the concentration of scaffold and alkynyl bromide.

Order determination with respect to silyl substrate 1a

Run	**1a** (mmol)	alkynyl bromide (mmol)	$[Rh(COD)Cl]_2$ (mmol)	$Cu_2Cr_2O_5$ (mmol)	Ag_2SO_4 (mmol)	Na_2CO_3 (mmol)	Admantane-1-COOH (mmol)
1	0.1	0.15	0.005	0.1	0.1	0.2	0.2
2	0.05	0.15	0.0025	0.05	0.05	0.1	0.1

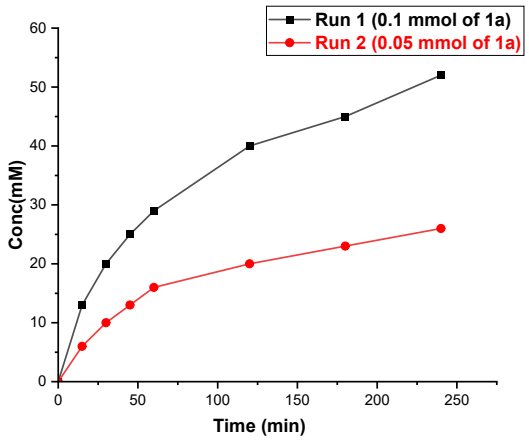

Figure S1: Order determination with respect to the substrate

As both arene and alkyne were involved in this reaction, we can assume the rate of the reaction is dependent on the concentration of substrate and alkyne.

Now, Rate = k. [**substrate**]^x [**alkyne**]^y

For run 1, initial rate = Rate 1

So, Rate 1= k. [**substrate**]^x [**alkyne**]^y

or, $0.86 = k_H . [0.1]^x [0.3]^y$ (1)

So, Rate 2= k. [**substrate**]^x [**alkyne**]^y

or, $0.4 = k_H . [0.05]^x [0.3]^y$ (2)

hence from equation (1) and (2)

We get, $[\text{Rate 1}/ \text{Rate 2}] = [0.1/ 0.05]^x$

or, x = [log (Rate 1) – log (Rate 2)] / [log (0.1) – log (0.05)]

or, x = [log (0.86) – log (0.4)] / [log (0.1) – log (0.05)]

or, x = 0.332/0.301 = 1.10

So, order with respect to scaffold (1a) is ~ 1

Order determination with respect to alkynye

Run	**1a** (mmol)	alkynyl bromide (mmol)	$[Rh(COD)Cl]_2$ (mmol)	$Cu_2Cr_2O_5$ (mmol)	Ag_2SO_4 (mmol)	Na_2CO_3 (mmol)	Admantane-1-COOH (mmol)
2	0.05	0.15	0.0025	0.05	0.05	0.1	0.1
3	0.05	0.075	0.0025	0.05	0.05	0.1	0.1

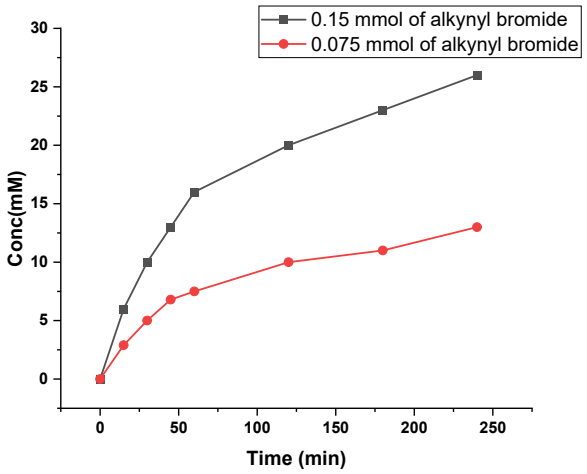

Figure S2: Order determination with respect to the alkynyl bromide

Now, Rate = k. [**substrate**]^{x} [**alkyne**]^{y}

For run 2, initial rate = Rate 2

So, Rate 2= k. [**substrate**]^{x} [**alkyne**]^{y}

or, $0.4 = k_H . [0.05]^x [0.15]^y$ (1)

So, Rate 3= k. [**substrate**]^{x} [**alkyne**]^{y}

For run 3, initial rate = Rate 3

or, $0.19 = k_H . [0.05]^x [0.075]^y$ (3)

hence from equation (1) and (3)

We get, $[\text{Rate 2}/ \text{Rate 3}] = [0.15/ 0.075]^x$

or, x = [log (Rate 2) – log (Rate 3)] / [log (0.15) – log (0.075)]

or, x = [log (0.4) – log (Rate 0.19)] / [log (0.15) – log (0.075)]

or, x = 0.280/0.301 = 1.07

So, order with respect to alkynyl bromide is ~ 1.

k_H/k_D determination: Kinetic isotopic study was performed under the standard condition by using the deuterium containing substrate.

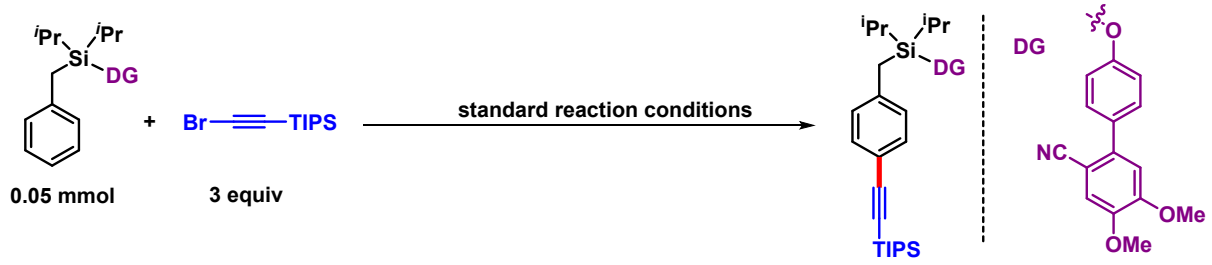

Run	**1a** (mmol)	alkynyl bromide (mmol)	$[Rh(COD)Cl]_2$ (mmol)	$Cu_2Cr_2O_5$ (mmol)	Ag_2SO_4 (mmol)	Na_2CO_3 (mmol)	Admantane-1-COOH (mmol)
1	0.05	0.15	0.0025	0.05	0.05	0.1	0.1

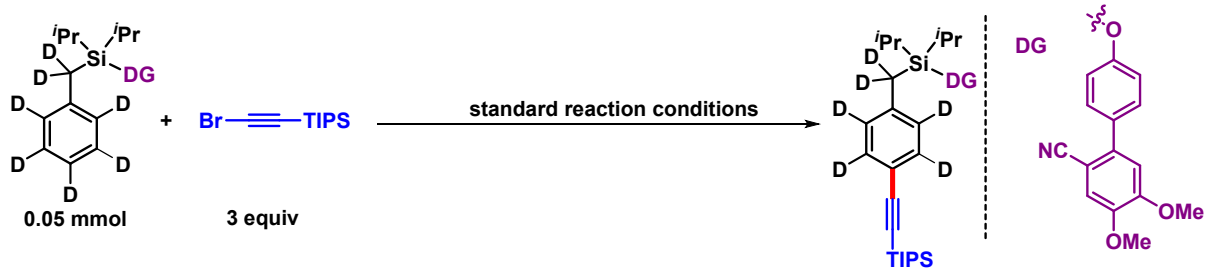

Run	**d-7 1a** (mmol)	alkynyl bromide (mmol)	$[Rh(COD)Cl]_2$ (mmol)	$Cu_2Cr_2O_5$ (mmol)	Ag_2SO_4 (mmol)	Na_2CO_3 (mmol)	Admantane-1-COOH (mmol)
4	0.05	0.15	0.0025	0.05	0.05	0.1	0.1

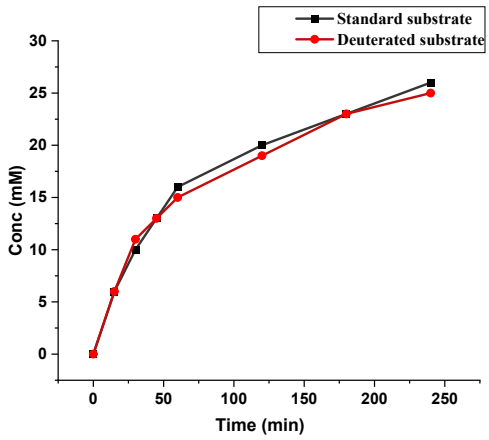

Figure S3: k_H/k_D determination

As both arene and alkyne were involved in this reaction, we can assume the rate of the reaction is dependent on the concentration of substrate and alkyne.

Now, Rate = k. [**substrate**]^x [**alkyne**]^y

For run 1, initial rate = Rate 1

So, Rate 1= k_H. [**substrate**]^x [**alkyne**]^y

or, 0.4 = k_H. $[0.05]^x$ $[0.15]^y$ (1)

For run 4, initial rate = Rate 4

So, Rate 4= k_D. [**deuterated substrate**]^x [**alkyne**]^y

or, 0.39 = k_D. $[0.05]^x$ $[0.15]^y$ (2)

So, k_H / k_D = Rate 1/ Rate 4

or, k_H / k_D = 0.4 / 0.39

or k_H / k_D = 1.03 ~ 1

Intermolecular KIE experiment:

In an oven-dried screw cap reaction tube charged with a magnetic stir-bar silyl-ether scaffold (0.1 mmol), deuterated-silyl-ether scaffold (deuterated-1aD_7), $[Rh(COD)Cl]_2$ (5 mol%, 0.01 mmol), $Cu_2Cr_2O_5$ (1 *equiv.*, 0.2 mmol), Ad-COOH (2 *equiv.*, 0.4 mmol), Na_2CO_3 (2 *equiv.*, 0.4 mmol),

Ag_2SO_4 (1 equiv, 0.2 mmol) were taken. After that 2 mL DCE was added followed by bromo acetylene (3 *equiv.*) was added with a microlitre pipette under aerobic condition. The tube was tightly capped and placed in a preheated oil bath at 120 ºC and the reaction mixture was stirred for 24 h. After completion of the reaction, the reaction mixture was then cooled to room temperature and filtered through a celite pad with ethyl acetate. The filtrate was washed with warm sat. $NaHCO_3$ solution and then the organic layers are collected and concentrated and the desired *para*-alkynylated compounds were purified using column chromatography using silica gel and ethyl acetate/petroleum ether as the eluent. P_H/P_D was calculated from ^{1}H NMR spectrum of the isolated product. From NMR spectrum product distribution P_H/P_D was found 1.04.

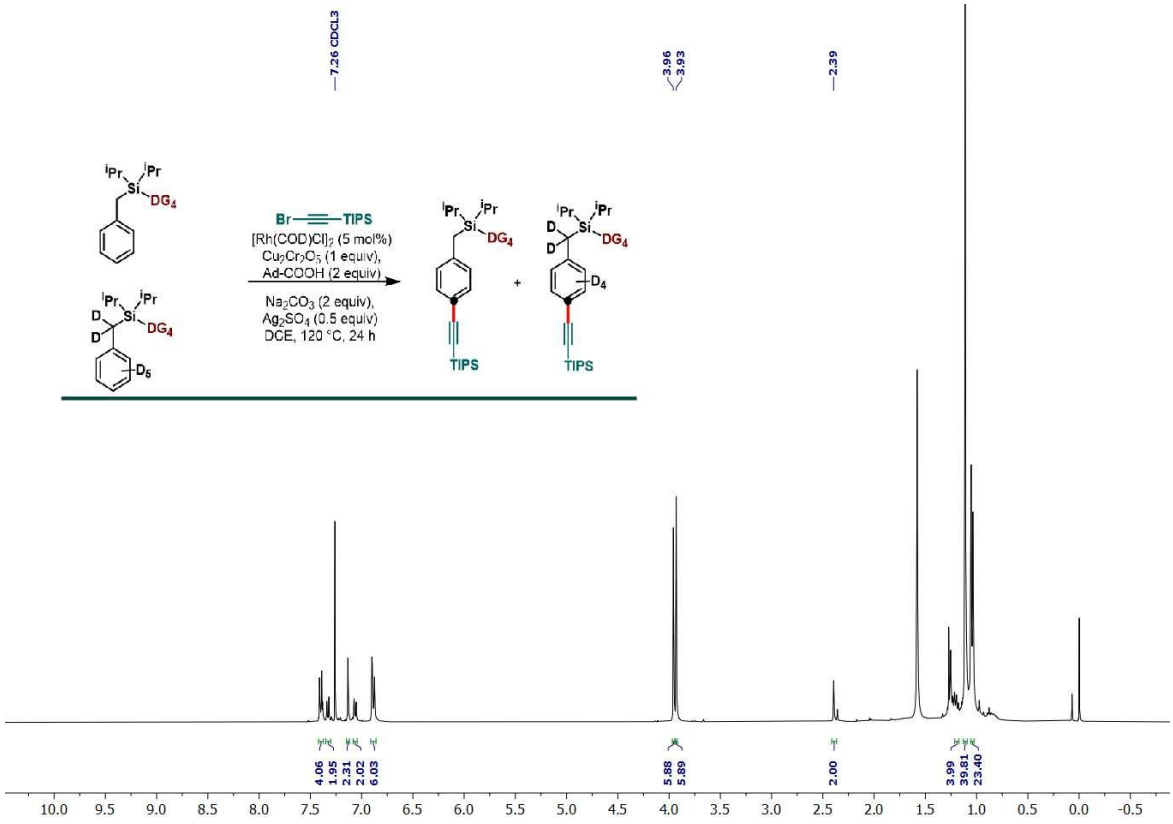

In this spectrum peak at 2.39 ppm corresponds to two benzylic protons and total integration is 2.0 and the singlet at 3.96 ppm coming from the one of the methoxy proton of directing group of deuterated and non-deuterated product. Among this 5.88 protons, three protons are coming from compound 2a (non-deuterated product) and rest 2.88 protons is the contribution of deuterated substrate (D_7-1a). And hence [P_H/P_D] = 3/2.88 = 1.04.

6. Computational Methods

Density functional theory (DFT) calculations were performed with *Gaussian 16* rev. B.01.[12] Geometry optimizations were initially performed using the global-hybrid meta-NGA (nonseparable gradient approximation) MN15 functional[13] with the def2-SVP[14,15] Karlsruhe-family basis set and the optimized structures further refined with a mix of larger basis set consisting of triple-ζ valence def2-TZVPD (where 'D' indicates diffuse basis functions) for Br[16], Rh[17,18] and Ag[16,17] atoms and def2-SVP[14,15] for all other atoms (BS1). MN15 functional was chosen as it performs much better than many other functionals (e.g. ωB97X-D and TPSS) in predicting transition metal (TM) reaction barrier heights and giving better geometries for both TM complexes and organic molecules.[2] Minima and transition structures on the potential energy surface (PES) were confirmed using harmonic frequency analysis at the same level of theory, showing respectively zero and one imaginary frequency. Where appropriate for cases where visual inspection of TS imaginary frequency is not obvious (e.g., for the beta-bromide elimination TS), intrinsic reaction coordinate (IRC) analyses[18,19] were performed to confirm that the found TSs connect to the right reactants and products. Single point (SP) corrections were performed using MN15 functional and def2-QZVP[14] basis set for all atoms. The SMD implicit continuum solvation model[20] was used to account for the effect of dichloroethane solvent on the computed Gibbs energy profile. Gibbs energies were evaluated at the reaction temperature of 393.15 K (120°C), using a quasi-RRHO treatment of vibrational entropies.[21,22] Vibrational entropies of frequencies below 100 cm^{-1} were obtained according to a free rotor description, using a smooth damping function to interpolate between the two limiting descriptions. The free energies were further corrected using standard concentration of 1 mol/L, which were used in solvation calculations. Unless otherwise stated, the final SMD (dichloroethane)-MN15/def2-QZVP//MN15/BS1 Gibbs energies are used for discussion throughout. *All Gibbs energy values in the text and figures are quoted in kcal mol^{-1}.* Molecular orbitals are generated from solvent-corrected SMD(1,4-dioxane)-MN15/def2-QZVPP checkpoint files and visualized using an isosurface value of 0.05 throughout. All molecular structures and molecular orbitals were visualized using *PyMOL* software.[23]

Geometries of all optimized structures (in *.xyz* format with their associated energy in Hartrees) are included in a separate folder named *DFT_structures*. All these data have been deposited with this Supporting Information and uploaded to zenodo.org under https://zenodo.org/record/7585280.

6.1 Model Simplification and Conformational considerations

Structure **SM1**, where the isopropyl (^{i}Pr) groups on the Si-atom are replaced by methyl (Me) groups, was used as a simplified model for computational modelling. The use of ^{i}Pr groups on Si probably benefits from favorable Thorpe–Ingold effect making the formation of rhodacycle easier than Me groups, but this simplification should not affect the reaction mechanism – any favorable barriers calculated with this simplified model are expected to be favorable for the ^{i}Pr analogue as well. The adamantane-1-carboxylate is simplified to acetate to save computational cost. The adamantyl group provides sterics to the molecules and in computational modelling we avoid conformations with any possible clashes that would arise if adamantane-1-carboxylate was used instead of acetate.

The starting material for computational modelling, **SM1**, was first conformationally sampled. The possible rotamers for **SM1** were generated by systematically varying a combination of key dihedral angles shown in red (Scheme S9) and optimizing the structures. The lowest energy conformer was used for subsequent calculations. For the Rh complexes involved in the reaction, such as **INT1** shown, the conformational flexibility is rather limited due to the rigidity of the coordinating sites of substrate **SM1** to Rh metal center. The conformations of the coordinating substrate (shown in blue in Scheme S9) are kept the same throughout the computational modelling.

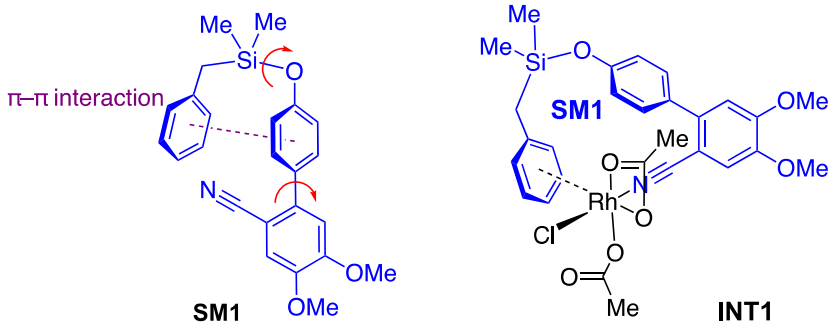

Scheme S9. Rotamers were generated by varying the dihedral angles in red in conformational sampling of the most stable conformer used for reaction modelling.

6.2 Rh(III) species in the reaction

Figure S4 compares the relative energies of the different species of rodacycles with varying coordinating ligands occupying different coordination sites. **INT1**, having Cl^{-} anion as one of the ligands is the most stable species and this is used for computational mechanistic investigations.

The regioisomeric **INT1a**, where Cl^- anion is at a different coordination site (*cis* to the nitrile group), is 5.7 kcal mol^{-1} higher in energy than where the Cl^- anion is *trans* to the nitrile group. The species with AcO^- anion instead of Cl^- anion, **INT1'**, is 21.4 kcal mol^{-1} higher in energy. The corresponding high spin Rh-species of **INT1** is 86.9 kcal mol^{-1} higher in energy and is thus not the ground state for this complex.

INT1	**INT1'**	**INT1a**
ΔΔG = 0.0 kcal mol^{-1}	ΔΔG = 21.4 kcal mol^{-1}	ΔΔG = 5.7 kcal mol^{-1}
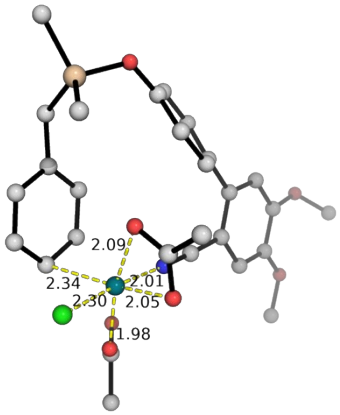	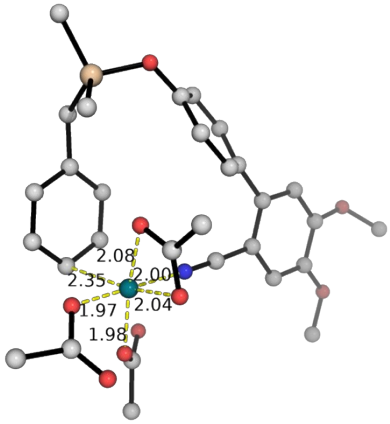	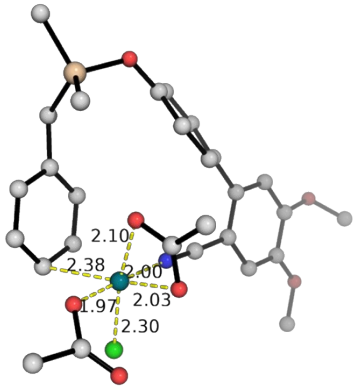

Figure S4. DFT optimized rodacyclic complexes. Relative Gibbs energies are given in kcal mol^{-1}.

6.3 C–H activation step

Although the C–H activation step is not the overall rate-limiting step of the Rh-catalyzed alkynylation (Figure 1, main text), it is the regio-determining step, as the formation of the rhodacycle after C–H activation is highly exergonic and irreversible.

Figure S5 shows all the TSs for the C–H activation step. C–H activation at *para*-position has a barrier of 4.6 kcal mol^{-1}, while the lowest barrier for C–H activation at *meta*-position is 6.8 kcal mol^{-1} (***meta*-TS1-site1**) and the lowest barrier for C–H activation at *ortho*-position is 15.7 kcal mol^{-1} (***ortho*-TS1-site1**). This higher barrier of 2.2 kcal mol^{-1} for *meta*- over *para*-selectivity indicates a 16:1 selectivity in favor of *para*-position over *meta*-position; the higher barrier of 11.1 kcal mol^{-1} for *ortho*- over *para*-selectivity indicates a 1.5 milion:1 selectivity in favor of *para*-position over *ortho*-position.

Comparing the two *meta* TS (**meta-TS1-site1** and **meta-TS1-site2**) and the two *ortho* TSs (**ortho-TS1-site1** and **ortho-TS1-site2**), we can see that the more the arene is positioned away from the favorable π-π interaction with the phenyl ring on the directing group and the more the rhodacyle is twisted, the higher the activation barriers (**site2** TSs over and **site1** TSs).

TS1 (para)	**meta-TS1-site1**	**meta-TS1-site2**
$\Delta G^{\ddagger}$ = 4.6 kcal mol^{-1}	$\Delta G^{\ddagger}$ = 6.8 kcal mol^{-1}	$\Delta G^{\ddagger}$ = 8.5 kcal mol^{-1}
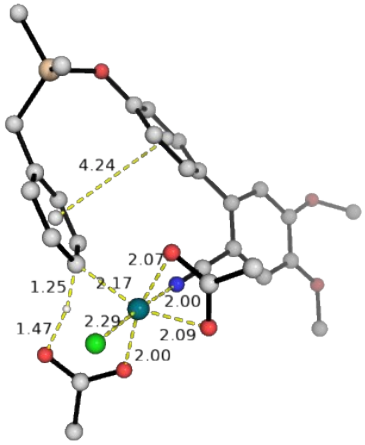	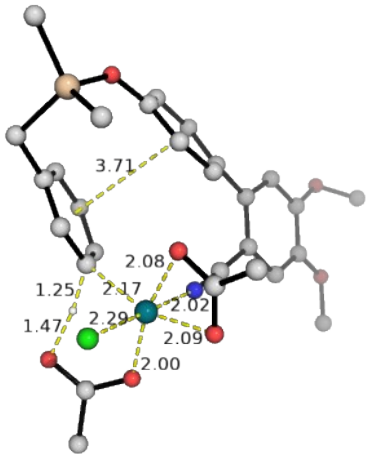	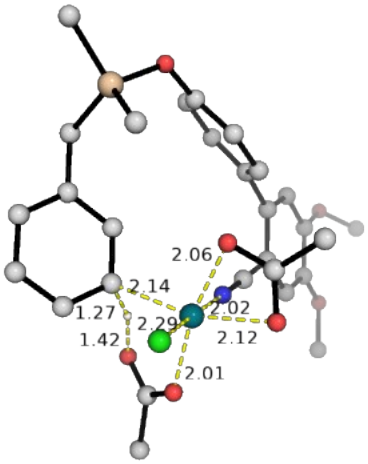
ortho-TS1-site1	**ortho-TS1-site2**	
$\Delta G^{\ddagger}$ = 15.7 kcal mol^{-1}	$\Delta G^{\ddagger}$ = 18.5 kcal mol^{-1}	
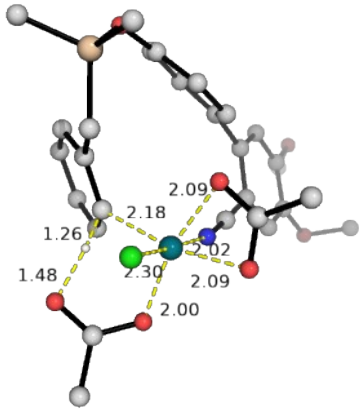	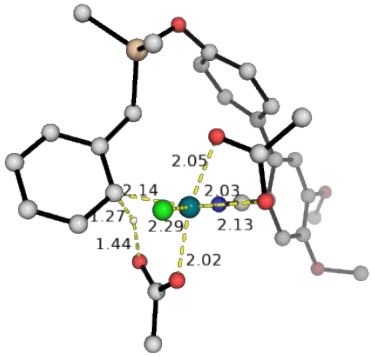	

Figure S5. DFT optimized TS structures for the C–H activation step at different arene sites.

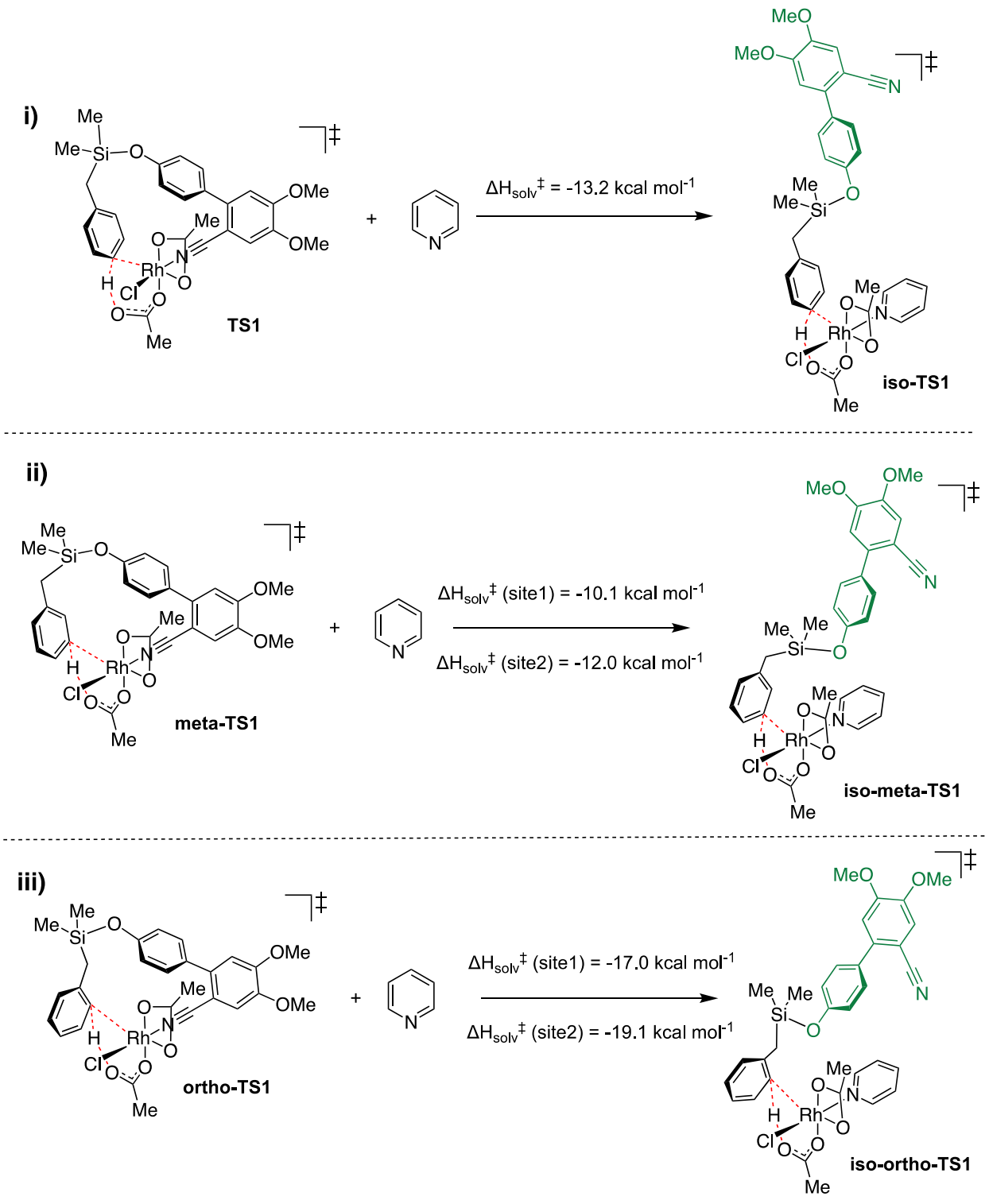

Scheme S10. Computed ring strain involving a hypothetical pyridine ligand for the C–H activation step.

We further performed isodesmic studies[24,25] to estimate the ring strains in these C–H activation TSs: a hypothetical pyridine ligand was used to displace the Rh–N(nitrile) interaction in these TSs

to release the ring strain so that the directing group (DG) gets uncoordinated (Scheme S10, see refs[26,27] for examples of such calculations). The starting conformation for the DG (highlighted in green, Scheme S10) in all 3 cases was made the same in a linear geometry for subsequent TS searches. The enthalpies of the reactions were corrected with SMD solvation model:

$$\Delta H_{sol}^{\ddagger} = \Delta H_{gas}^{\ddagger} - \Delta E_{gas}^{\ddagger} + \Delta E_{sol}^{\ddagger}.$$

	Barrier	Barrier *relative* to para-activation	Ring strain	Ring strain *relative* to para-activation
TS1 (para)	4.6	0.0	13.2	0
meta-TS1-site1	6.8	2.2	10.1	-3.1
meta-TS1-site2	8.5	3.9	12.0	-1.2
ortho-TS1-site1	15.7	11.1	17.0	3.8
ortho-TS1-site2	18.5	13.9	19.1	5.9

Table S9. Comparison of relative barriers and computed ring strains from isodesmic studies for C–H activation TSs. All values are given in kcal mol^{-1}. Although C–H activation at *meta*-positions have higher barriers, they have smaller ring strains (highlighted in grey) compared to C–H activation at *para*-position.

From the enthalpic changes, we can see that there is 13.2 kcal mol^{-1} ring strain in **TS1** vs 10.1 kcal mol^{-1} in ***meta*-TS1-site1** and 17.0 kcal mol^{-1} in ***ortho*-TS1-site1**. These values are summarized in Table S9. From the table, we see that ring strain only contributes partially to the activation barrier heights in the current system: the *ortho*-C–H activations (***ortho*-TS1-site1** and ***ortho*-TS1-site2**) have barriers 11.1 and 13.9 kcal mol^{-1} higher than *para*-C–H activation, however, ring strains are only 3.8 and 5. 9 kcal mol^{-1} respectively. In addition, the *meta*-C–H activations (***meta*-TS1-site1** and ***meta*-TS1-site2**) have barriers 2.2 and 3.9 kcal mol^{-1} higher than *para*-C–H activation, but they both have lower ring strains than *para*-C–H activation. Therefore, electronic factors and non-covalent interactions could be important for the regioselectivities in the C–H activation step.

Figure S6 shows the HOMOs for the lowest energy TSs in the C–H activation step at various positions. These demonstrate that at the *para*-position, the orbital overlap is the best between the d-orbital on Rh-metal and the π-orbital on the arene, whereas the *meta*- and *ortho*- C–H activation

TSs have poor orbital overlap. Thus, the good orbital overlaps in *para*-C–H activation lowers the C–H activation barrier.

TS1 (para)	**meta-TS1-site1**	**ortho-TS1-site1**
$\Delta G^{\ddagger}$ = 4.6 kcal mol^{-1}	$\Delta G^{\ddagger}$ = 6.8 kcal mol^{-1}	$\Delta G^{\ddagger}$ = 15.7 kcal mol^{-1}
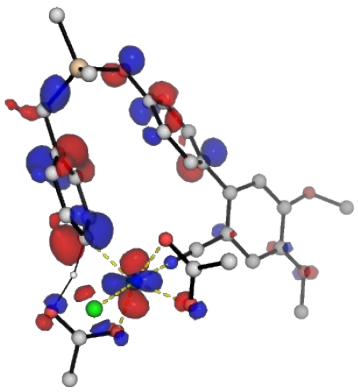	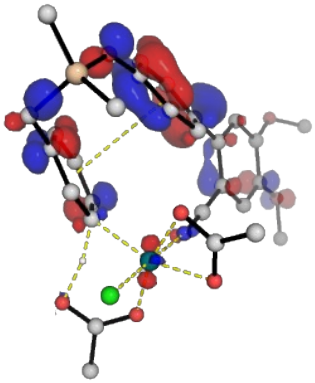	

Figure S6. HOMOs for the lowest energy C–H activation TSs at various positions at an isosurface value of 0.05.

6.4. Optimized structures and absolute energies, zero-point energies

Geometries of all optimized structures (in *.xyz* format with their associated energy in Hartrees) are included in a separate folder named *final_xyz_structures* with an associated readme.txt file. All these data have been deposited with this Supporting Information and uploaded to zenodo.org under https://zenodo.org/record/7585280 (DOI: 10.5281/zenodo.7585280).

Absolute values (in Hartrees) for SCF energy, zero-point vibrational energy (ZPE), enthalpy and quasi-harmonic Gibbs free energy (at 120°C/393.15 K) for optimized structures are given below. Single point corrections in SMD dichloroethane using MN15/def2-QZVP level of theory are also included.

Structure	**E/au**	**ZPE/au**	**H/au**	**T.S/au**	**qh-G/au**	**SP MN15-2X/def2-QZVP**
acetate	-228.059294	0.048236	-228.00312	0.042052	-228.044074	-228.58196816
cl_anion	-459.94618	0	-459.94307	0.019458	-459.962525	-460.35548536
acetic_acid	-228.644533	0.062197	-228.57411	0.041723	-228.61541	-229.06955302
para_prd	-1981.081338	0.546187	-1980.4703	0.171415	-1980.629273	-1984.01198130
SM1	-1496.88555	0.434538	-1496.4017	0.137658	-1496.530029	-1499.27458900

AgBr_monomer	-2721.225319	0.000564	-2721.2196	0.035623	-2721.255255	-2721.39785166
AgBr_dimer	-5442.524491	0.001782	-5442.5119	0.057735	-5442.568098	-5442.84035785
AgOAc_monomer	-374.748696	0.050645	-374.68765	0.052241	-374.738021	-375.18550671
AgOAc_dimer	-749.614004	0.104042	-749.48872	0.080731	-749.564698	-750.44446144
pyridine	-247.762761	0.089473	-247.66485	0.04235	-247.707207	-248.22280239
bromide_anion	-2574.568731	0	-2574.5656	0.020978	-2574.586596	-2574.79169029
INT1'	-2291.480019	0.593629	-2290.8113	0.19471	-2290.990623	-2295.11328959
INT1a	-2523.377463	0.543043	-2522.7649	0.182377	-2522.93338	-2526.87032898
INT1	-2523.387198	0.543315	-2522.7745	0.181615	-2522.942522	-2526.87365115
TS1	-2523.375553	0.538406	-2522.7684	0.181045	-2522.935902	-2526.86128572
INT2	-2523.422867	0.543207	-2522.8102	0.182821	-2522.978994	-2526.90216367
meta-TS1-site1	-2523.377822	0.538772	-2522.7706	0.178007	-2522.936478	-2526.85952134
meta-TS1-site2	-2523.370902	0.538089	-2522.7642	0.179235	-2522.930407	-2526.85587057
ortho-TS1-site1	-2523.363381	0.538104	-2522.7567	0.177348	-2522.923016	-2526.84425515
ortho-TS1-site2	-2523.357095	0.538074	-2522.7507	0.177225	-2522.916189	-2526.84047622
TIPS_ethynyl_bromide	-3294.590028	0.292704	-3294.266	0.096914	-3294.358717	-3295.72618549
INT3	-5589.359989	0.774064	-5588.4932	0.230722	-5588.706268	-5593.55152672
TS2	-5589.340178	0.772675	-5588.4754	0.230546	-5588.68775	-5593.53371449
INT4	-5589.391612	0.776455	-5588.5237	0.226948	-5588.733939	-5593.58151479
TS2-c2	-5589.336832	0.772709	-5588.4721	0.230284	-5588.684317	-5593.53129885
TS3	-5589.351953	0.774786	-5588.4857	0.226652	-5588.695722	-5593.551563
INT5	-5589.355253	0.774633	-5588.4877	0.233164	-5588.701594	-5593.556881
INT4prime	-5735.888644	0.776531	-5735.0173	0.23592	-5735.235146	-5740.141028
TS3prime	-5735.88473	0.775398	-5735.0148	0.236191	-5735.232237	-5740.13771
INT5prime	-5735.909927	0.775979	-5735.0381	0.243622	-5735.259463	-5740.170937
iso-meta-TS1	-2771.161608	0.629032	-2770.4539	0.208236	-2770.642855	-2775.10100132
iso-ortho-TS1	-2771.166312	0.629765	-2770.4587	0.200443	-2770.643758	-2775.09712330

7. References:

1. U. Dutta, S. Maiti, S. Pimparkar, S. Maiti, L. R. Gahan, E. H. Krenske, D.W. Lupton and D. Maiti, *Chem. Sci*. **2019**, *10*, 7426–7432;

2. S. Sasmal, G. Prakash, U. Dutta, R. Laskar, G. K. Lahiri, D. Maiti. *Chem. Sci.* **2022**, *13*, 5616-5621.

3. S. Bag, T. Patra, A. Modak, A. Deb, S. Maity, U. Dutta, A. Dey, R. Kancherla, A. Maji, A. Hazra, M. Bera, D. Maiti, *J. Am. Chem. Soc.* **2015**, *137*, 11888-11891.

4. C. Wang, H. Ge, *Chem. Eur. J*. **2011**, *17*, 14371 – 14374.

5. E. Richmond, J. Moran, *J. Org. Chem.* **2015**, *80*, 6922−6929.

6. U. Dutta, D. W. Lupton, D. Maiti, *Org. Lett.* **2016**, *18*, 860–863.

7. K. A. A. Kumara, V. Venkateswarlua, R. A. Vishwakarmaa, S. D. Sawant, *Synthesis* **2015**, *47*, 3161–3168

8. C. Li, P. Zhao, R. Li, B. Zhang, W. Zhao, *Angew. Chem. Int. Ed.* **2020**, *59*, 10913 –10917.

9. U. Dutta, S. Maity, R. Kancherla, D. Maiti, *Org. Lett.* **2014**, *16*, 6302–6305.

10. S. Madabhushi, R. Jillella, K. K. R. Mallu, K. R. Godala, V. S. Vangipuram, *Tetrahedron Letters* **2013,** *54*, 3993–3996.

11. S. Lin, M. Li, Z. Dong, F. Liang, J. Zhang, *Org. Biomol. Chem*., **2014**, *12*, 1341-1350.

Full reference Gaussian 16:

Gaussian 16, Revision B.01, Frisch, M. J.; Trucks, G. W.; Schlegel, H. B.; Scuseria, G. E.; Robb, M. A.; Cheeseman, J. R.; Scalmani, G.; Barone, V.; Mennucci, B.; Petersson, G. A.; Nakatsuji, H.; Caricato, M.; Li, X.; Hratchian, H. P.; Izmaylov, A. F.; Bloino, J.; Zheng, G.; Sonnenberg, J. L.; Hada, M.; Ehara, M.; Toyota, K.; Fukuda, R.; Hasegawa, J.; Ishida, M.; Nakajima, T.; Honda, Y.; Kitao, O.; Nakai, H.; Vreven, T.; Montgomery Jr., J. A.; Peralta, J. E.; Ogliaro, F.; Bearpark, M.; Heyd, J. J.; Brothers, E.; Kudin, K. N.; Staroverov, V. N.; Kobayashi, R.; Normand, J.; Raghavachari, K.; Rendell, A.; Burant, J. C.; Iyengar, S. S.; Tomasi, J.; Cossi, M.; Rega, N.; Millam, J. M.; Klene, M.; Knox, J. E.; Cross, J. B.; Bakken, V.; Adamo, C.; Jaramillo, J.; Gomperts, R.; Stratmann, R. E.; Yazyev, O.; Austin, A. J.; Cammi, R.; Pomelli, C.; Ochterski, J. W.; Martin, R. L.; Morokuma, K.; Zakrzewski, V. G.; Voth, G. A.; Salvador, P.; Dannenberg, J. J.; Dapprich, S.; Daniels, A. D.; Farkas, Ö.; Foresman, J. B.; Ortiz, J. V; Cioslowski, J.; Fox, D. J.

Gaussian, Inc., Wallingford CT, 2016.

(12) M. J. Frisch, G. W. Trucks, H. B. Schlegel, G. E. Scuseria, M. A. Robb, J. R. Cheeseman, G. Scalmani, V. Barone, G. A. Petersson, H. Nakatsuji, et al. Gaussian 16, Revision B.01. 2016.

(13) H. S. Yu, X. He, S. L. Li, D. G. Truhlar, MN15: *Chem. Sci.* **2016**, *7*, 5032–5051.

(14) F. Weigend, R. Ahlrichs, *Phys. Chem. Chem. Phys.* **2005**, *7*, 3297–3305.

(15) F. Weigend, Accurate Coulomb-Fitting Basis Sets for H to Rn.. **2006**, *8*, 1057–1065.

(16) D. Rappoport, F. Furche, *J. Chem. Phys.* **2010**, *133*, 134105.

(17) D. Andrae, U. Häußermann, M. Dolg, H. Stoll, H. Preuß, *Theor. Chim. Acta* **1990**, *77*, 123–141.

(18) K. Fukui, *J. Phys. Chem.* **2005**, *74* (23), 4161–4163.

(19) K. Fukui, *Acc. Chem. Res.* **1981**, *14*, 363–368.

(20) A. V. Marenich, C. J. Cramer, D. G. Truhlar, *J. Phys. Chem. B* **2009**, *113*, 6378–6396.

(22) S. Grimme, *Chem.: Eur. J.* **2012**, *18*, 9955–9964.

(22) I. Funes-Ardoiz, R. S. Paton, GoodVibes v1.0.1 http://doi.org/10.5281/zenodo.56091.

(23) L. Schrödinger, *The PyMOL Molecular Graphics Development Component, Version 1.8*; 2015.

(24) S. E. Wheeler, K. N. Houk, P. V. R. Schleyer, W. D. Allen, *J. Am. Chem. Soc.* **2009**, *131*, 2547–2560.

(25) S. E. Wheeler, **2012**, *2*, 204–220.

(26) X. Zhang, G. Lu, M. Sun, M. Mahankali, Y. Ma, M. Zhang, W. Hua, Y. Hu, Q. Wang, J. Chen, *Nat. Chem.* **2018**, *10*, 540–548.

(27) S. Porey, X. Zhang, S. Bhowmick, V. Kumar Singh, S. Guin; R. S. Paton, D. Maiti, *J. Am. Chem. Soc.* **2020**, *142*, 3762–3774.

NMR SPECTRA

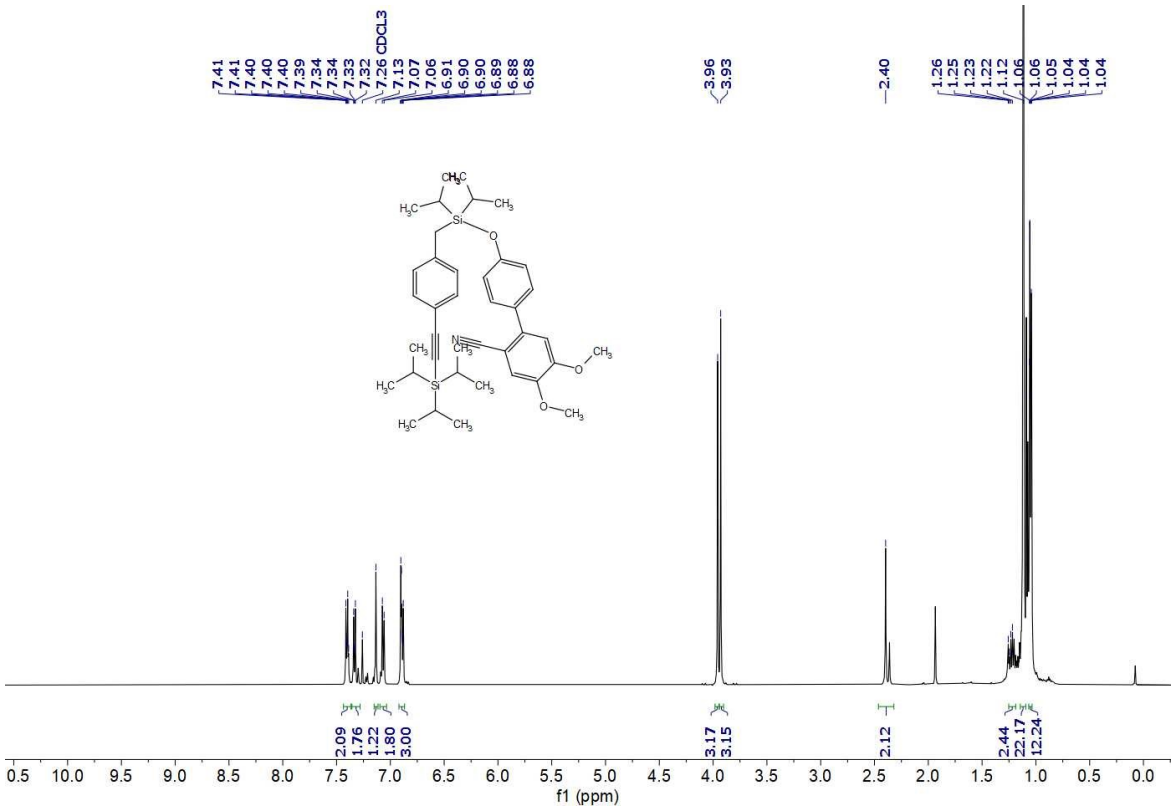
7.41
7.41
7.40
7.40
7.40
7.39
7.34
7.34
7.33
7.32
7.26 CDCL3
7.13
7.07
7.06
6.91
6.90
6.90
6.89
6.88
6.88
3.96
3.93
2.40
1.26
1.25
1.23
1.22
1.12
1.06
1.06
1.05
1.04
1.04
1.04
2.09
1.76
1.22
1.80
3.00
3.17
3.15
2.12
2.44
22.17
12.24
f1 (ppm)

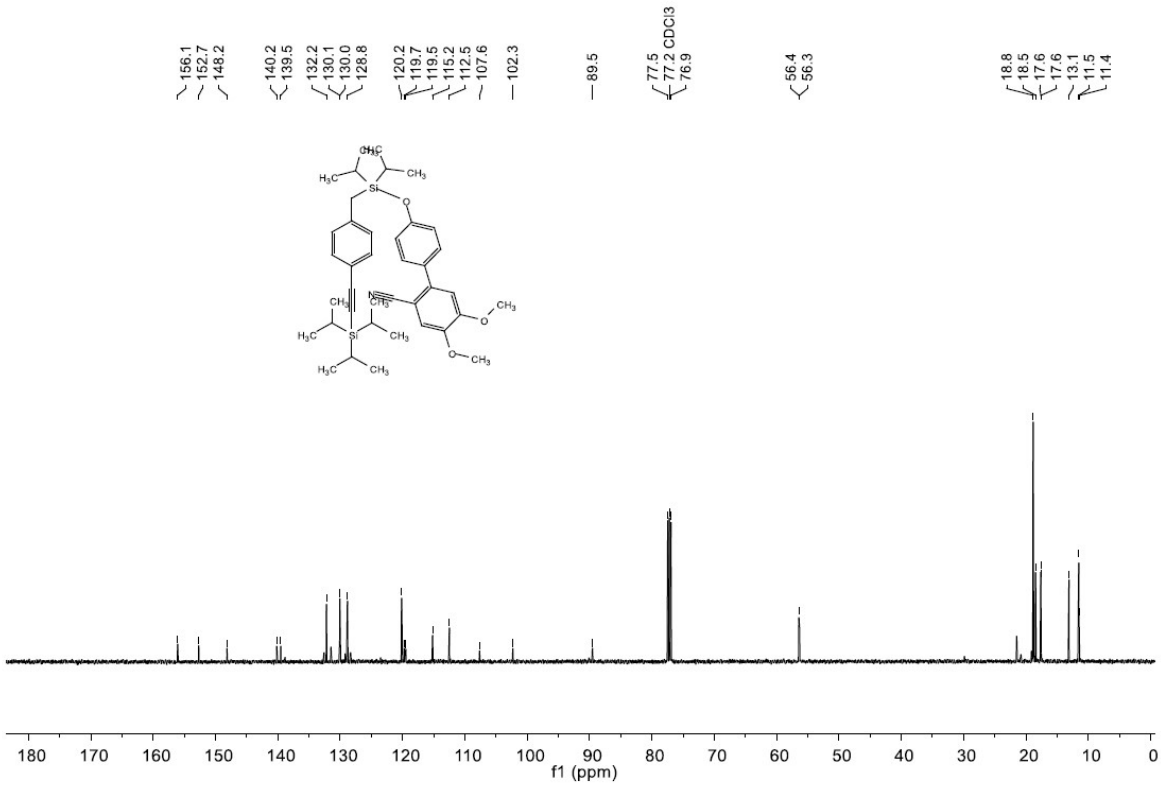
156.1
152.7
148.2
140.2
139.5
132.2
130.1
130.0
128.8
120.2
119.7
119.5
115.2
112.5
107.6
102.3
89.5
77.5
77.2 CDCl3
76.9
56.4
56.3
18.8
18.5
17.6
17.6
13.1
11.5
11.4
f1 (ppm)

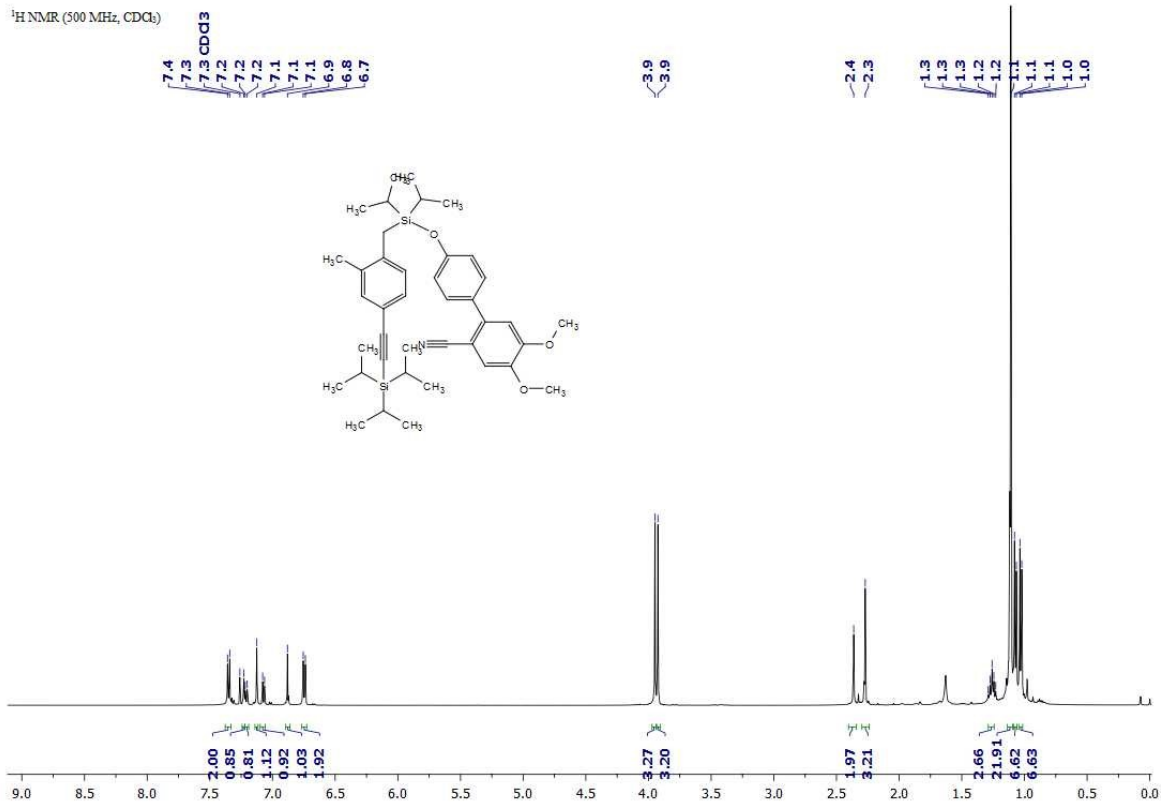
^{1}H NMR (500 MHz, CDCl$_3$)
7.4
7.3
7.3 CDCl3
7.2
7.2
7.2
7.1
7.1
7.1
6.9
6.8
6.7
3.9
3.9
2.4
2.3
1.3
1.3
1.3
1.2
1.2
1.1
1.1
1.1
1.0
1.0
2.00
0.85
0.81
1.12
0.92
1.03
1.92
3.27
3.20
1.97
3.21
2.66
21.91
6.62
6.63
9.0
8.5
8.0
7.5
7.0
6.5
6.0
5.5
5.0
4.5
4.0
3.5
3.0
2.5
2.0
1.5
1.0
0.5
0.0

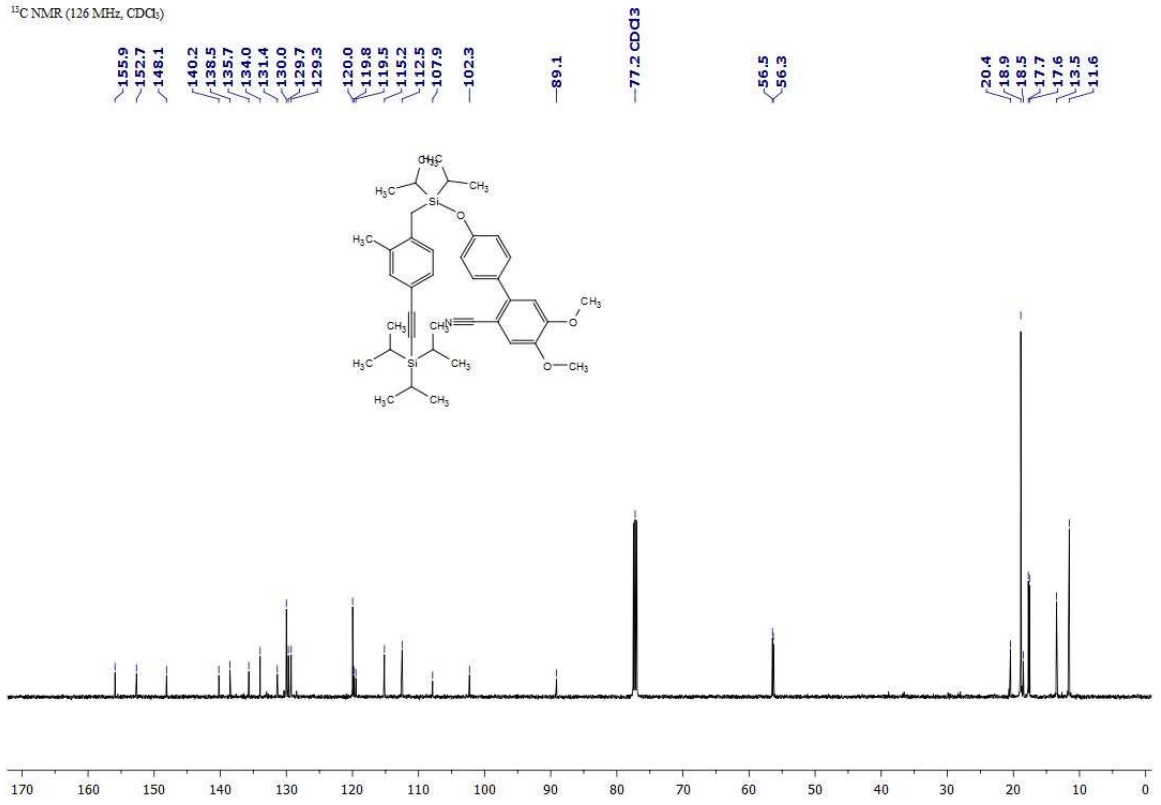
^{13}C NMR (126 MHz, CDCl$_3$)
155.9
152.7
148.1
140.2
138.5
135.7
134.0
131.4
130.0
129.7
129.3
120.0
119.8
119.5
115.2
112.5
107.9
102.3
89.1
77.2 CDCl3
56.5
56.3
20.4
18.9
18.5
17.7
17.6
13.5
11.6
170
160
150
140
130
120
110
100
90
80
70
60
50
40
30
20
10
0

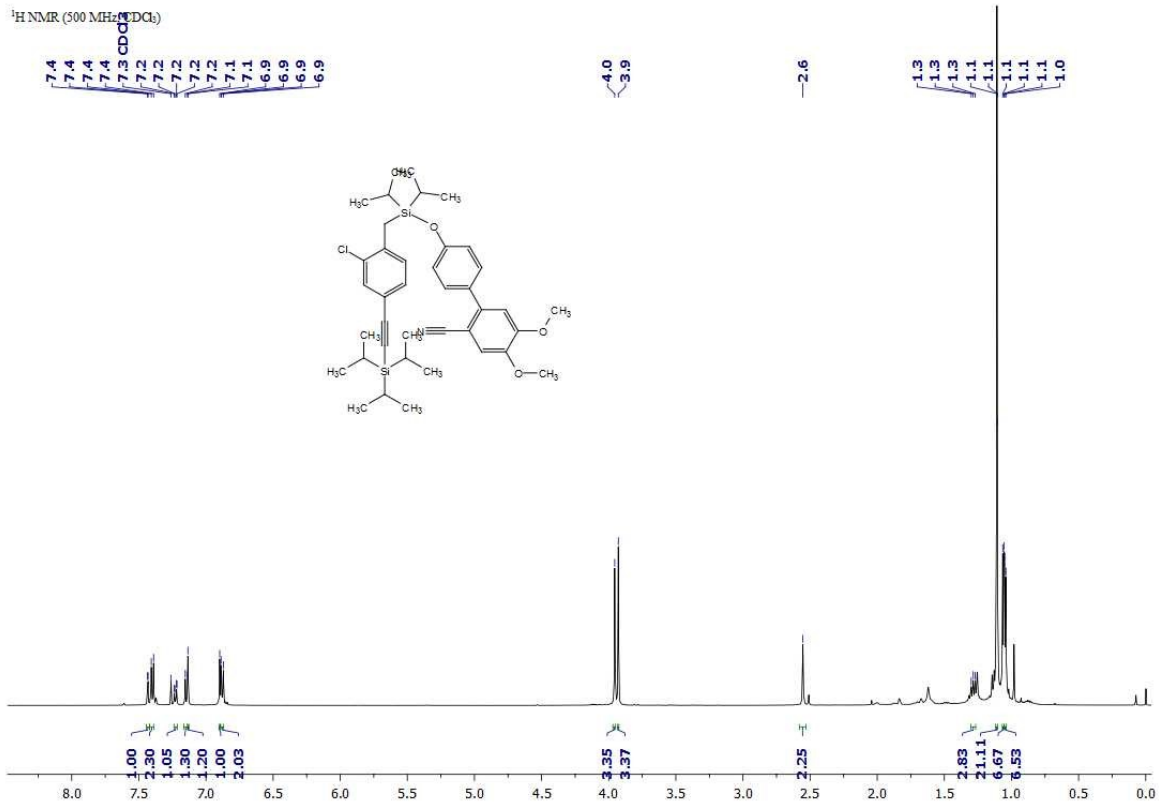
1H NMR (500 MHz, CDCl3)
7.4
7.4
7.4
7.4
7.3 CDCl3
7.2
7.2
7.2
7.2
7.2
7.1
7.1
6.9
6.9
6.9
6.9
4.0
3.9
2.6
1.3
1.3
1.3
1.1
1.1
1.1
1.1
1.0
1.00
2.30
1.05
1.30
1.20
1.00
2.03
3.35
3.37
2.25
2.83
21.11
6.67
6.53
8.0
7.5
7.0
6.5
6.0
5.5
5.0
4.5
4.0
3.5
3.0
2.5
2.0
1.5
1.0
0.5
0.0

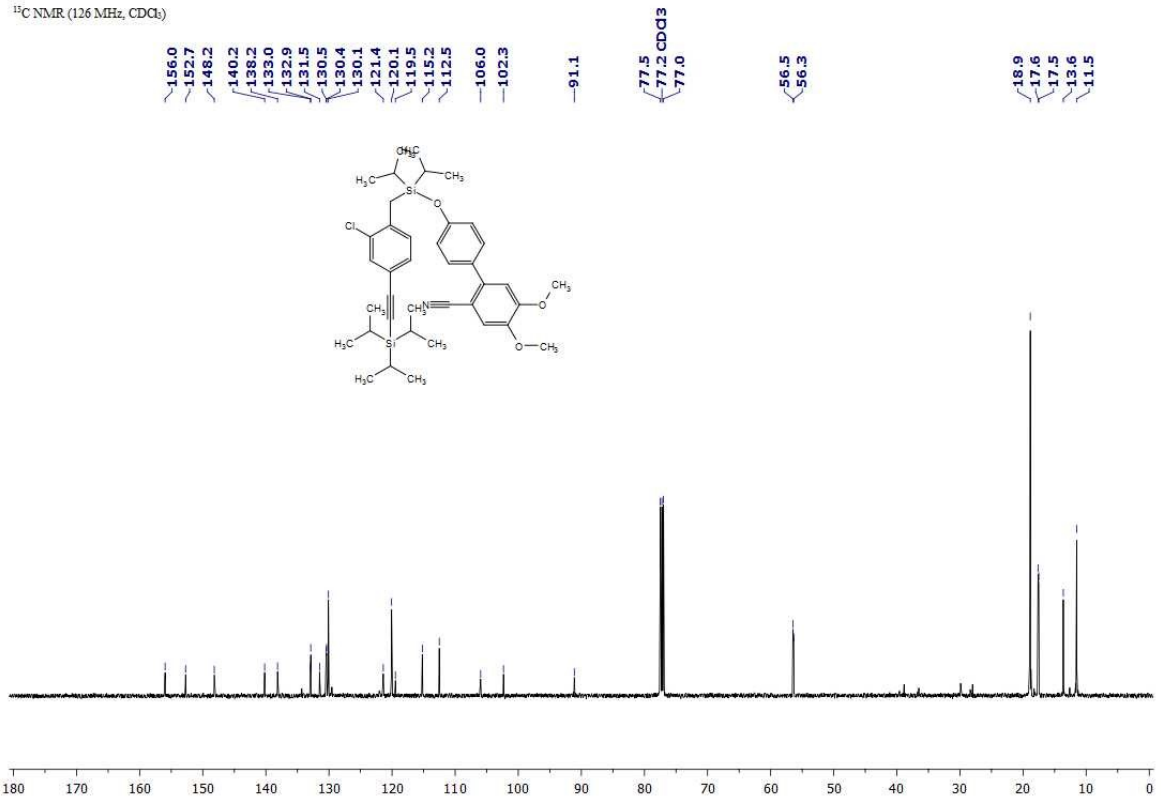
13C NMR (126 MHz, CDCl3)
156.0
152.7
148.2
140.2
138.2
133.0
132.9
131.5
130.5
130.4
130.1
121.4
120.1
119.5
115.2
112.5
106.0
102.3
91.1
77.5
77.2 CDCl3
77.0
56.5
56.3
18.9
17.6
17.5
13.6
11.5
180
170
160
150
140
130
120
110
100
90
80
70
60
50
40
30
20
10
0

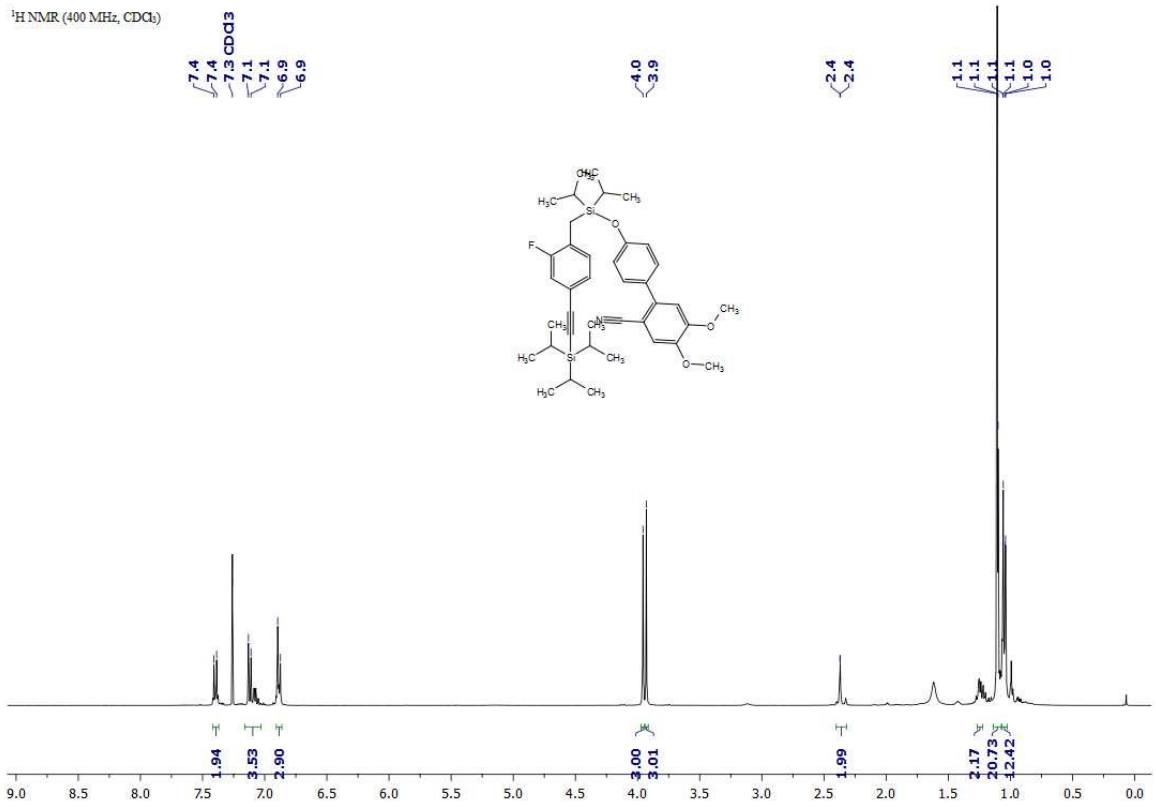
^{1}H NMR (400 MHz, CDCl$_3$)
7.4
7.4
7.3 CDCl3
7.1
7.1
6.9
6.9
4.0
3.9
2.4
2.4
1.1
1.1
1.1
1.1
1.0
1.0
1.94
3.53
2.90
3.00
3.01
1.99
2.17
20.73
12.42
9.0
8.5
8.0
7.5
7.0
6.5
6.0
5.5
5.0
4.5
4.0
3.5
3.0
2.5
2.0
1.5
1.0
0.5
0.0

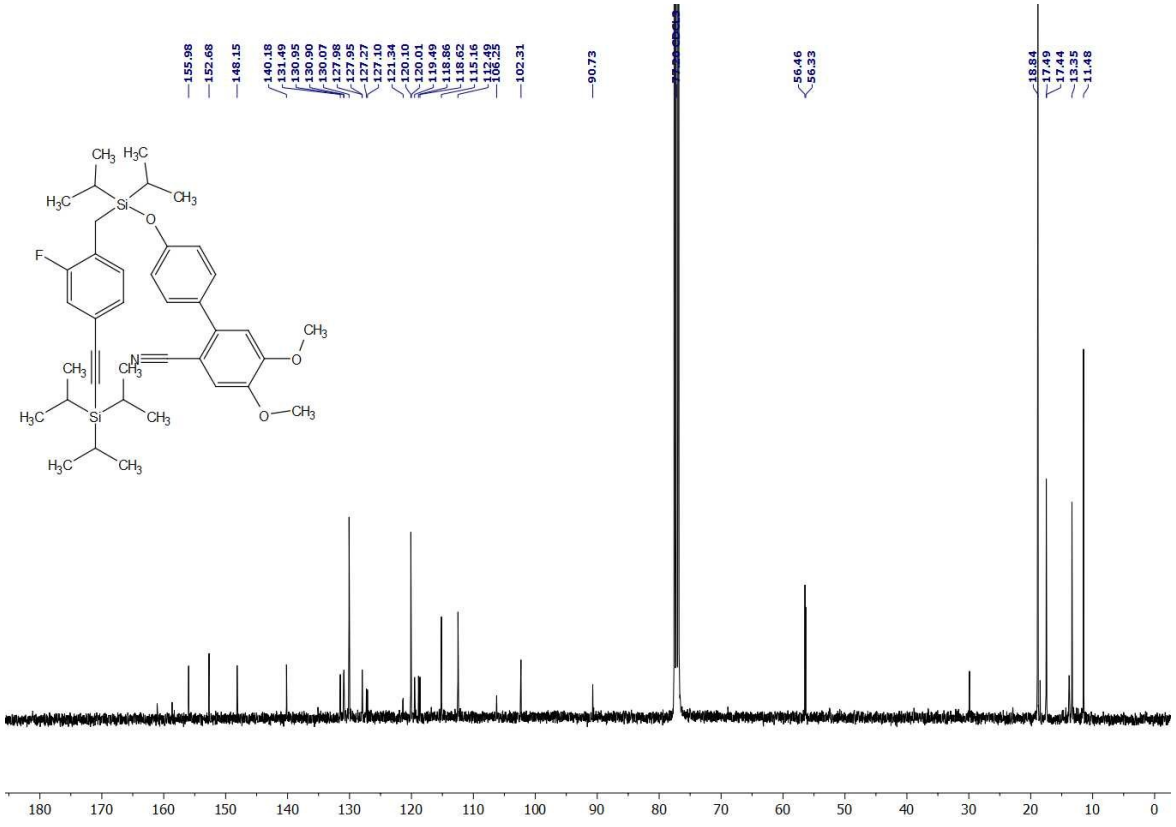
155.98
152.68
148.15
140.18
131.49
130.95
130.90
130.07
127.98
127.95
127.27
127.10
121.34
120.10
120.01
119.49
118.86
118.62
115.16
102.31
90.73
56.46
56.33
18.84
17.49
17.44
13.35
11.48
180
170
160
150
140
130
120
110
100
90
80
70
60
50
40
30
20
10
0

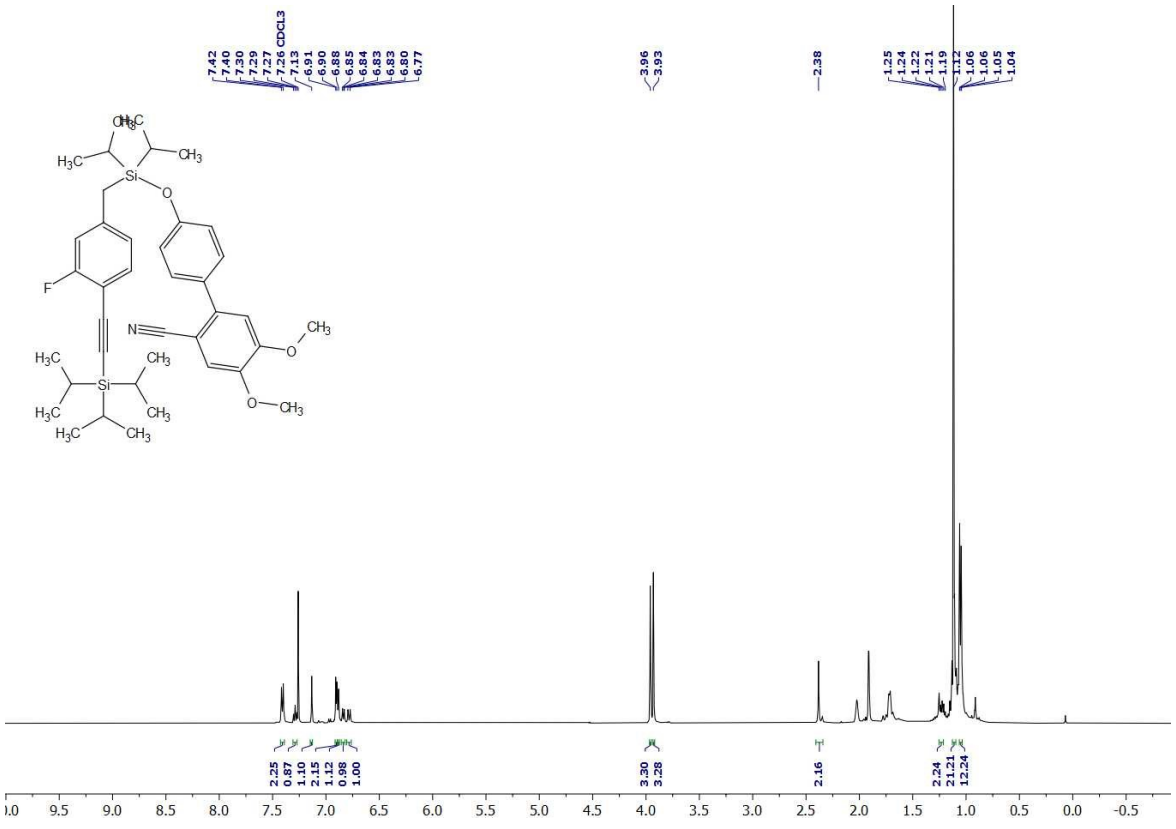
7.42
7.40
7.30
7.29
7.27
7.26 CDCL3
7.13
6.91
6.90
6.88
6.85
6.84
6.83
6.83
6.80
6.77
3.96
3.93
2.38
1.25
1.24
1.22
1.21
1.19
1.12
1.06
1.06
1.05
1.04
2.25
0.87
1.10
2.15
1.12
0.98
1.00
3.30
3.28
2.16
2.24
21.21
12.24

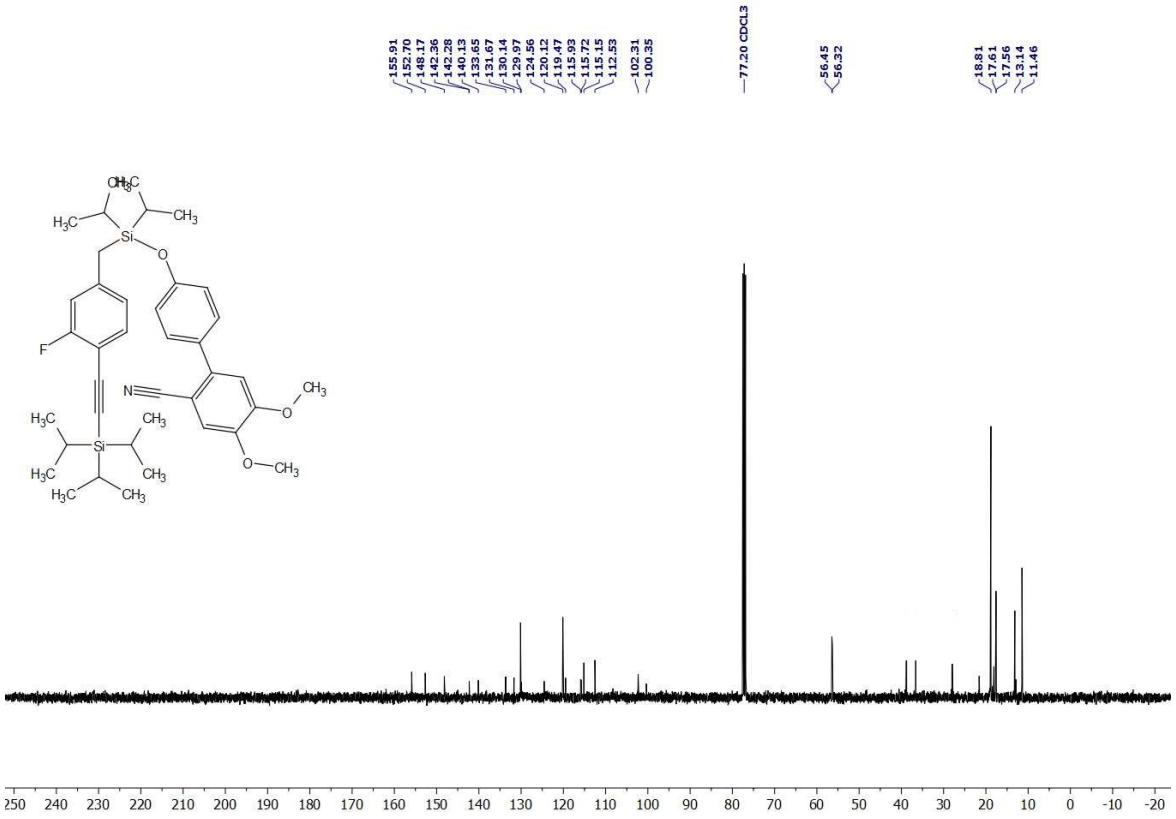
155.91
152.70
148.17
142.36
142.28
140.13
133.65
131.67
130.14
129.97
124.56
120.12
119.47
115.93
115.72
115.15
112.53
102.31
100.35
77.20 CDCL3
56.45
56.32
18.81
17.61
17.56
13.14
11.46

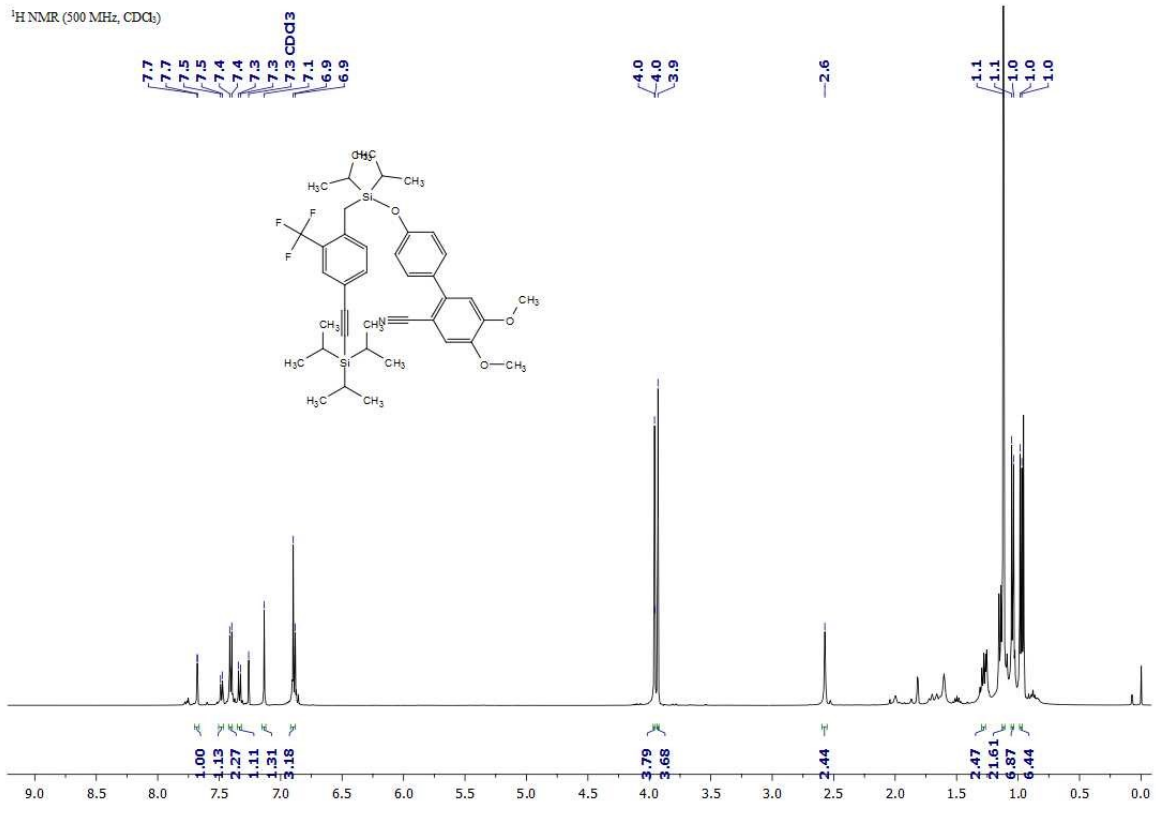
^{1}H NMR (500 MHz, CDCl$_3$)
7.7
7.7
7.5
7.5
7.4
7.4
7.3
7.3
7.3 CDCl3
7.1
6.9
6.9
4.0
4.0
3.9
2.6
1.1
1.1
1.0
1.0
1.0
1.00
1.13
2.27
1.11
1.31
3.18
3.79
3.68
2.44
2.47
21.61
6.87
6.44
9.0
8.5
8.0
7.5
7.0
6.5
6.0
5.5
5.0
4.5
4.0
3.5
3.0
2.5
2.0
1.5
1.0
0.5
0.0

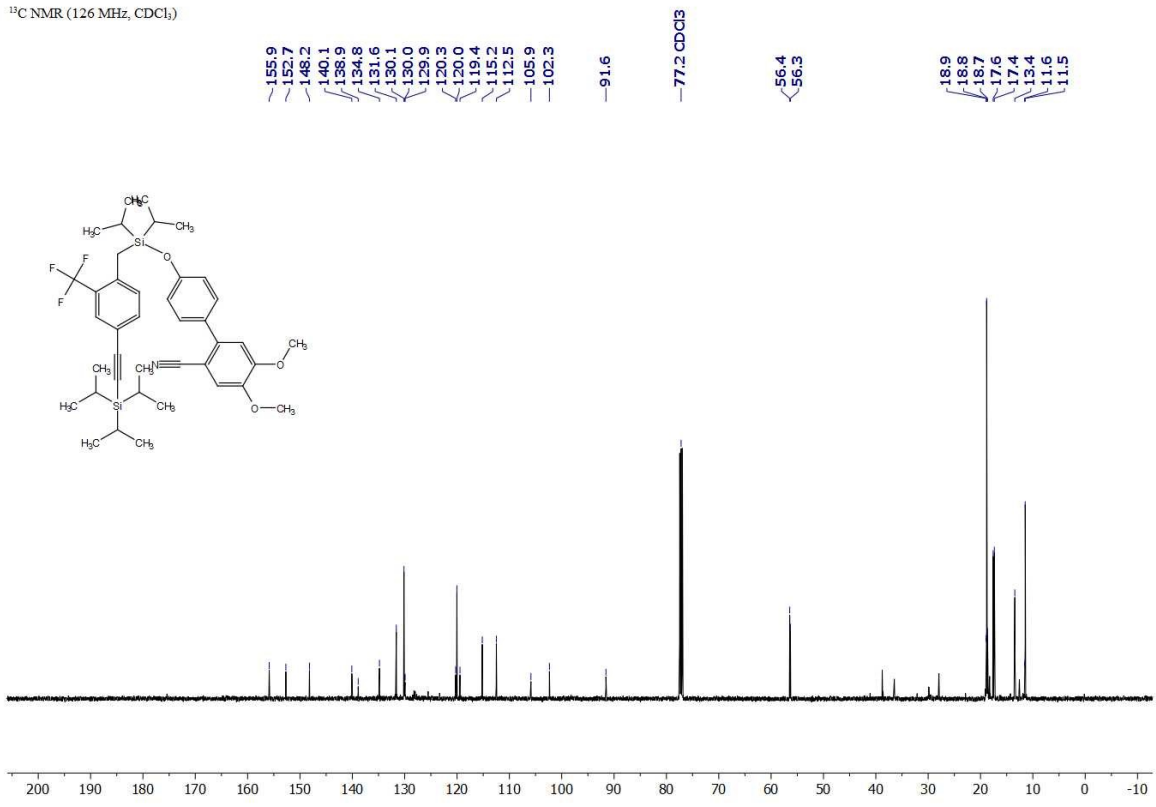
^{13}C NMR (126 MHz, CDCl$_3$)
155.9
152.7
148.2
140.1
138.9
134.8
131.6
130.1
130.0
129.9
120.3
120.0
119.4
115.2
112.5
105.9
102.3
91.6
77.2 CDCl3
56.4
56.3
18.9
18.8
18.7
17.6
17.4
13.4
11.6
11.5
200
190
180
170
160
150
140
130
120
110
100
90
80
70
60
50
40
30
20
10
0
-10

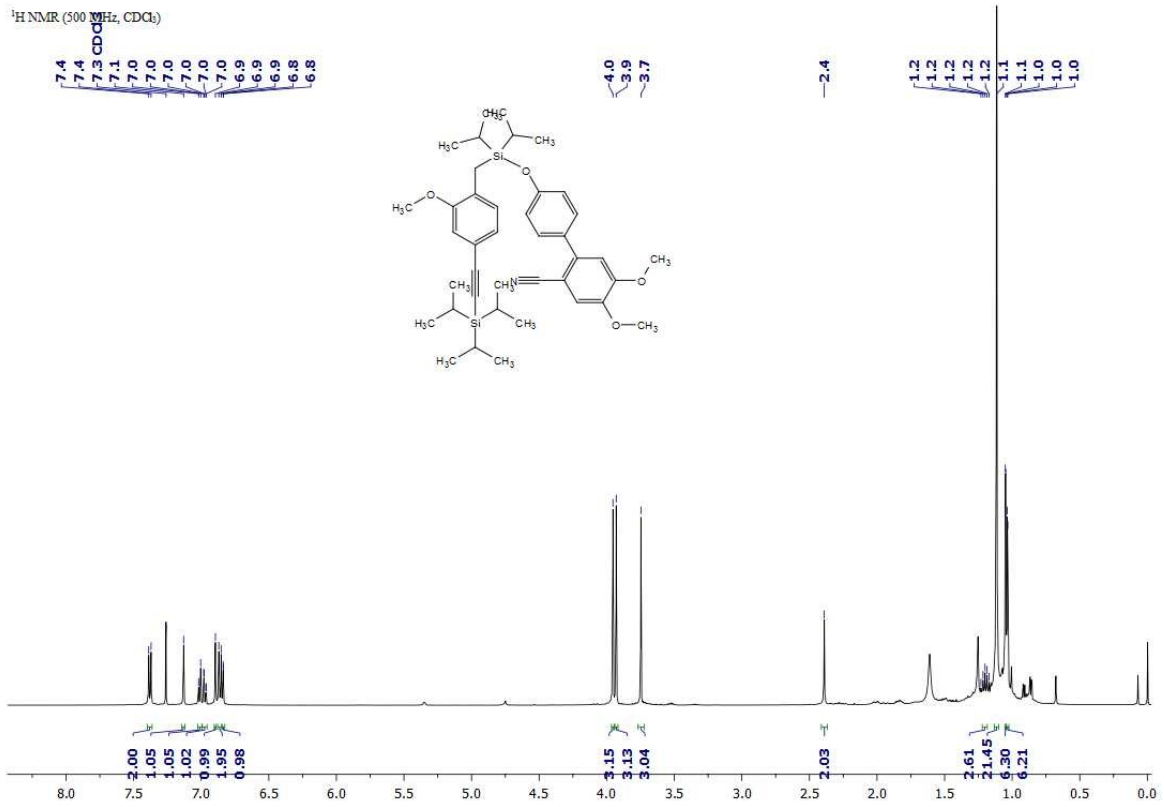
¹H NMR (500 MHz, CDCl₃)
7.4
7.4
7.3 CDCl3
7.1
7.0
7.0
7.0
7.0
7.0
7.0
6.9
6.9
6.9
6.8
6.8
4.0
3.9
3.7
2.4
1.2
1.2
1.2
1.2
1.2
1.1
1.1
1.0
1.0
1.0
2.00
1.05
1.05
1.02
0.99
1.95
0.98
3.15
3.13
3.04
2.03
2.61
21.45
6.30
6.21
8.0
7.5
7.0
6.5
6.0
5.5
5.0
4.5
4.0
3.5
3.0
2.5
2.0
1.5
1.0
0.5
0.0

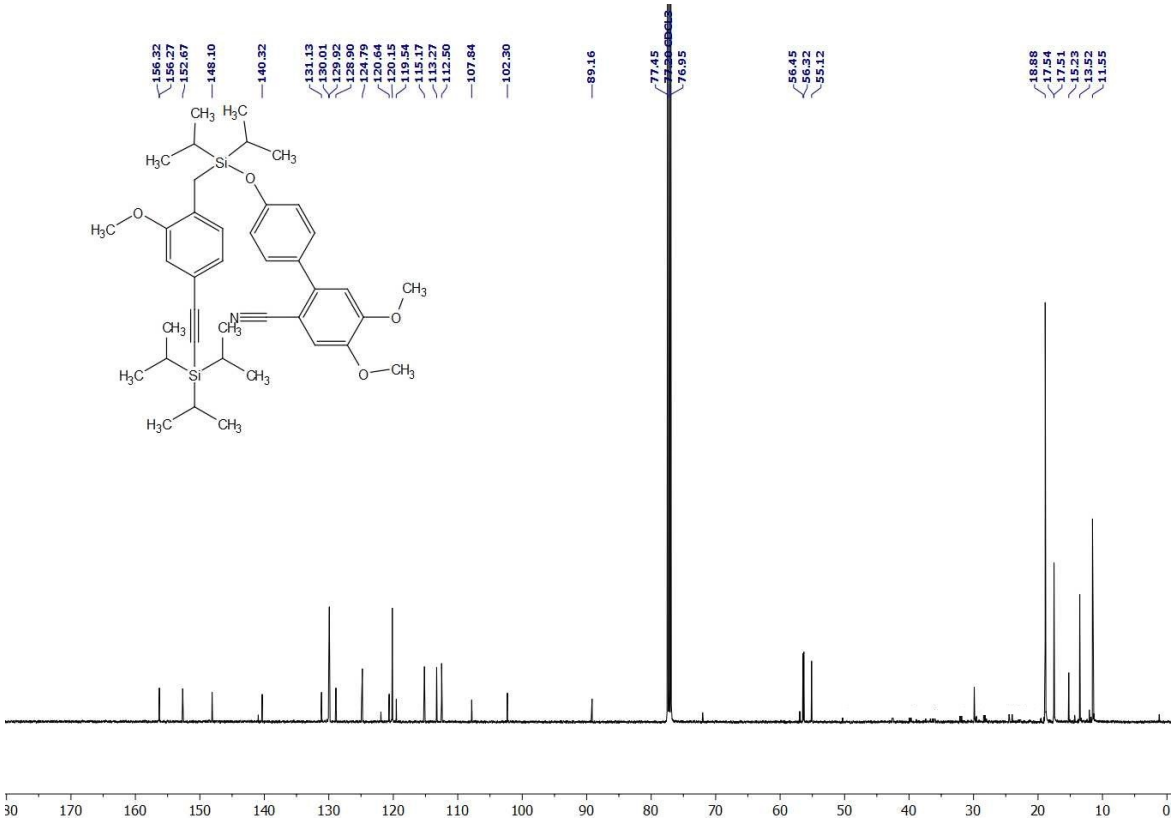
156.32
156.27
152.67
148.10
140.32
131.13
130.01
129.92
128.90
124.79
120.64
120.15
119.54
115.17
113.27
112.50
107.84
102.30
89.16
77.45
76.95
56.45
56.32
55.12
18.88
17.54
17.51
15.23
13.52
11.55
230
220
210
200
190
180
170
160
150
140
130
120
110
100
90
80
70
60
50
40
30
20
10
0

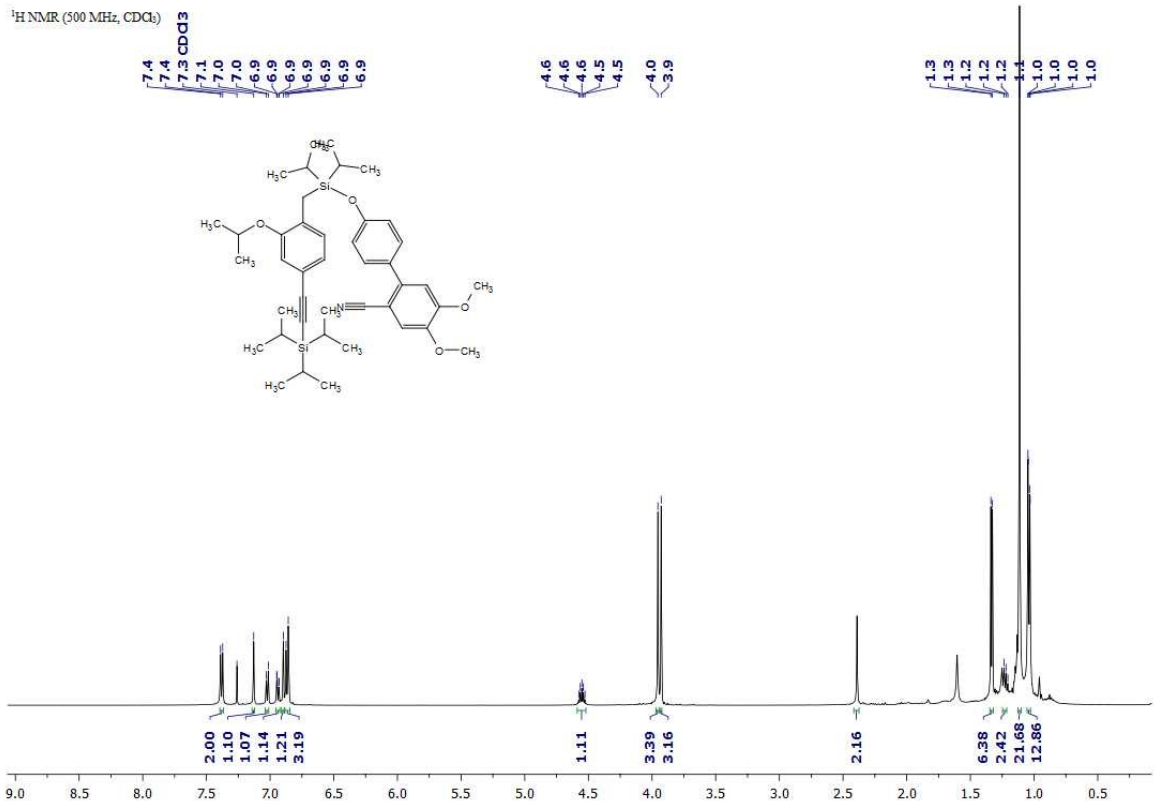
^{1}H NMR (500 MHz, CDCl$_3$)
7.4
7.4
7.3 CDCl3
7.1
7.0
7.0
6.9
6.9
6.9
6.9
6.9
6.9
4.6
4.6
4.6
4.5
4.5
4.0
3.9
1.3
1.3
1.2
1.2
1.2
1.1
1.0
1.0
1.0
1.0
2.00
1.10
1.07
1.14
1.21
3.19
1.11
3.39
3.16
2.16
6.38
2.42
21.68
12.86
9.0
8.5
8.0
7.5
7.0
6.5
6.0
5.5
5.0
4.5
4.0
3.5
3.0
2.5
2.0
1.5
1.0
0.5

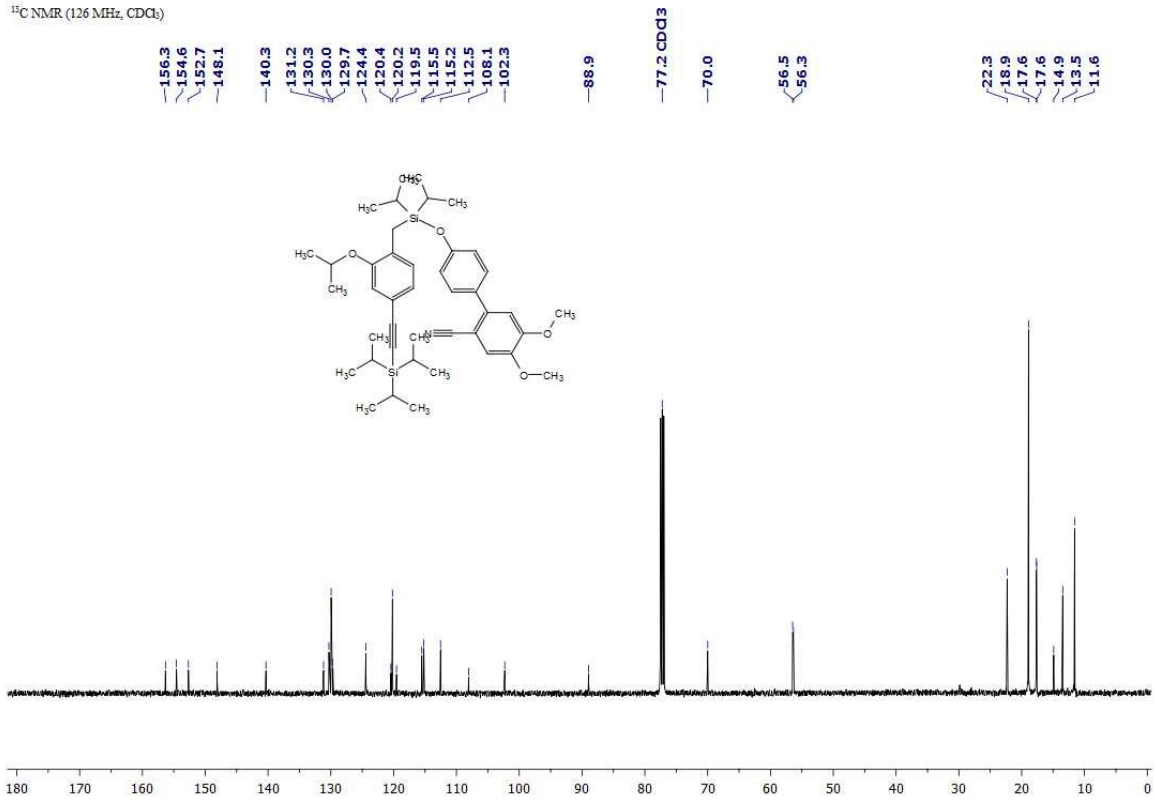
^{13}C NMR (126 MHz, CDCl$_3$)
156.3
154.6
152.7
148.1
140.3
131.2
130.3
130.0
129.7
124.4
120.4
120.2
119.5
115.5
115.2
112.5
108.1
102.3
88.9
77.2 CDCl3
70.0
56.5
56.3
22.3
18.9
17.6
17.6
14.9
13.5
11.6
180
170
160
150
140
130
120
110
100
90
80
70
60
50
40
30
20
10
0

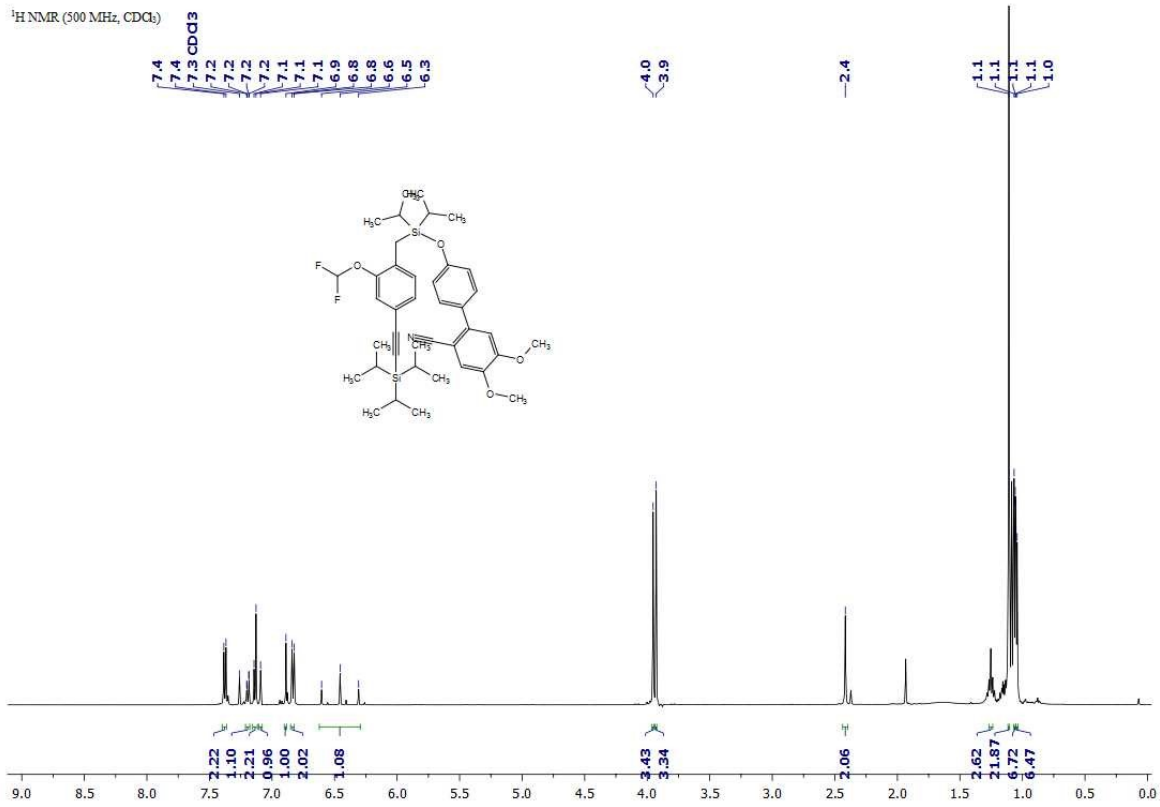
^{1}H NMR (500 MHz, CDCl$_3$)
7.4
7.4
7.3 CDCl3
7.2
7.2
7.2
7.2
7.1
7.1
7.1
6.9
6.8
6.8
6.6
6.5
6.3
4.0
3.9
2.4
1.1
1.1
1.1
1.0
2.22
1.10
2.21
0.96
1.00
2.02
1.08
3.43
3.34
2.06
2.62
21.87
6.72
6.47

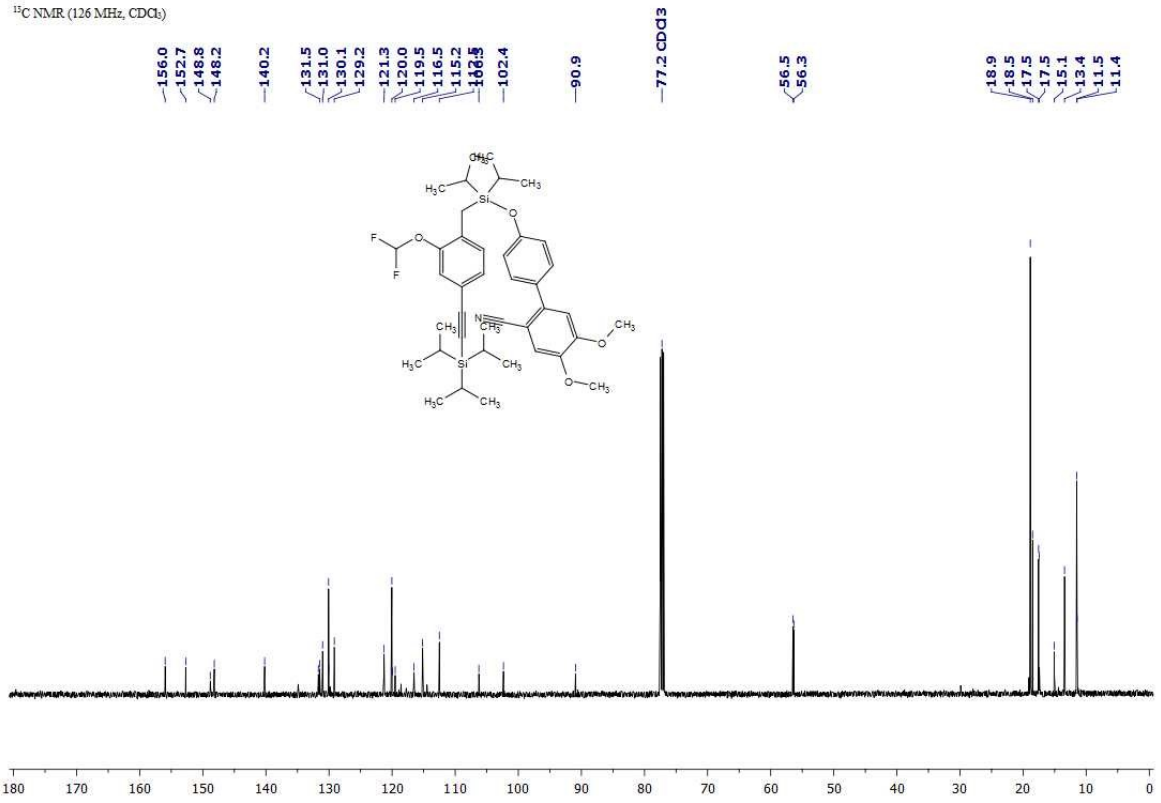
^{13}C NMR (126 MHz, CDCl$_3$)
156.0
152.7
148.8
148.2
140.2
131.5
131.0
130.1
129.2
121.3
120.0
119.5
116.5
115.2
102.4
90.9
77.2 CDCl3
56.5
56.3
18.9
18.5
17.5
17.5
15.1
13.4
11.5
11.4

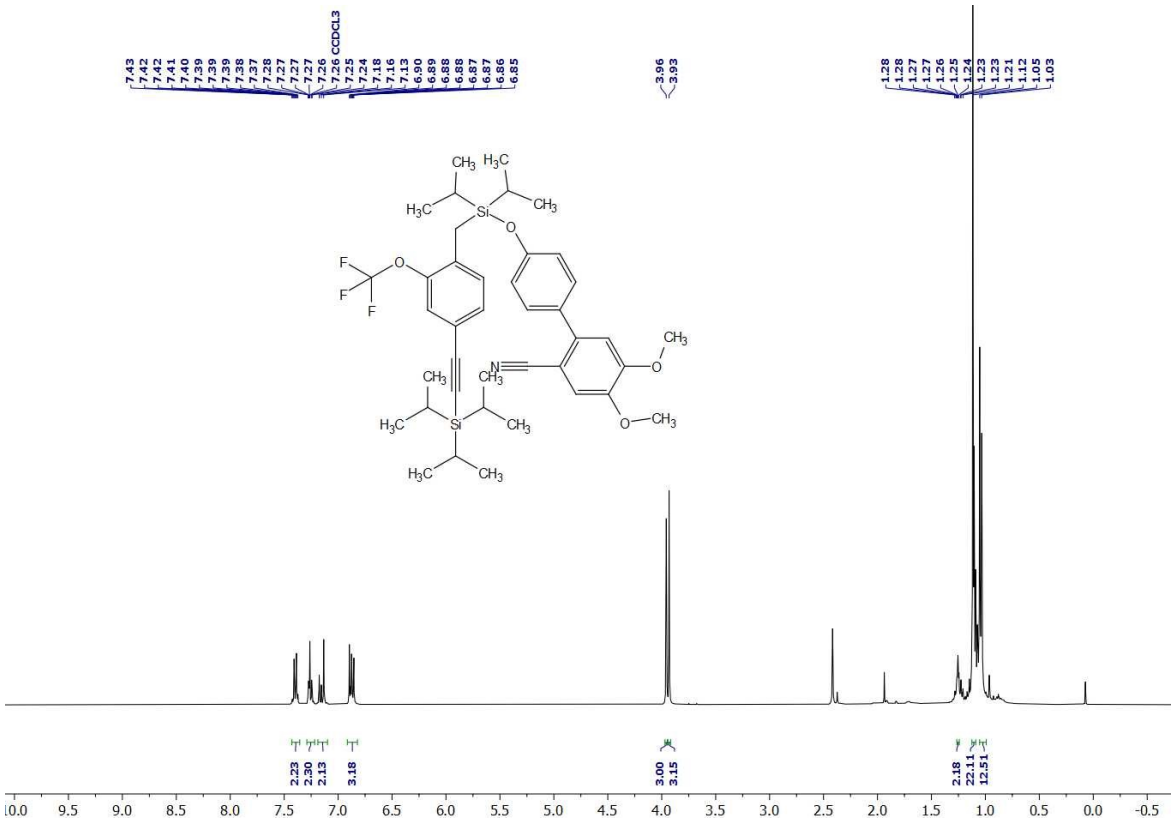

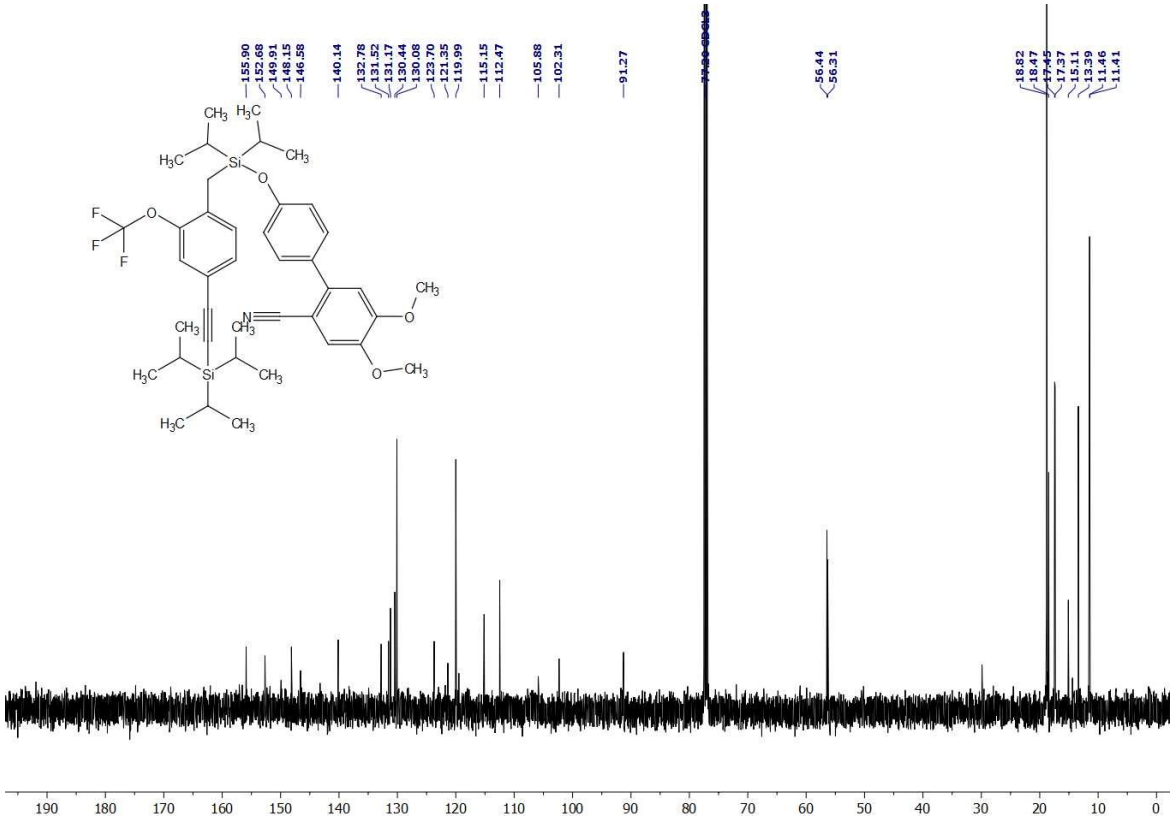

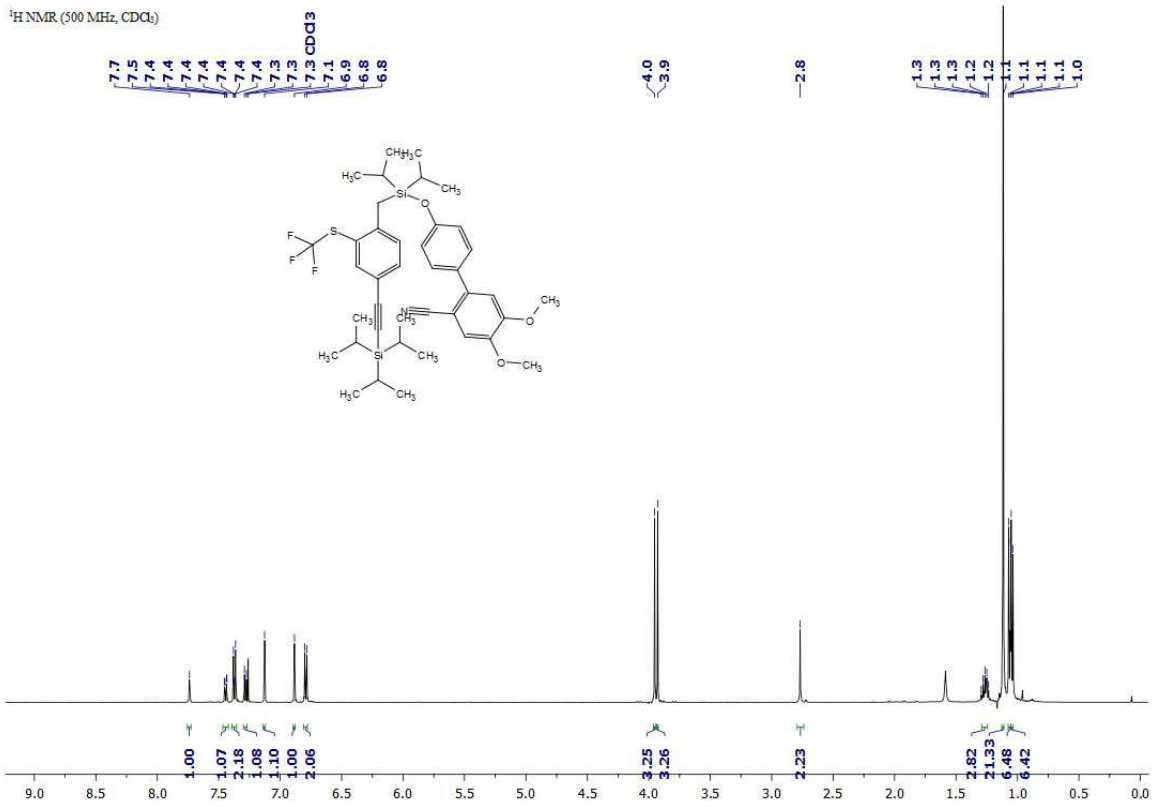
^{1}H NMR (500 MHz, CDCl$_3$)
7.7
7.5
7.4
7.4
7.4
7.4
7.4
7.4
7.3
7.3
7.3 CDCl3
7.1
6.9
6.8
6.8
4.0
3.9
2.8
1.3
1.3
1.3
1.2
1.2
1.1
1.1
1.1
1.1
1.0
1.00
1.07
2.18
1.08
1.10
1.00
2.06
3.25
3.26
2.23
2.82
21.33
6.48
6.42
9.0
8.5
8.0
7.5
7.0
6.5
6.0
5.5
5.0
4.5
4.0
3.5
3.0
2.5
2.0
1.5
1.0
0.5
0.0

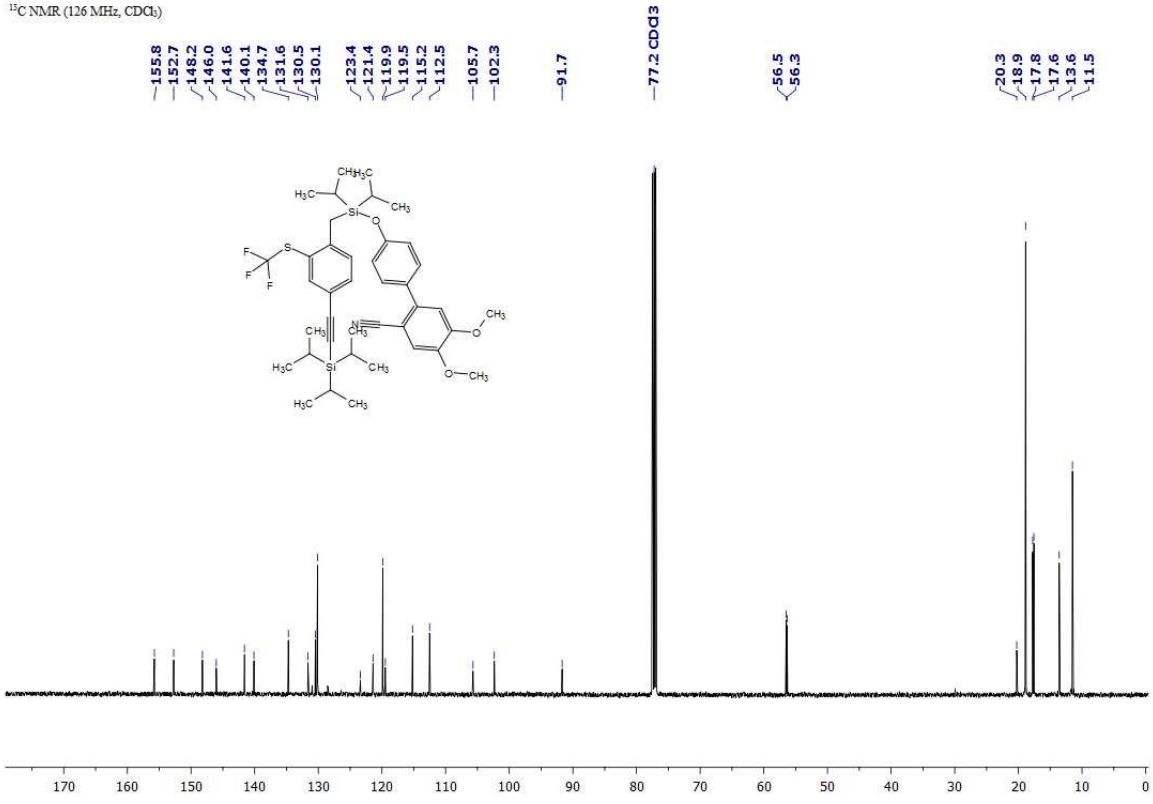
^{13}C NMR (126 MHz, CDCl$_3$)
155.8
152.7
148.2
146.0
141.6
140.1
134.7
131.6
130.5
130.1
123.4
121.4
119.9
119.5
115.2
112.5
105.7
102.3
91.7
77.2 CDCl3
56.5
56.3
20.3
18.9
17.8
17.6
13.6
11.5
170
160
150
140
130
120
110
100
90
80
70
60
50
40
30
20
10
0

^{1}H NMR (400 MHz, $CDCl_3$)

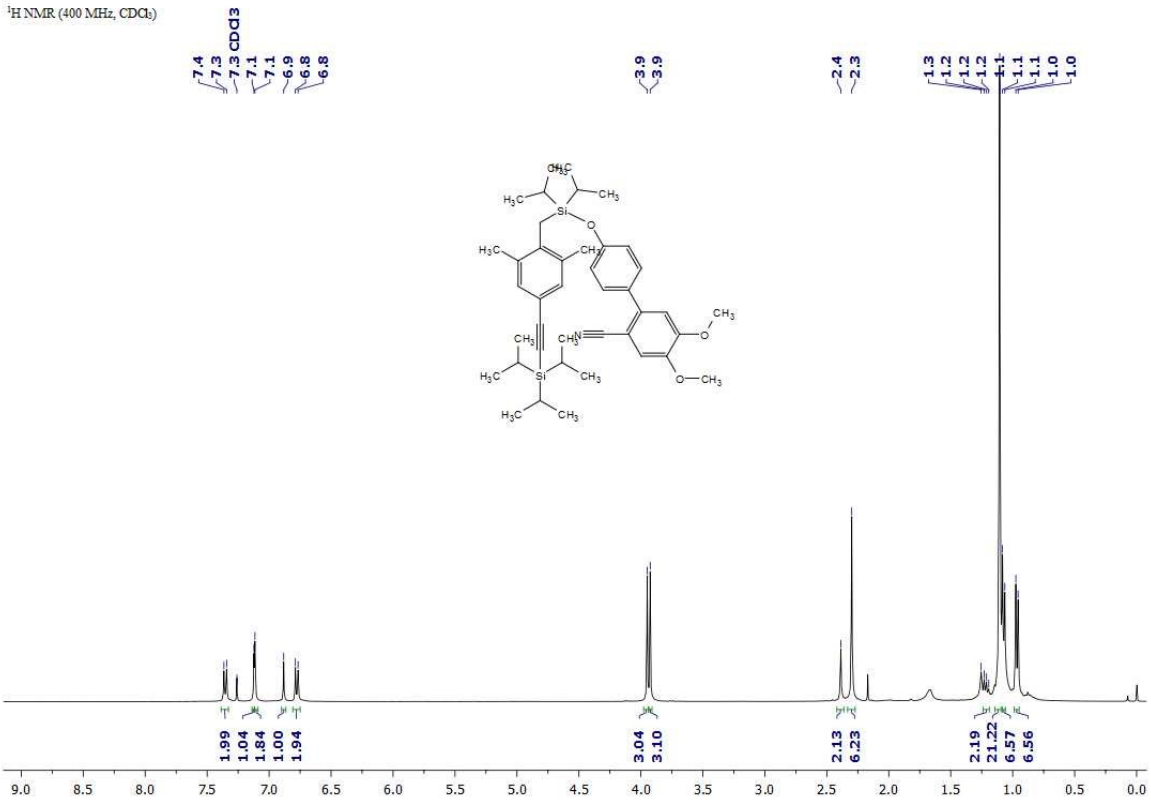

^{13}C NMR (101 MHz, $CDCl_3$)

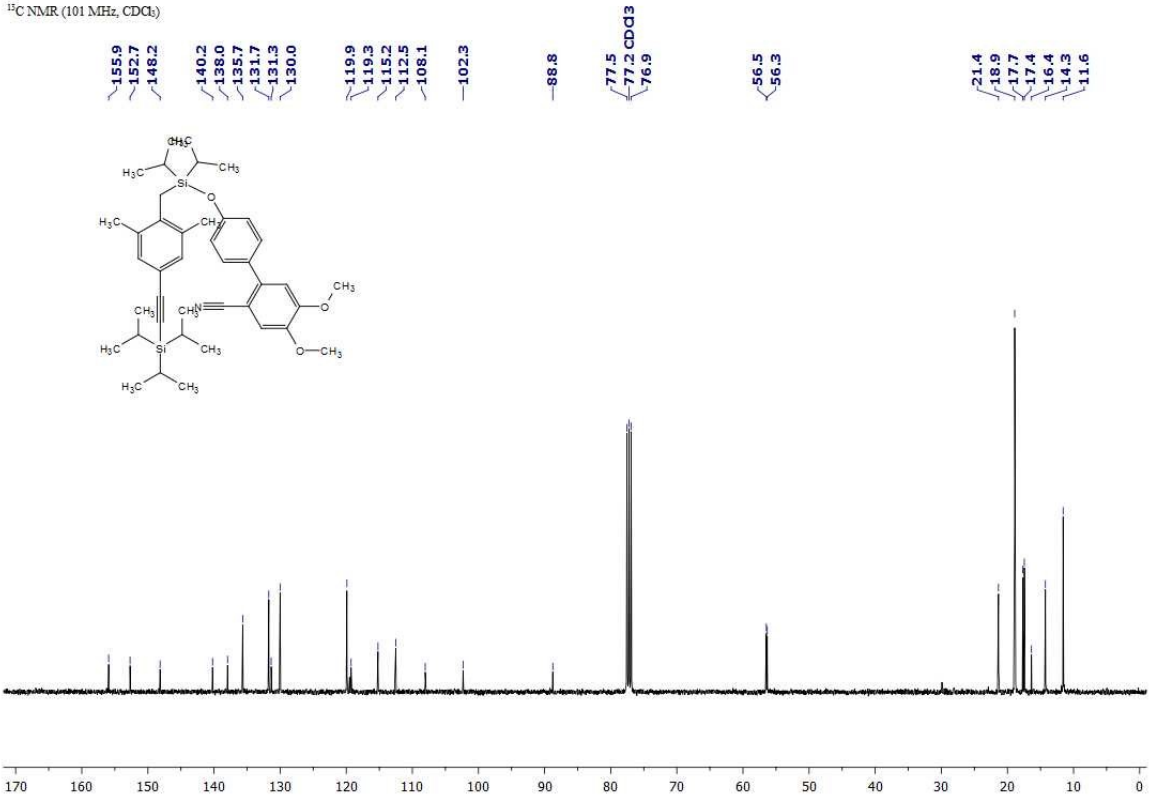

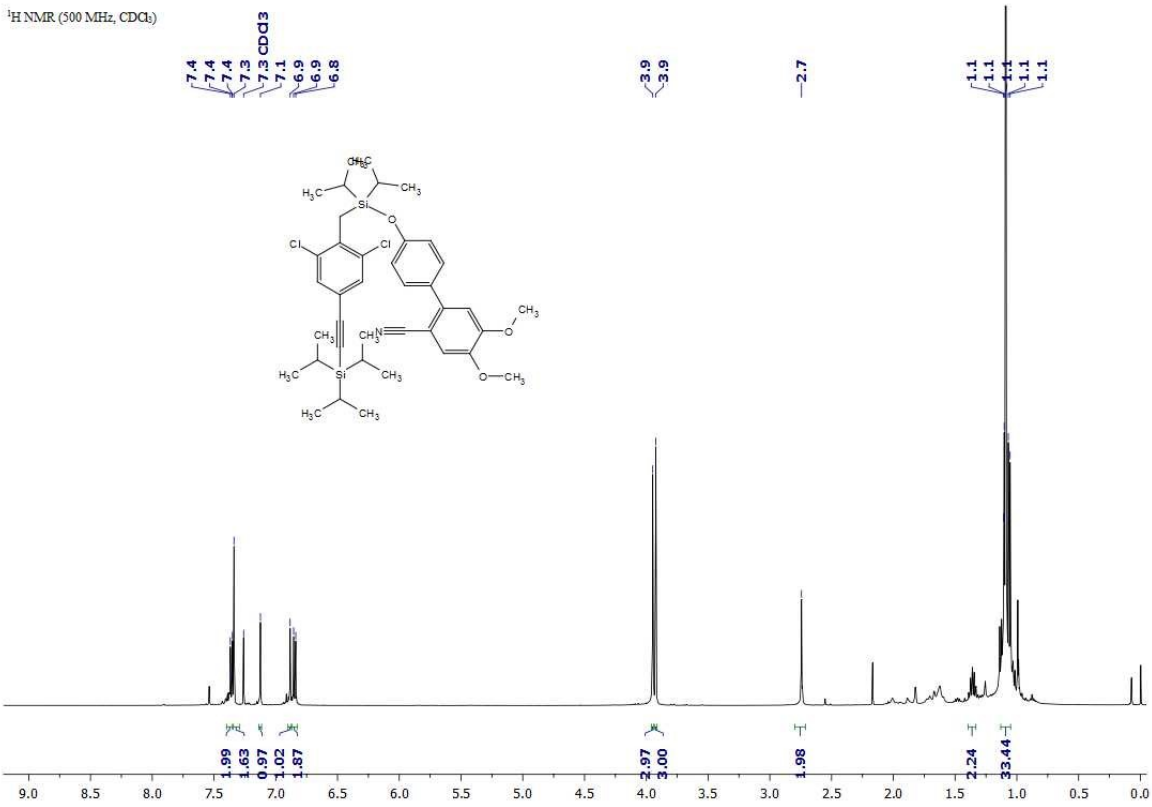
^{1}H NMR (500 MHz, CDCl$_3$)
7.4
7.4
7.4
7.3
7.3 CDCl3
7.1
6.9
6.9
6.8
3.9
3.9
2.7
1.1
1.1
1.1
1.1
1.1
1.99
1.63
0.97
1.02
1.87
2.97
3.00
1.98
2.24
33.44

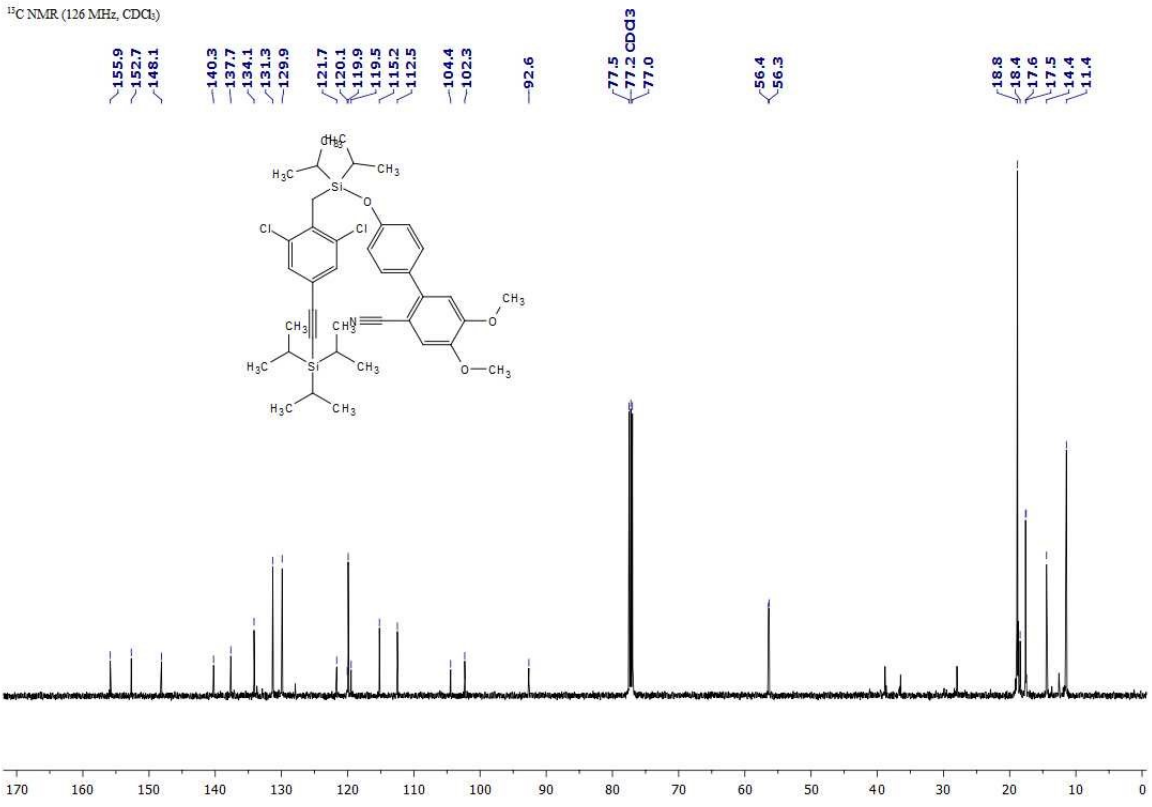
^{13}C NMR (126 MHz, CDCl$_3$)
155.9
152.7
148.1
140.3
137.7
134.1
131.3
129.9
121.7
120.1
119.9
119.5
115.2
112.5
104.4
102.3
92.6
77.5
77.2 CDCl3
77.0
56.4
56.3
18.8
18.4
17.6
17.5
14.4
11.4

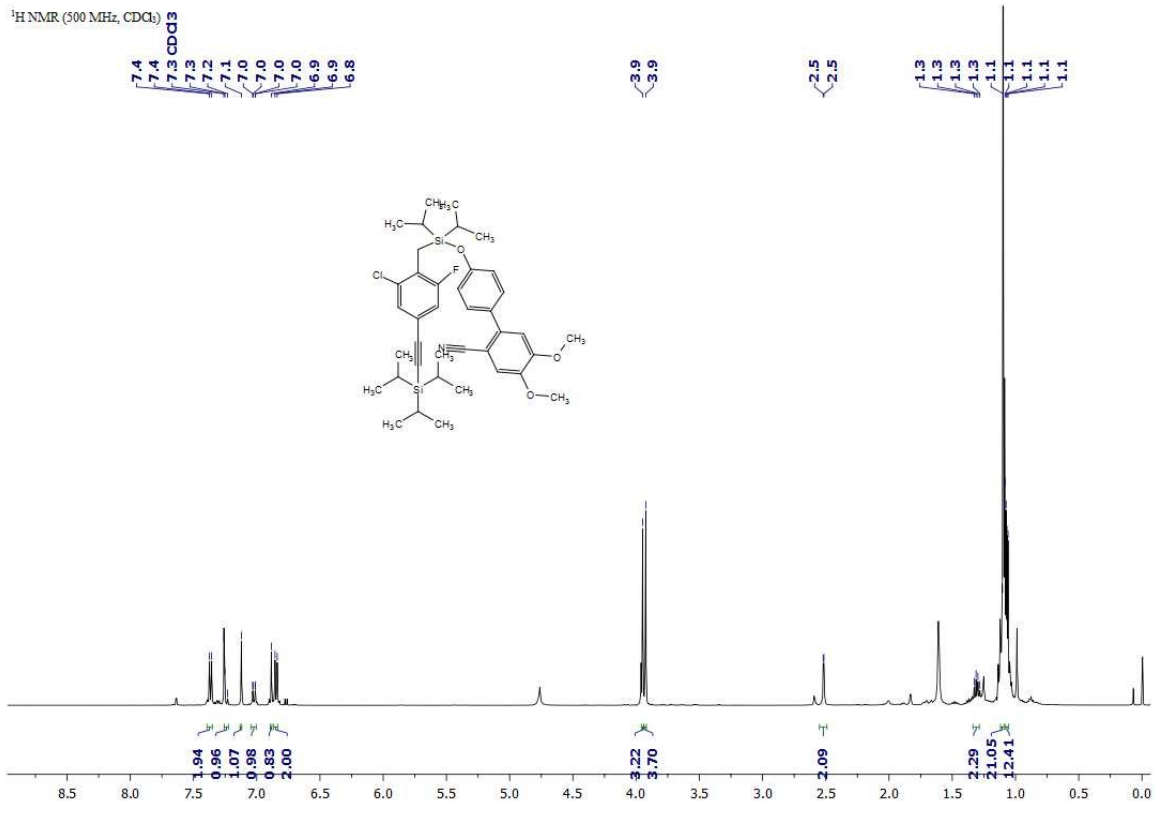
1H NMR (500 MHz, CDCl3)
7.4
7.4
7.3 CDCl3
7.3
7.2
7.1
7.0
7.0
7.0
7.0
6.9
6.9
6.8
3.9
3.9
2.5
2.5
1.3
1.3
1.3
1.3
1.1
1.1
1.1
1.1
1.1
1.94
0.96
1.07
0.98
0.83
2.00
3.22
3.70
2.09
2.29
21.05
12.41
8.5
8.0
7.5
7.0
6.5
6.0
5.5
5.0
4.5
4.0
3.5
3.0
2.5
2.0
1.5
1.0
0.5
0.0

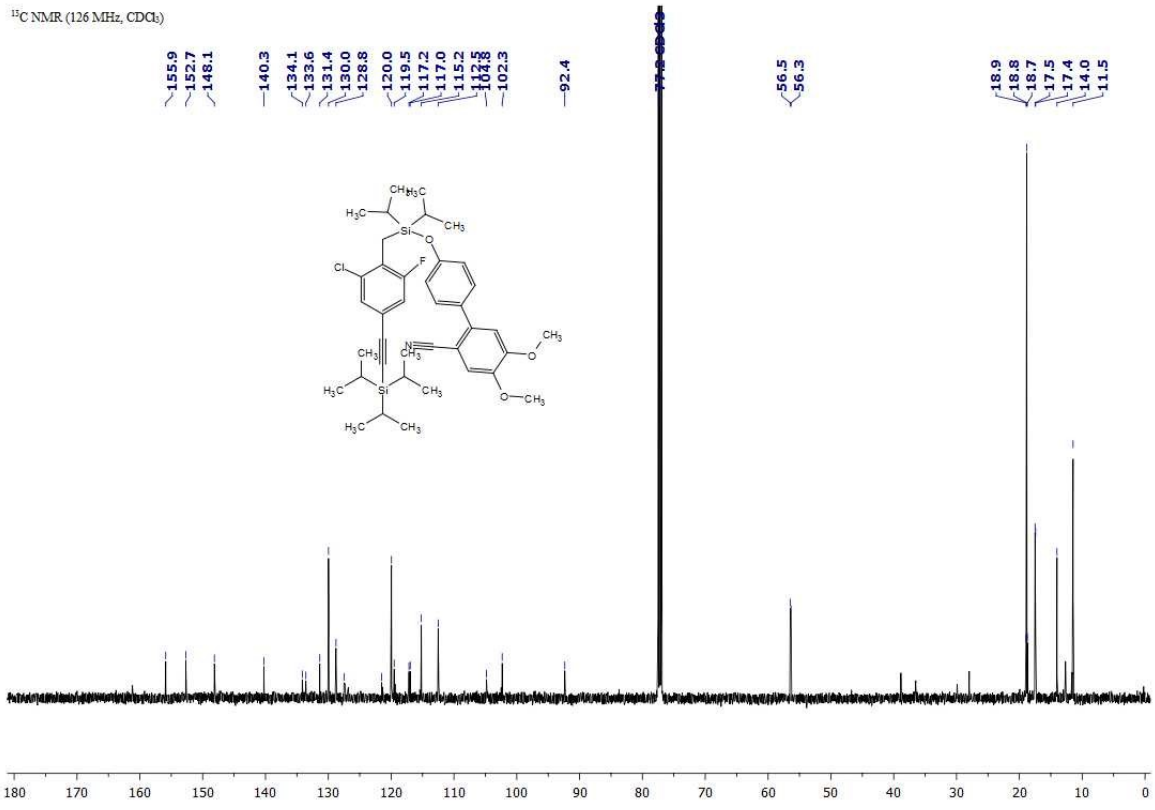
13C NMR (126 MHz, CDCl3)
155.9
152.7
148.1
140.3
134.1
133.6
131.4
130.0
128.8
120.0
119.5
117.2
117.0
115.2
112.5
104.8
102.3
92.4
77.0
56.5
56.3
18.9
18.8
18.7
17.5
17.4
14.0
11.5
180
170
160
150
140
130
120
110
100
90
80
70
60
50
40
30
20
10
0

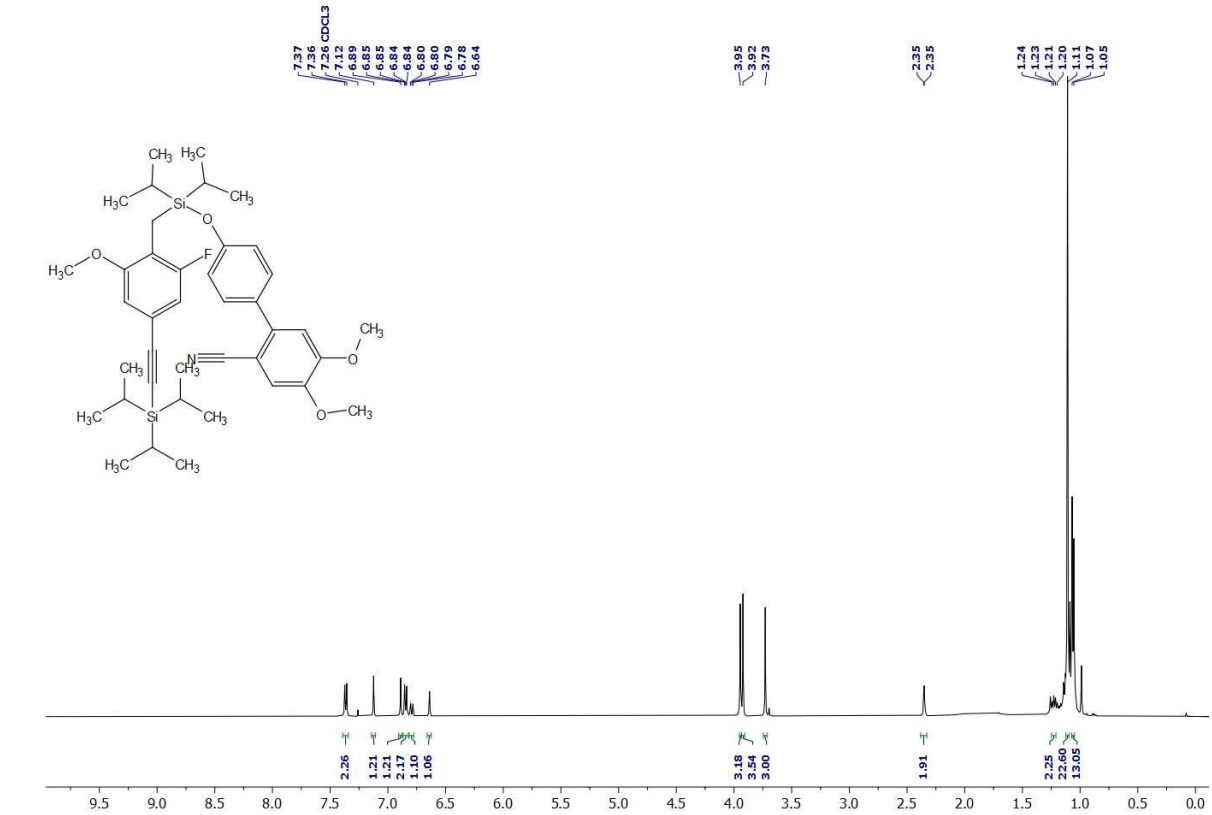

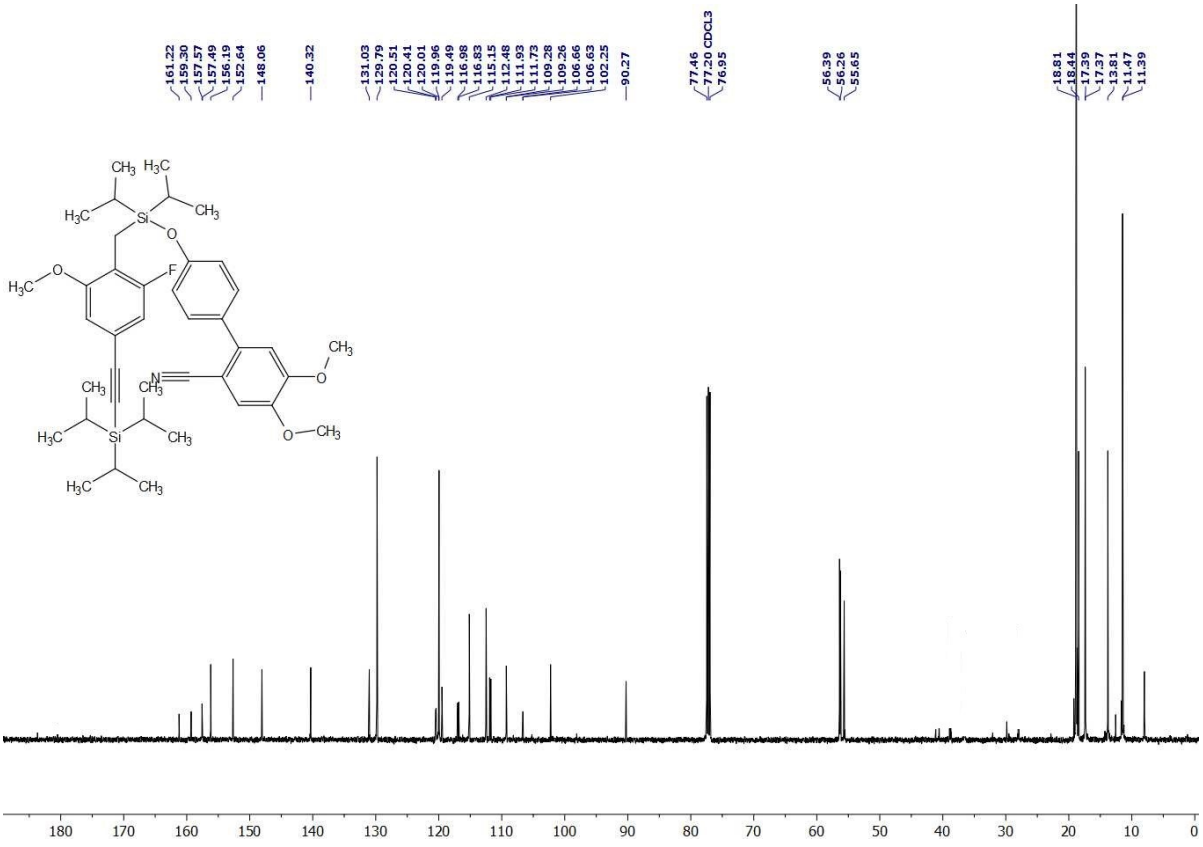

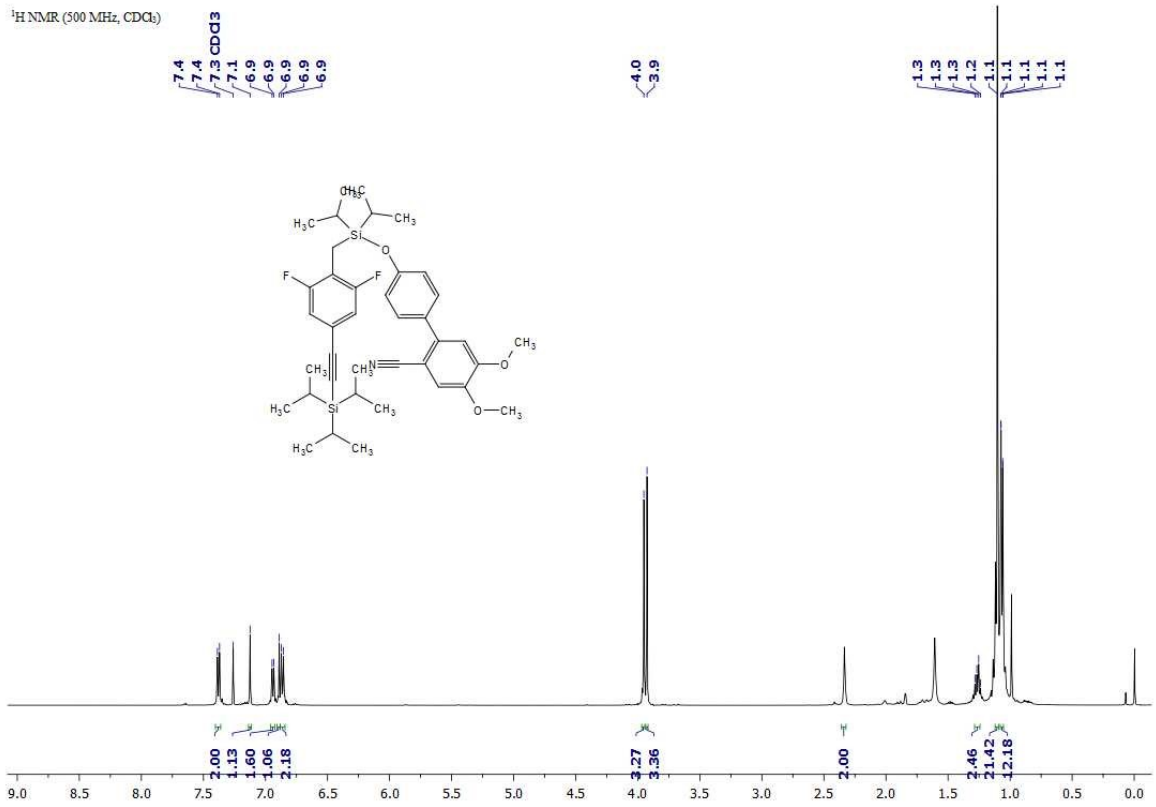
^{1}H NMR (500 MHz, CDCl$_3$)
7.4
7.4
7.3 CDCl3
7.1
6.9
6.9
6.9
6.9
6.9
4.0
3.9
1.3
1.3
1.3
1.2
1.1
1.1
1.1
1.1
1.1
2.00
1.13
1.60
1.06
2.18
3.27
3.36
2.00
2.46
21.42
12.18
9.0
8.5
8.0
7.5
7.0
6.5
6.0
5.5
5.0
4.5
4.0
3.5
3.0
2.5
2.0
1.5
1.0
0.5
0.0

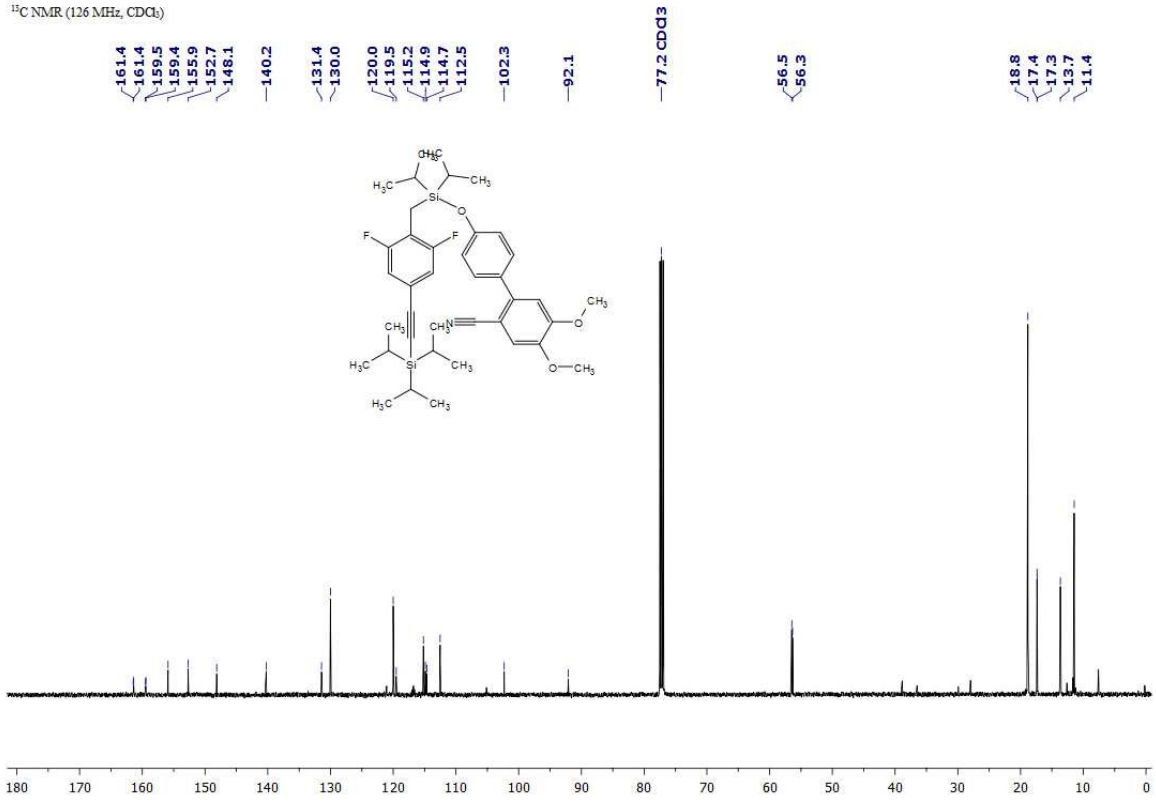
^{13}C NMR (126 MHz, CDCl$_3$)
161.4
161.4
159.5
159.4
155.9
152.7
148.1
140.2
131.4
130.0
120.0
119.5
115.2
114.9
114.7
112.5
102.3
92.1
77.2 CDCl3
56.5
56.3
18.8
17.4
17.3
13.7
11.4
180
170
160
150
140
130
120
110
100
90
80
70
60
50
40
30
20
10
0

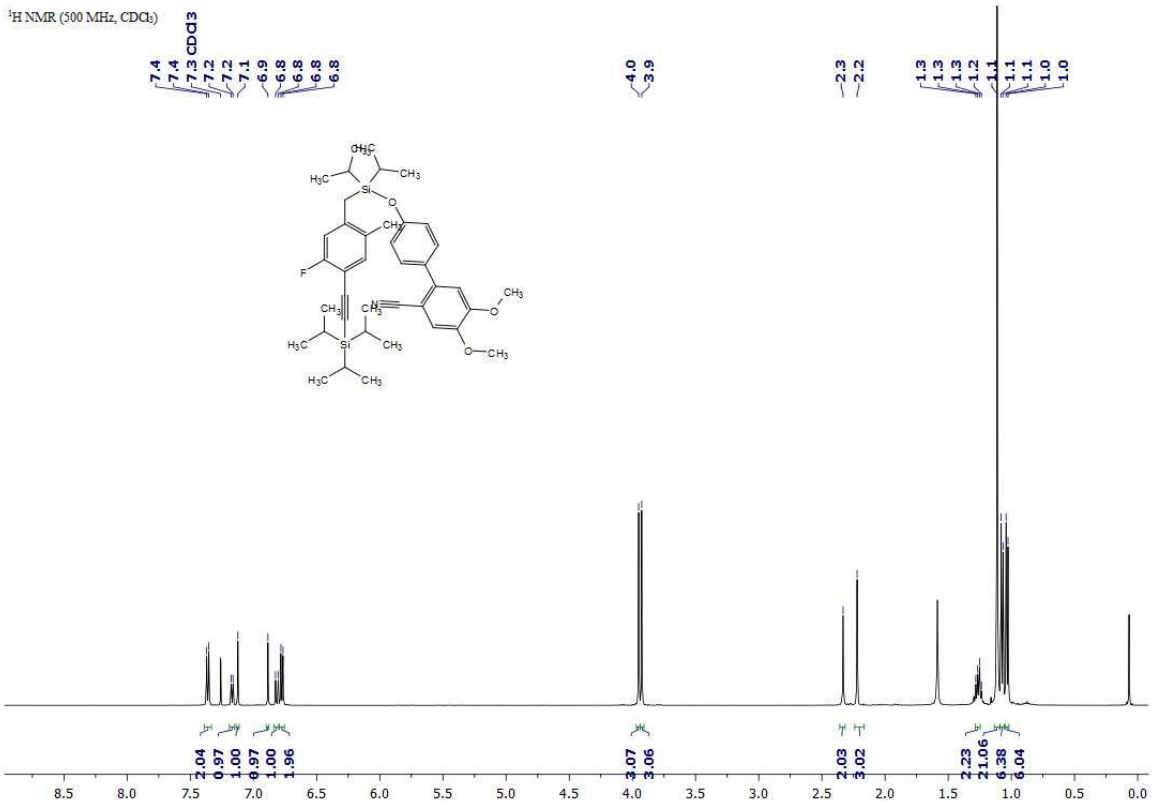
^{1}H NMR (500 MHz, CDCl$_3$)
7.4
7.4
7.3 CDCl3
7.2
7.2
7.1
6.9
6.8
6.8
6.8
6.8
4.0
3.9
2.3
2.2
1.3
1.3
1.3
1.2
1.1
1.1
1.1
1.0
1.0
2.04
0.97
1.00
0.97
1.00
1.96
3.07
3.06
2.03
3.02
2.23
21.06
6.38
6.04
8.5
8.0
7.5
7.0
6.5
6.0
5.5
5.0
4.5
4.0
3.5
3.0
2.5
2.0
1.5
1.0
0.5
0.0

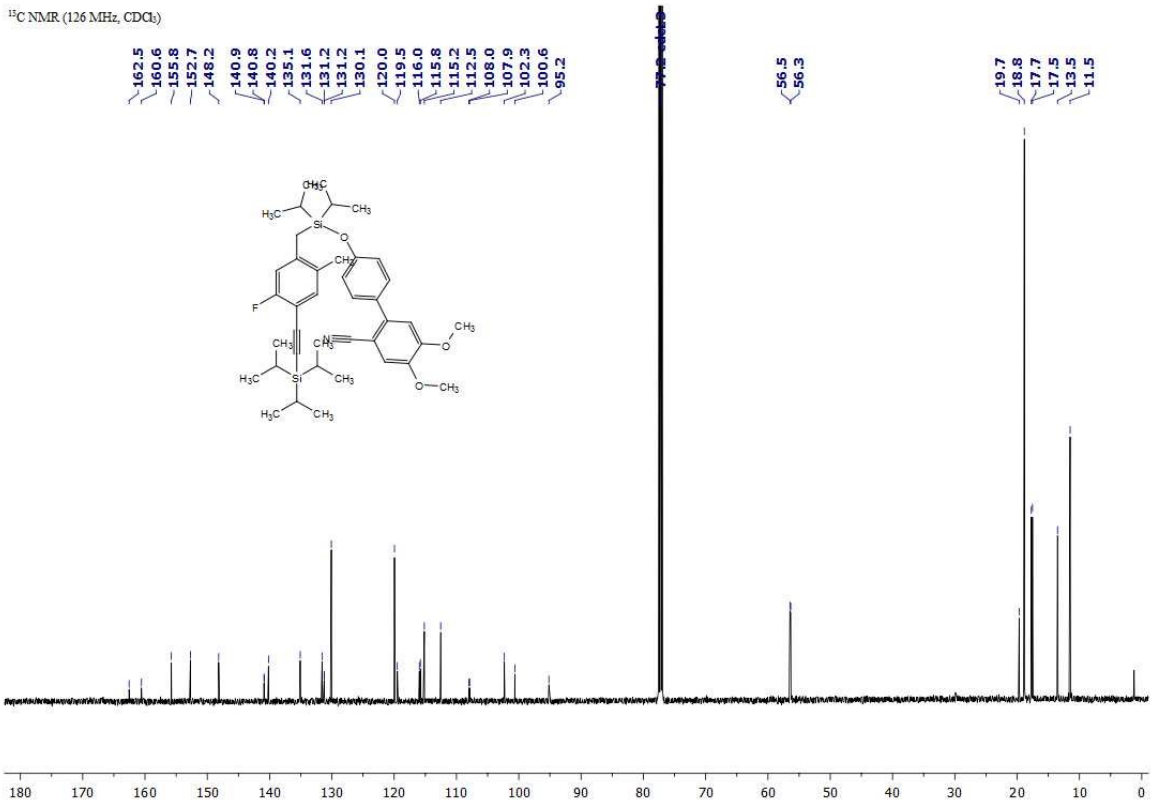
^{13}C NMR (126 MHz, CDCl$_3$)
162.5
160.6
155.8
152.7
148.2
140.9
140.8
140.2
135.1
131.6
131.2
131.2
130.1
120.0
119.5
116.0
115.8
115.2
112.5
108.0
107.9
102.3
100.6
95.2
77.2 ctd
56.5
56.3
19.7
18.8
17.7
17.5
13.5
11.5
180
170
160
150
140
130
120
110
100
90
80
70
60
50
40
30
20
10
0

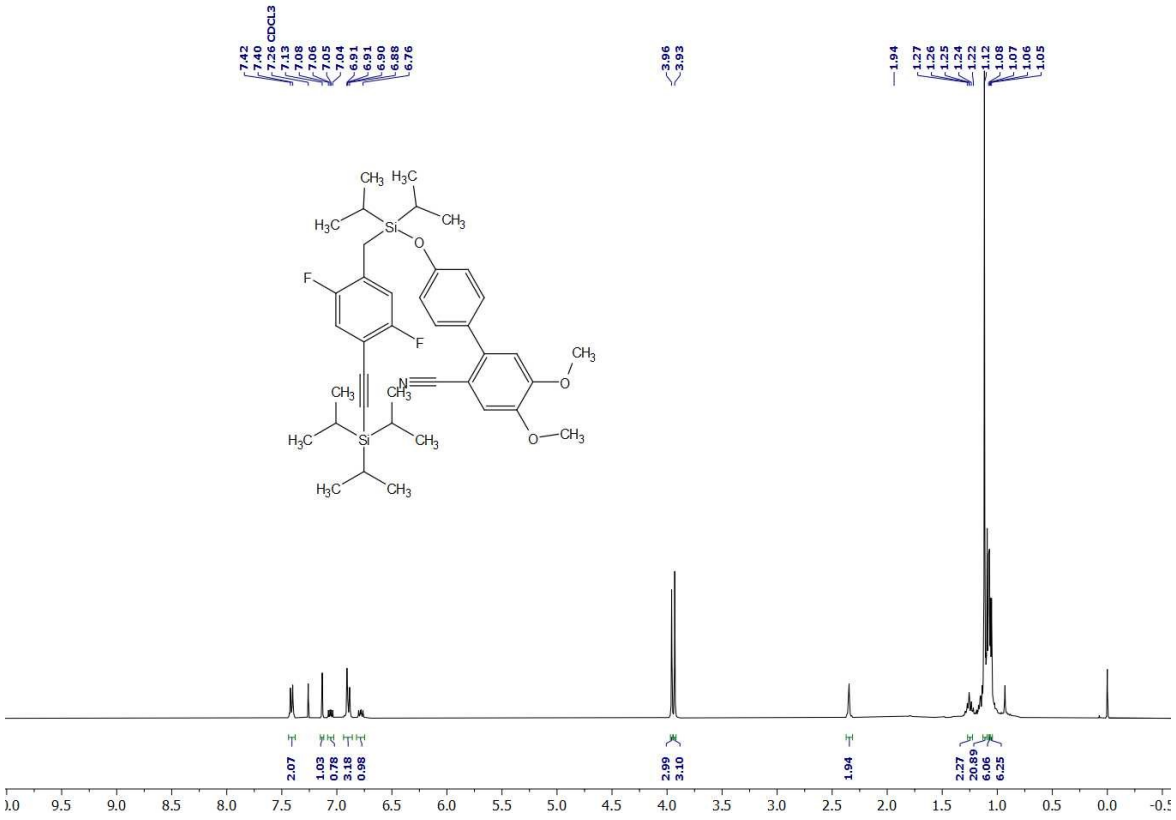
7.42
7.40
7.26 CDCL3
7.13
7.08
7.06
7.05
7.04
6.91
6.91
6.90
6.88
6.76
3.96
3.93
1.94
1.27
1.26
1.25
1.24
1.22
1.12
1.08
1.07
1.06
1.05
2.07
1.03
0.78
3.18
0.98
2.99
3.10
1.94
2.27
20.89
6.06
6.25

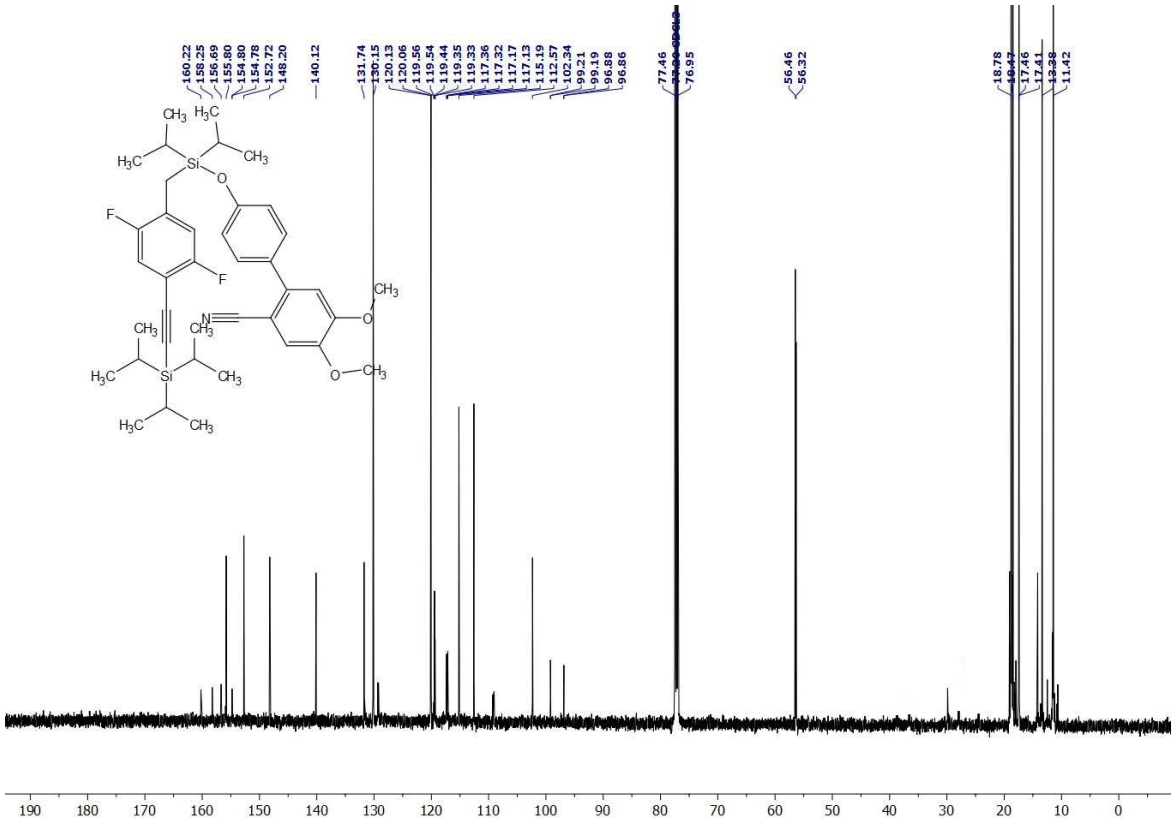
160.22
158.25
156.69
155.80
154.80
154.78
152.72
148.20
140.12
131.74
130.15
120.13
120.06
119.56
119.54
119.44
119.35
119.33
117.36
117.32
117.17
117.13
115.19
112.57
102.34
99.21
99.19
96.88
96.86
77.46
76.95
56.46
56.32
18.78
17.46
17.41
13.38
11.42

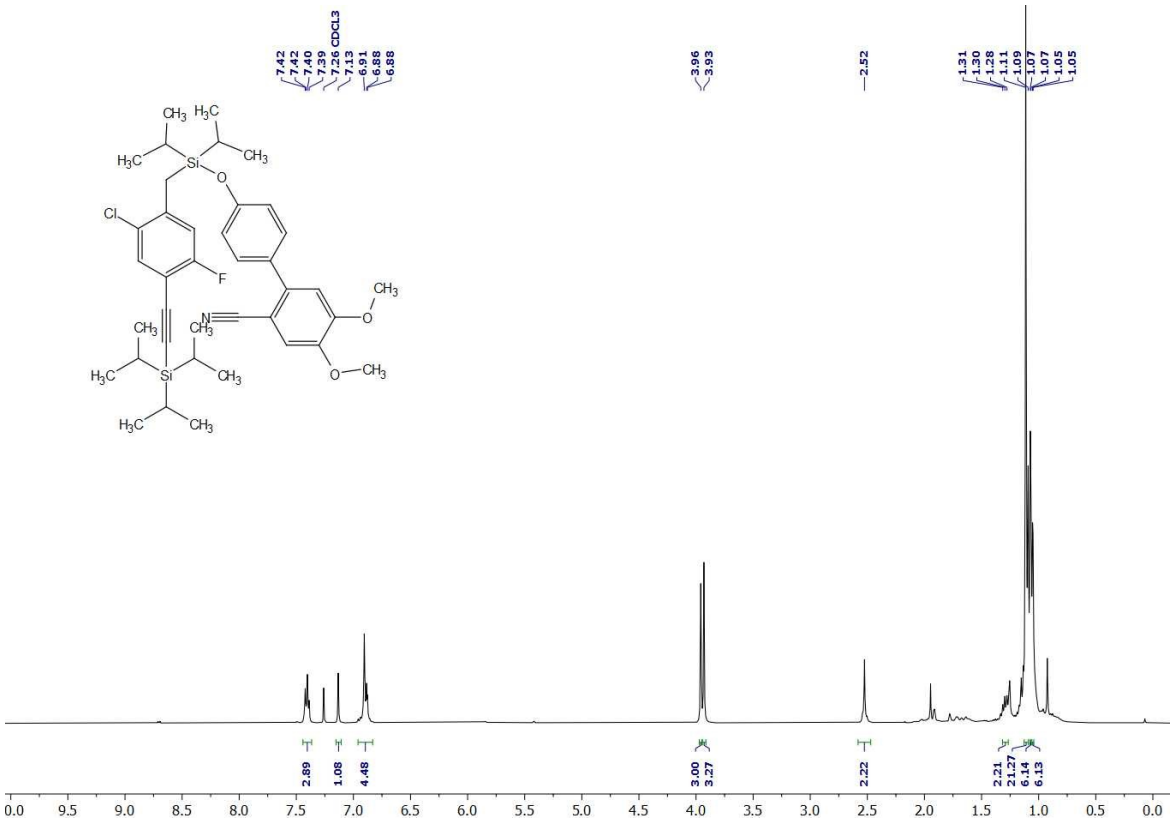
7.42
7.42
7.40
7.39
7.26 CDCL3
7.13
6.91
6.88
6.88
3.96
3.93
2.52
1.31
1.30
1.28
1.11
1.09
1.07
1.07
1.05
1.05
2.89
1.08
4.48
3.00
3.27
2.22
2.21
21.27
6.14
6.13
0.0 9.5 9.0 8.5 8.0 7.5 7.0 6.5 6.0 5.5 5.0 4.5 4.0 3.5 3.0 2.5 2.0 1.5 1.0 0.5 0.0

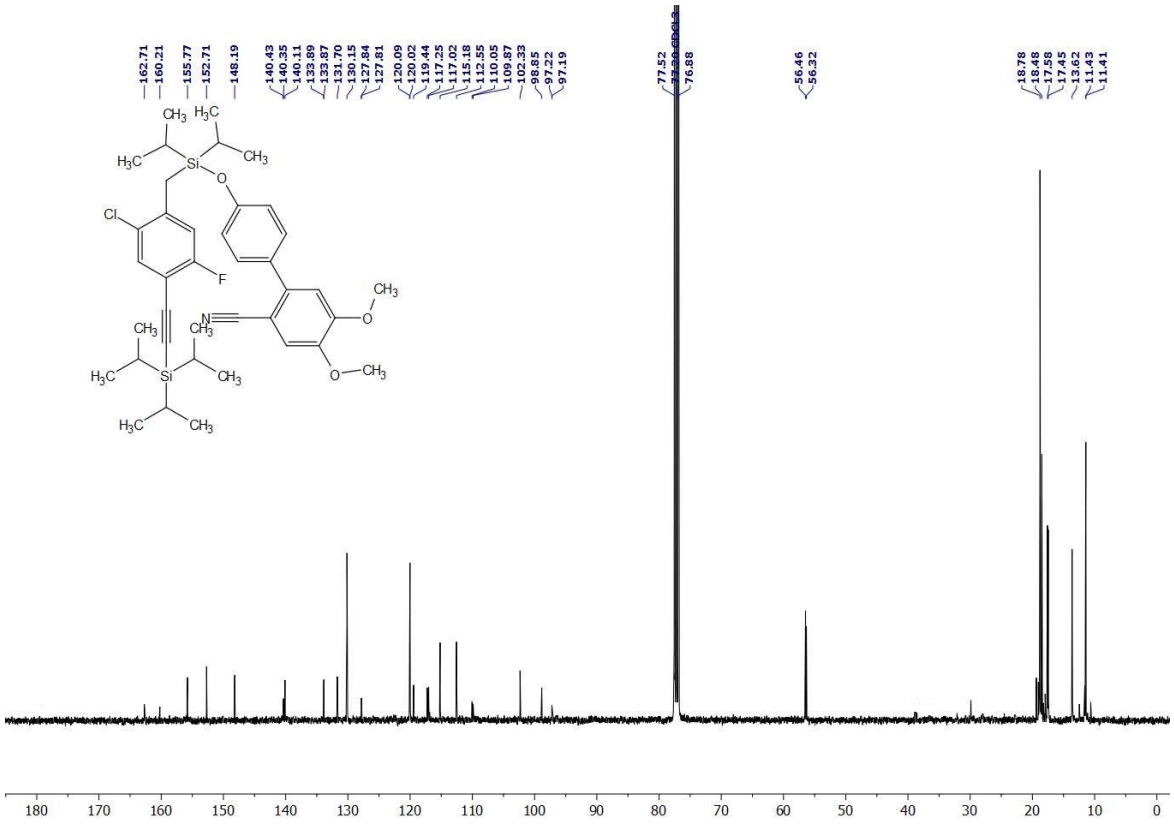
162.71
160.21
155.77
152.71
148.19
140.43
140.35
140.11
133.89
133.87
131.70
130.15
127.84
127.81
120.09
120.02
119.44
117.25
117.02
115.18
112.55
110.05
109.87
102.33
98.85
97.22
97.19
77.52
76.88
56.46
56.32
18.78
18.48
17.58
17.45
13.62
11.43
11.41
180 170 160 150 140 130 120 110 100 90 80 70 60 50 40 30 20 10 0

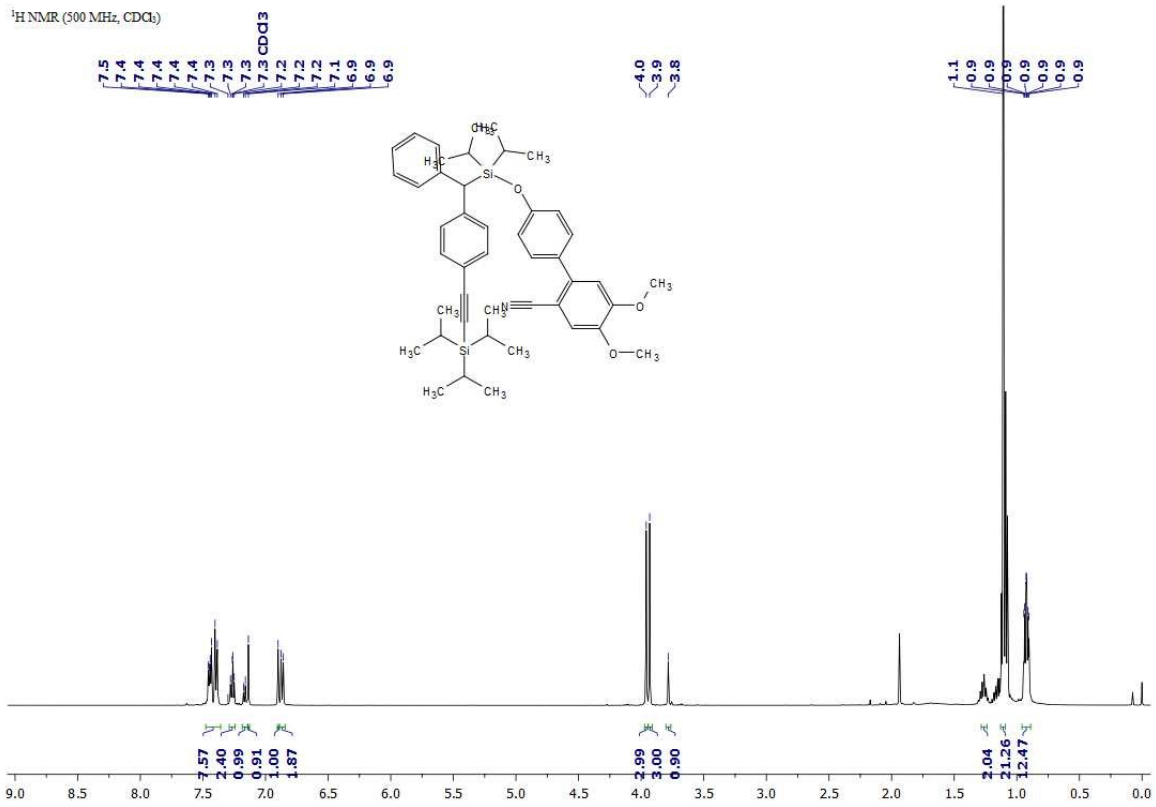
^{1}H NMR (500 MHz, CDCl$_3$)
CDCl3
7.57
2.40
0.99
0.91
1.00
1.87
2.99
3.00
0.90
2.04
21.26
12.47

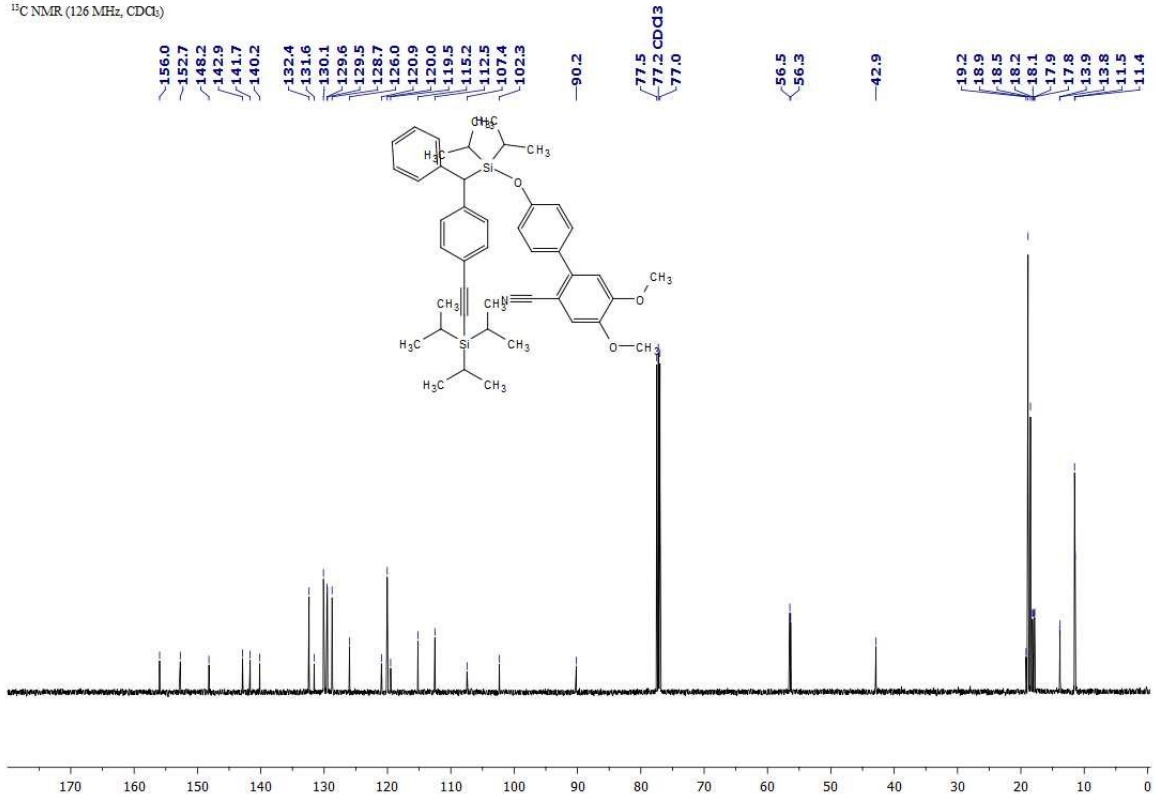
^{13}C NMR (126 MHz, CDCl$_3$)
CDCl3

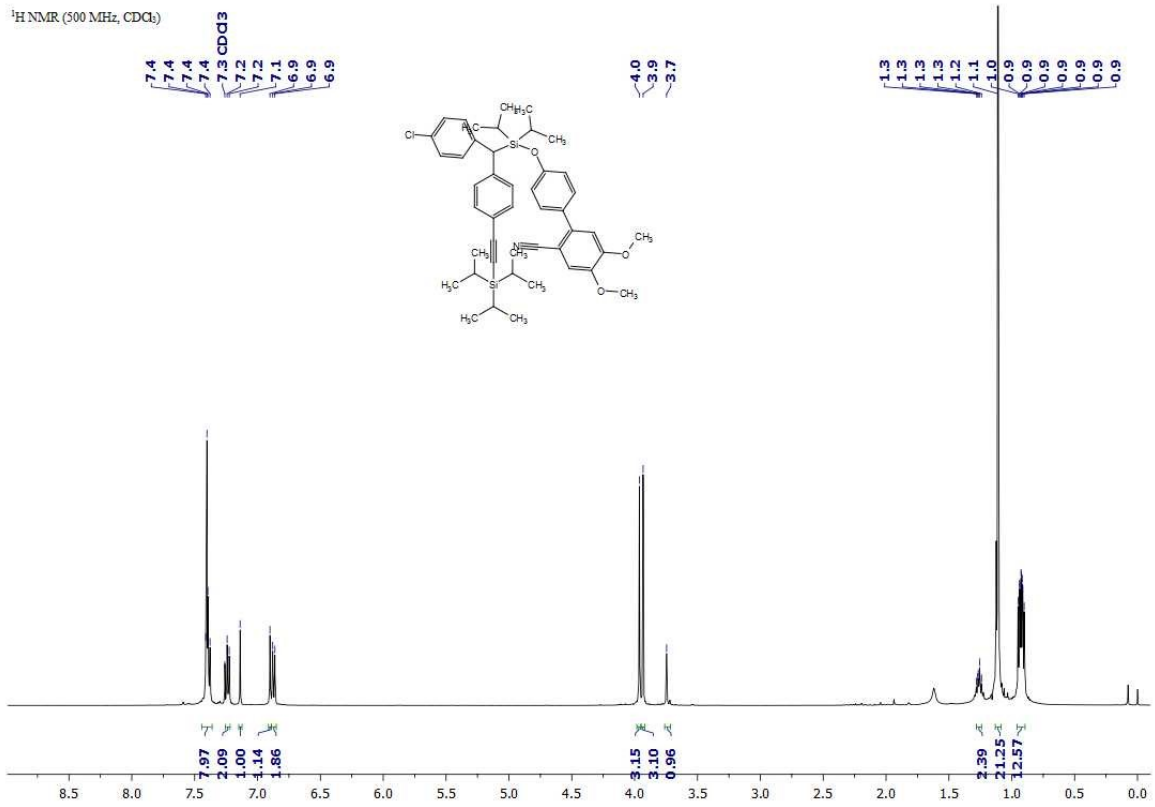
^{1}H NMR (500 MHz, CDCl$_3$)
7.4
7.4
7.4
7.4
7.3 CDCl3
7.2
7.2
7.1
6.9
6.9
6.9
4.0
3.9
3.7
1.3
1.3
1.3
1.3
1.2
1.1
1.0
0.9
0.9
0.9
0.9
0.9
0.9
0.9
7.97
2.09
1.00
1.14
1.86
3.15
3.10
0.96
2.39
21.25
12.57
8.5
8.0
7.5
7.0
6.5
6.0
5.5
5.0
4.5
4.0
3.5
3.0
2.5
2.0
1.5
1.0
0.5
0.0

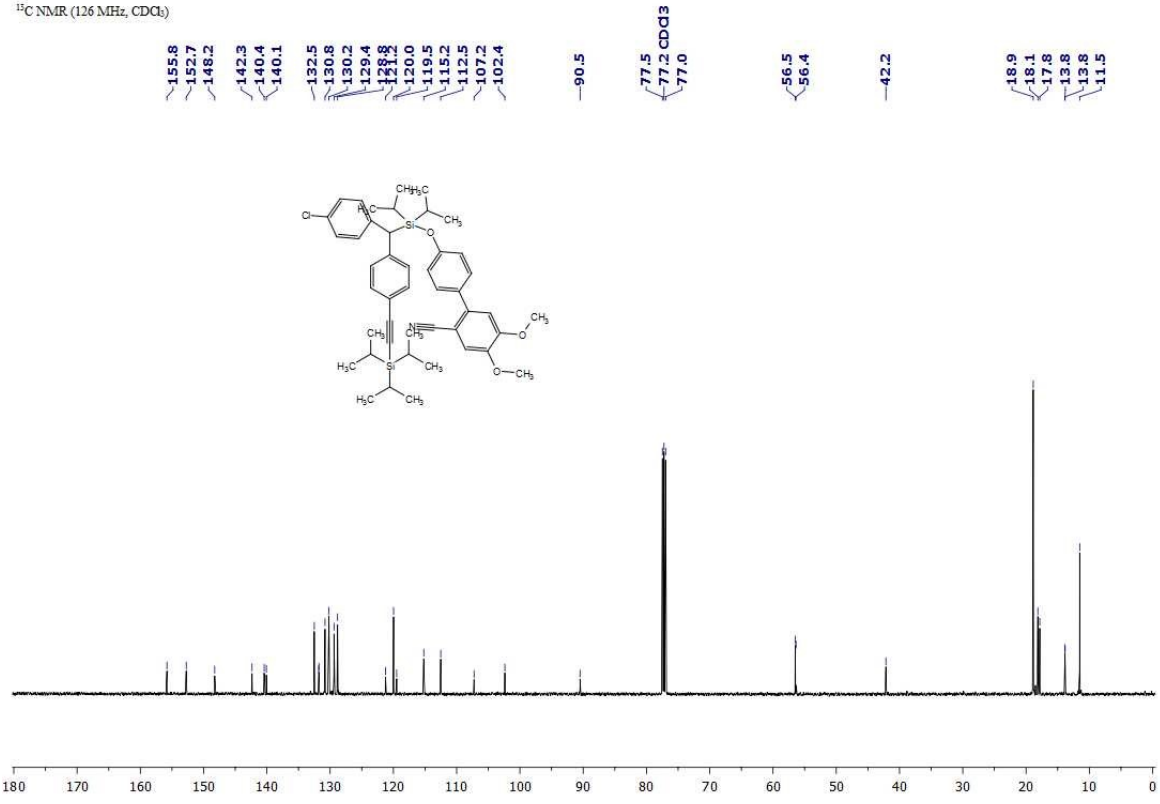
^{13}C NMR (126 MHz, CDCl$_3$)
155.8
152.7
148.2
142.3
140.4
140.1
132.5
130.8
130.2
129.4
120.0
119.5
115.2
112.5
107.2
102.4
90.5
77.5
77.2 CDCl3
77.0
56.5
56.4
42.2
18.9
18.1
17.8
13.8
13.8
11.5
180
170
160
150
140
130
120
110
100
90
80
70
60
50
40
30
20
10
0

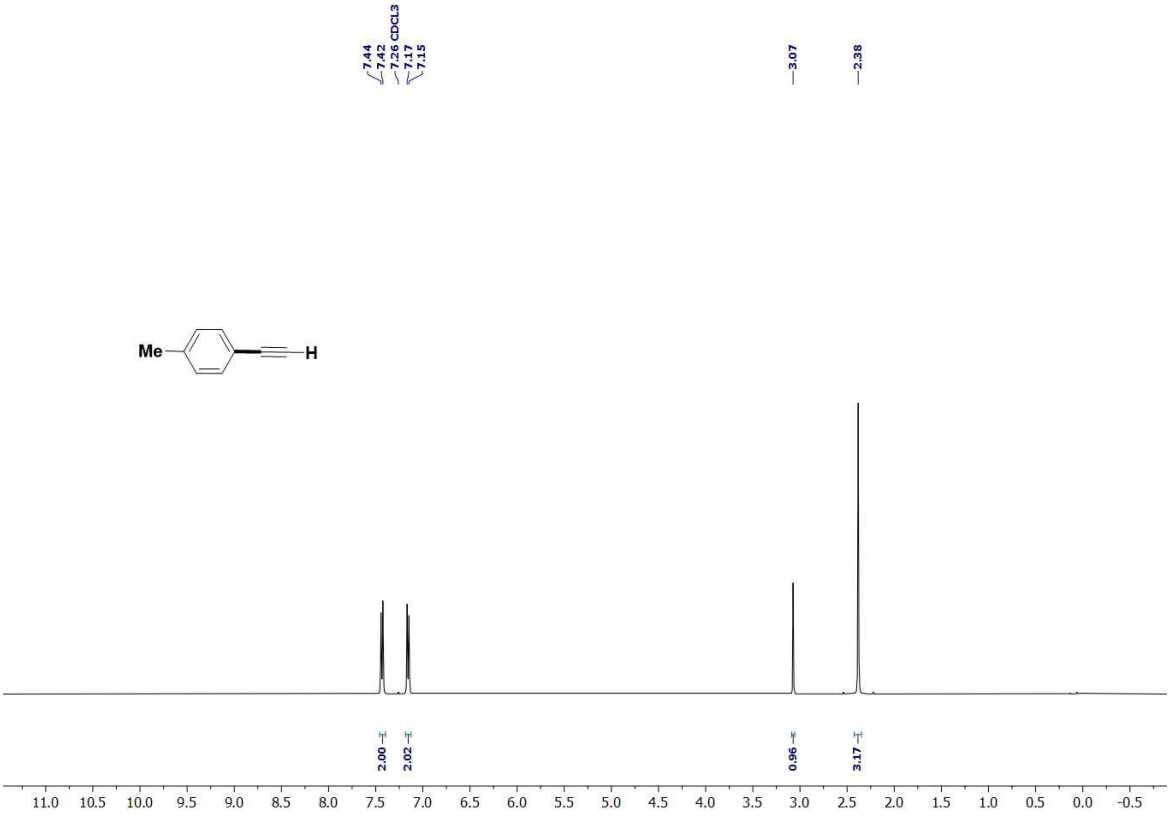
7.44
7.42
7.26 CDCL3
7.17
7.15
3.07
2.38
Me
H
2.00
2.02
0.96
3.17
11.0 10.5 10.0 9.5 9.0 8.5 8.0 7.5 7.0 6.5 6.0 5.5 5.0 4.5 4.0 3.5 3.0 2.5 2.0 1.5 1.0 0.5 0.0 -0.5

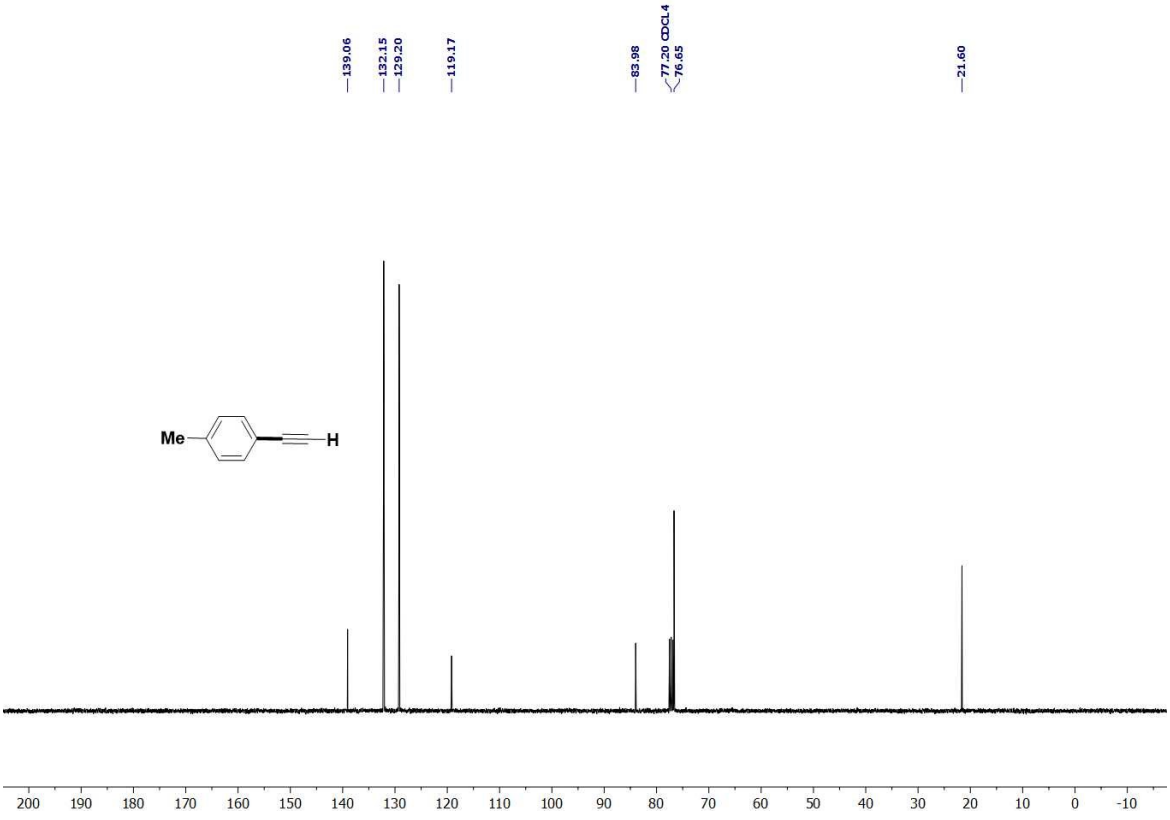
139.06
132.15
129.20
119.17
83.98
77.20 CDCL4
76.65
21.60
Me
H
200 190 180 170 160 150 140 130 120 110 100 90 80 70 60 50 40 30 20 10 0 -10

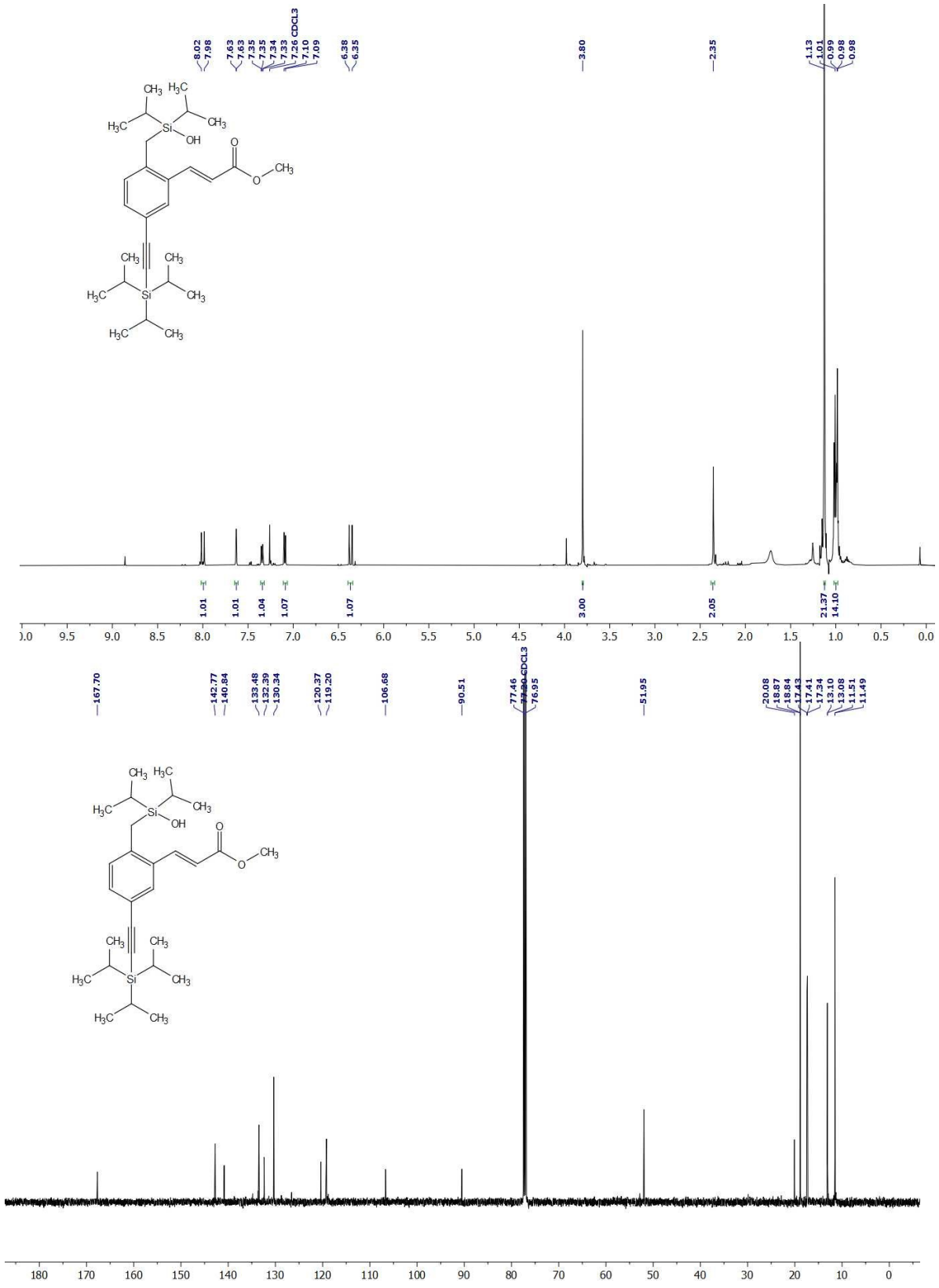

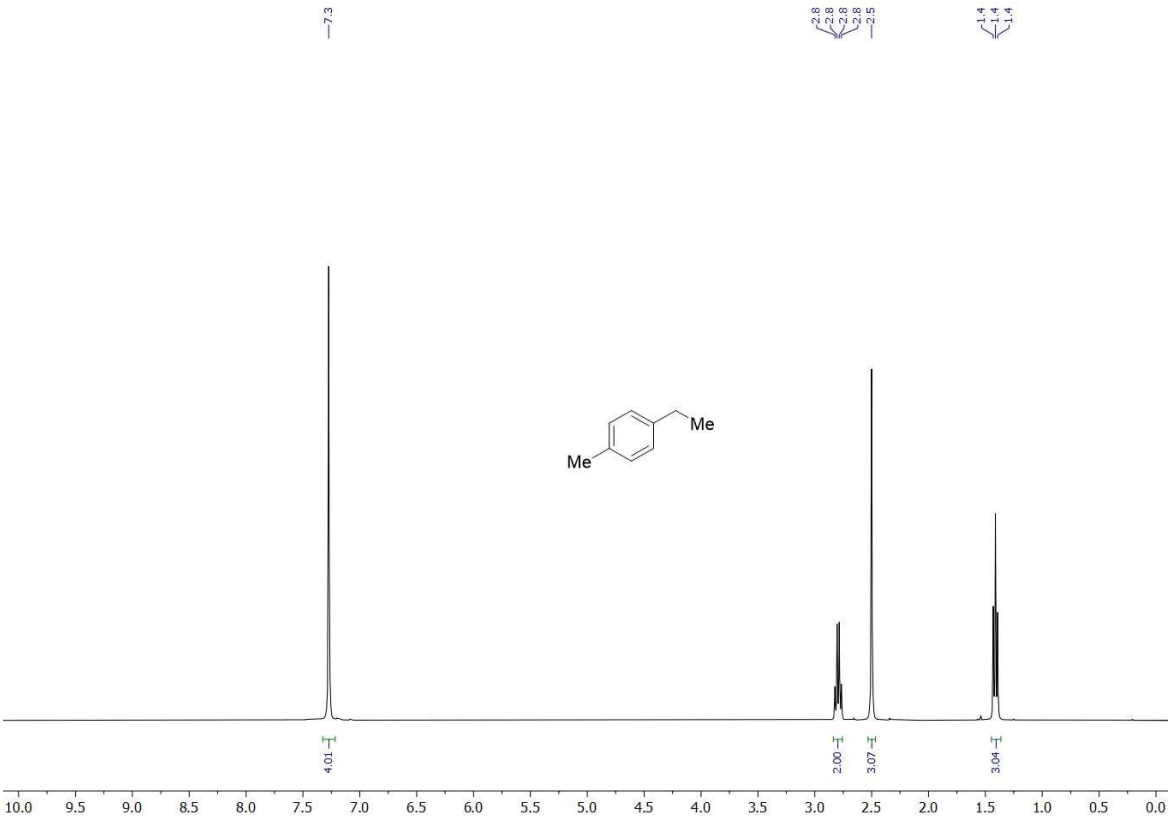
7.3
2.8
2.8
2.8
2.5
1.4
1.4
1.4
Me
Me
4.01
2.00
3.07
3.04
10.0
9.5
9.0
8.5
8.0
7.5
7.0
6.5
6.0
5.5
5.0
4.5
4.0
3.5
3.0
2.5
2.0
1.5
1.0
0.5
0.0

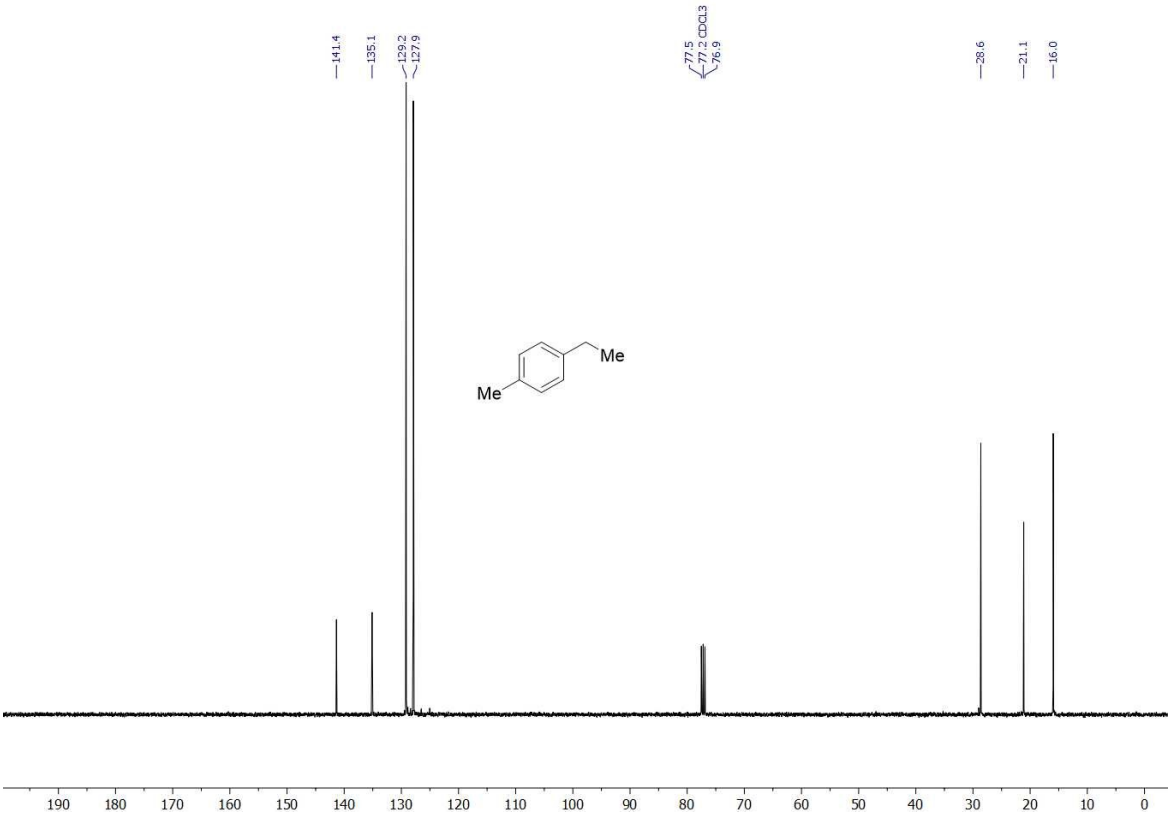
141.4
135.1
129.2
127.9
77.5
77.2 CDCl3
76.9
28.6
21.1
16.0
Me
Me
190
180
170
160
150
140
130
120
110
100
90
80
70
60
50
40
30
20
10
0

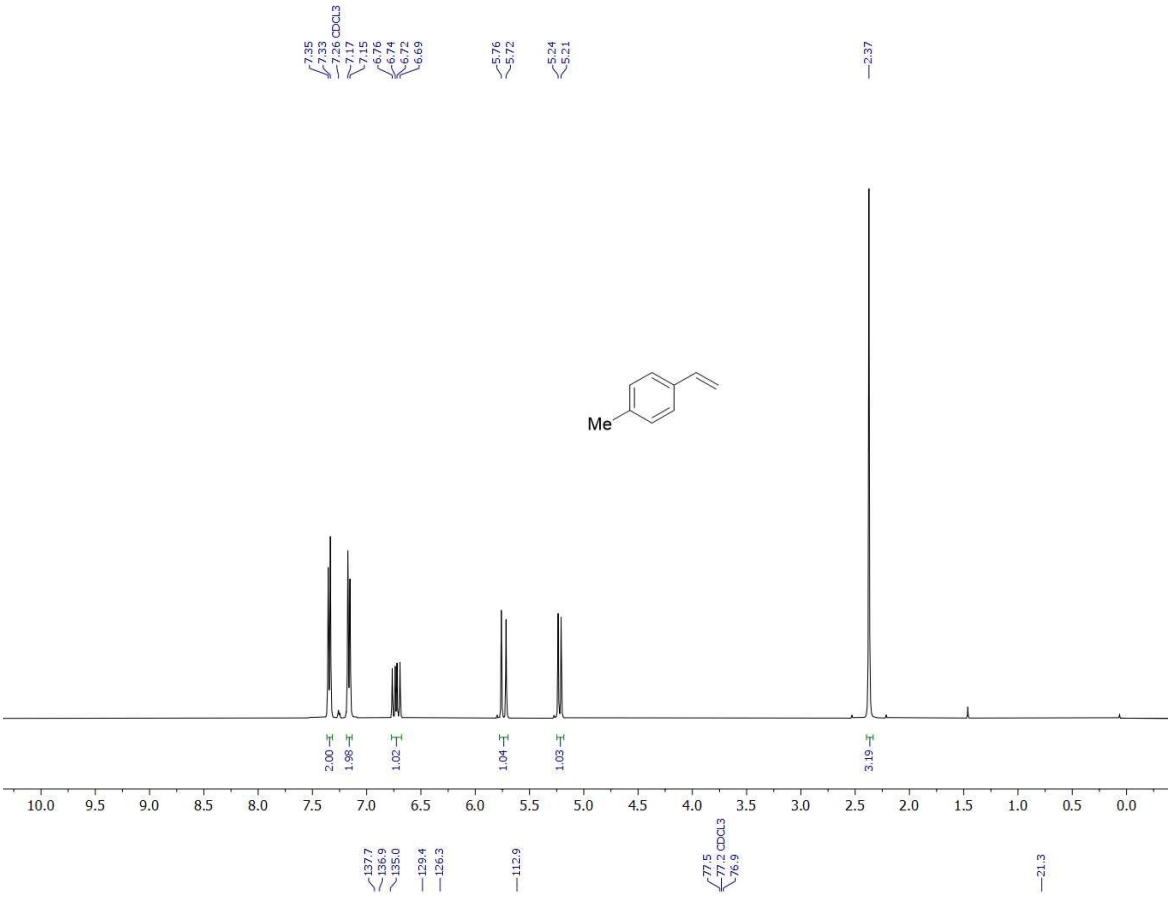
7.35
7.33
7.26 CDCl3
7.17
7.15
6.76
6.74
6.72
6.69
5.76
5.72
5.24
5.21
2.37
Me
2.00
1.98
1.02
1.04
1.03
3.19
10.0 9.5 9.0 8.5 8.0 7.5 7.0 6.5 6.0 5.5 5.0 4.5 4.0 3.5 3.0 2.5 2.0 1.5 1.0 0.5 0.0

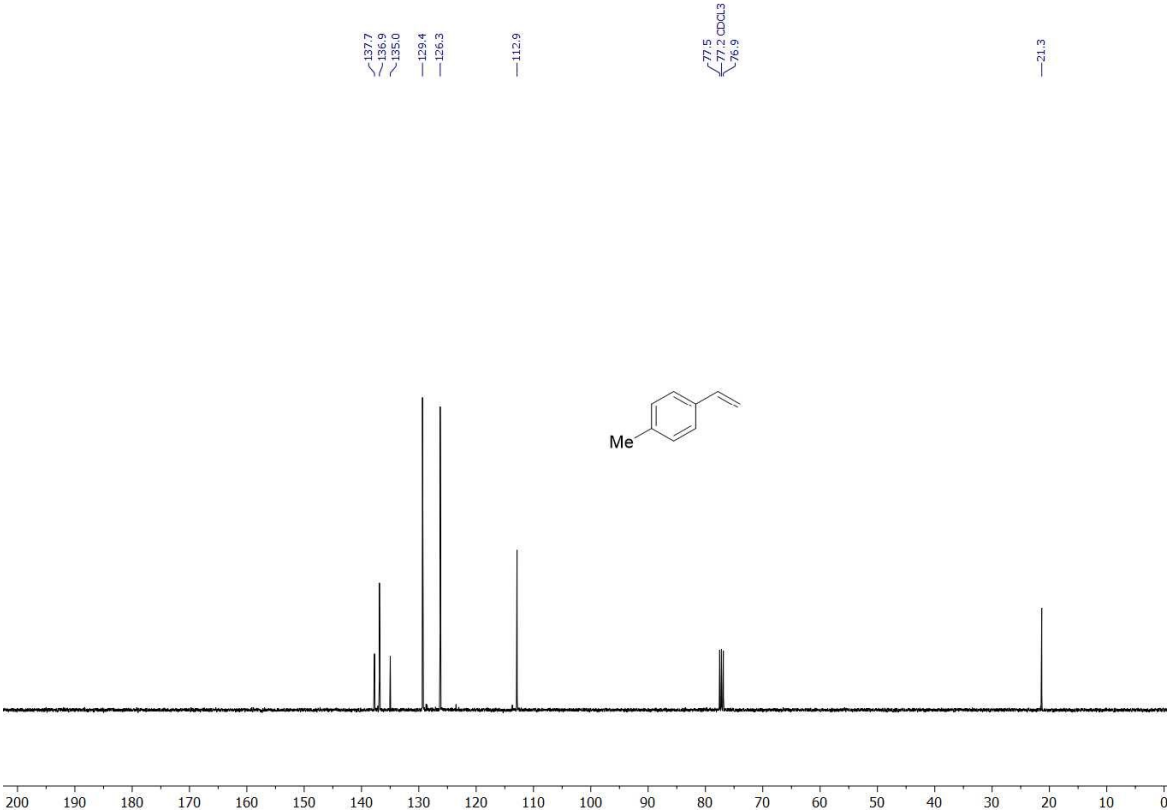
137.7
136.9
135.0
129.4
126.3
112.9
77.5
77.2 CDCl3
76.9
21.3
Me
200 190 180 170 160 150 140 130 120 110 100 90 80 70 60 50 40 30 20 10 0

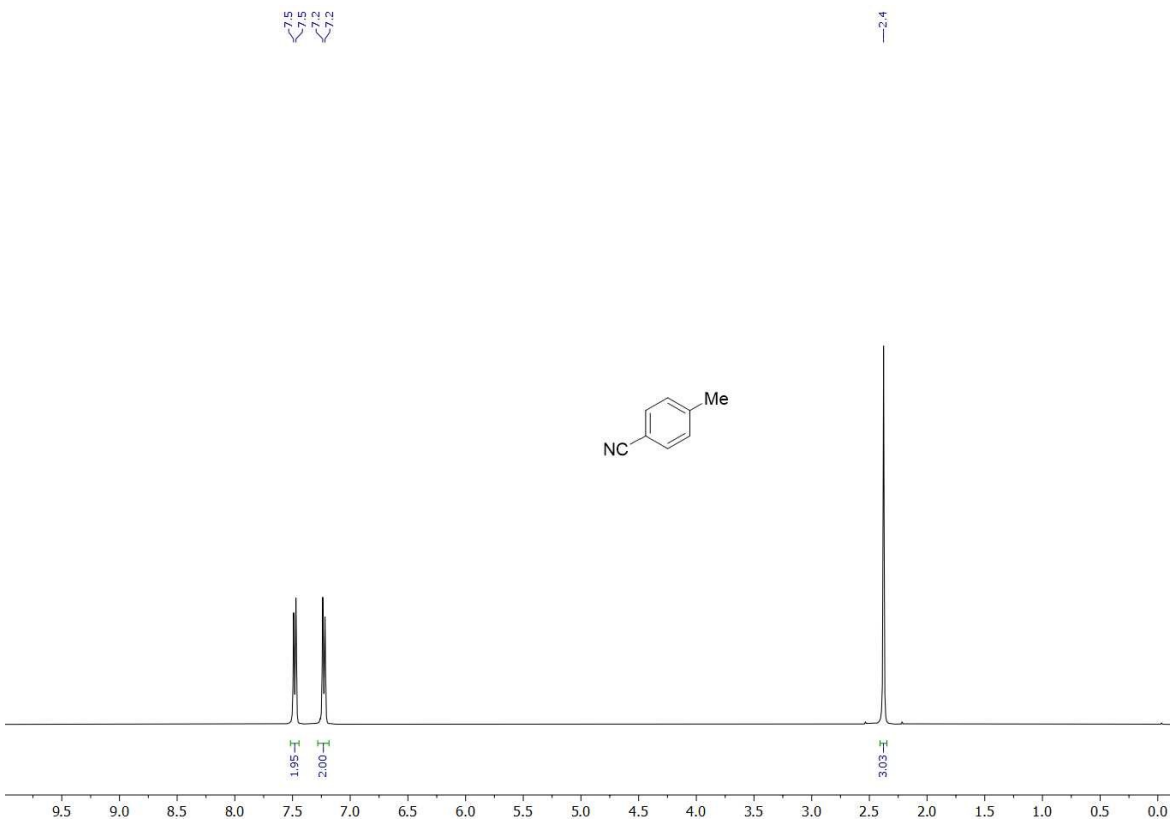
7.5
7.5
7.2
7.2
2.4
Me
NC
1.95
2.00
3.03
9.5 9.0 8.5 8.0 7.5 7.0 6.5 6.0 5.5 5.0 4.5 4.0 3.5 3.0 2.5 2.0 1.5 1.0 0.5 0.0

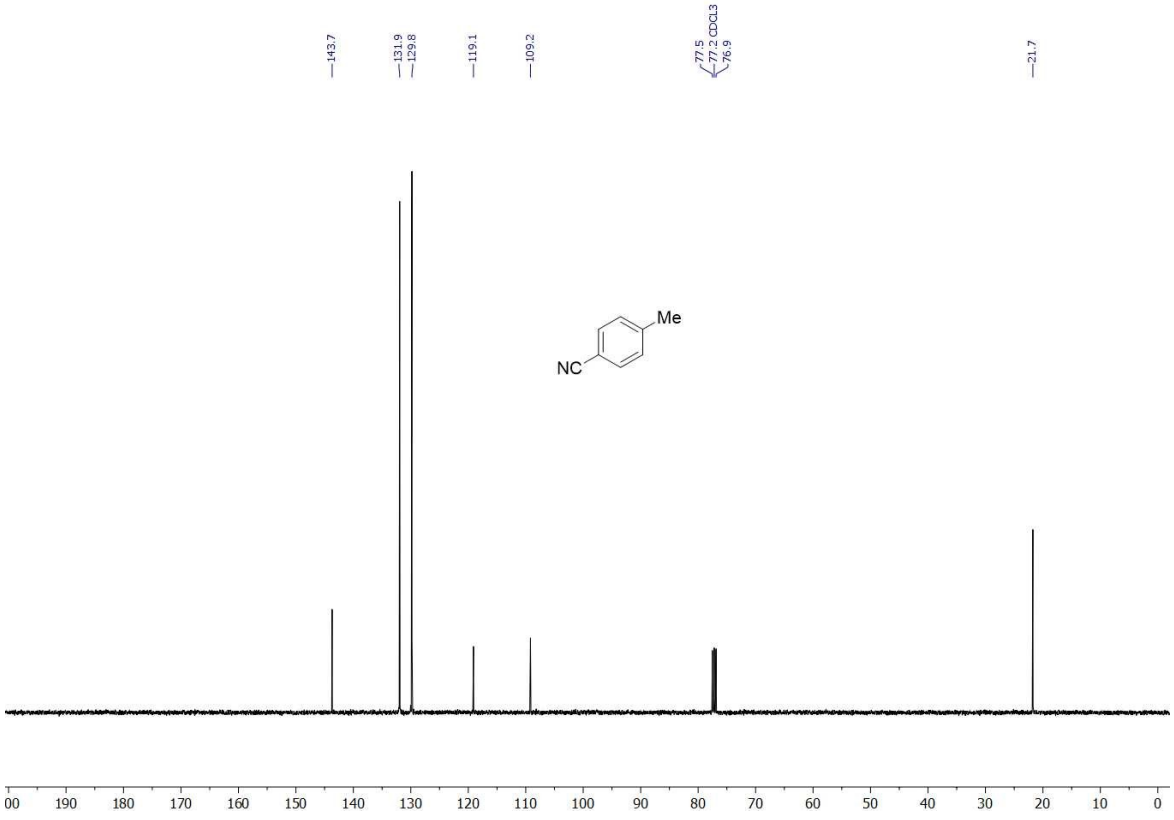
143.7
131.9
129.8
119.1
109.2
77.5
77.2 CDCl3
76.9
21.7
Me
NC
190 180 170 160 150 140 130 120 110 100 90 80 70 60 50 40 30 20 10 0

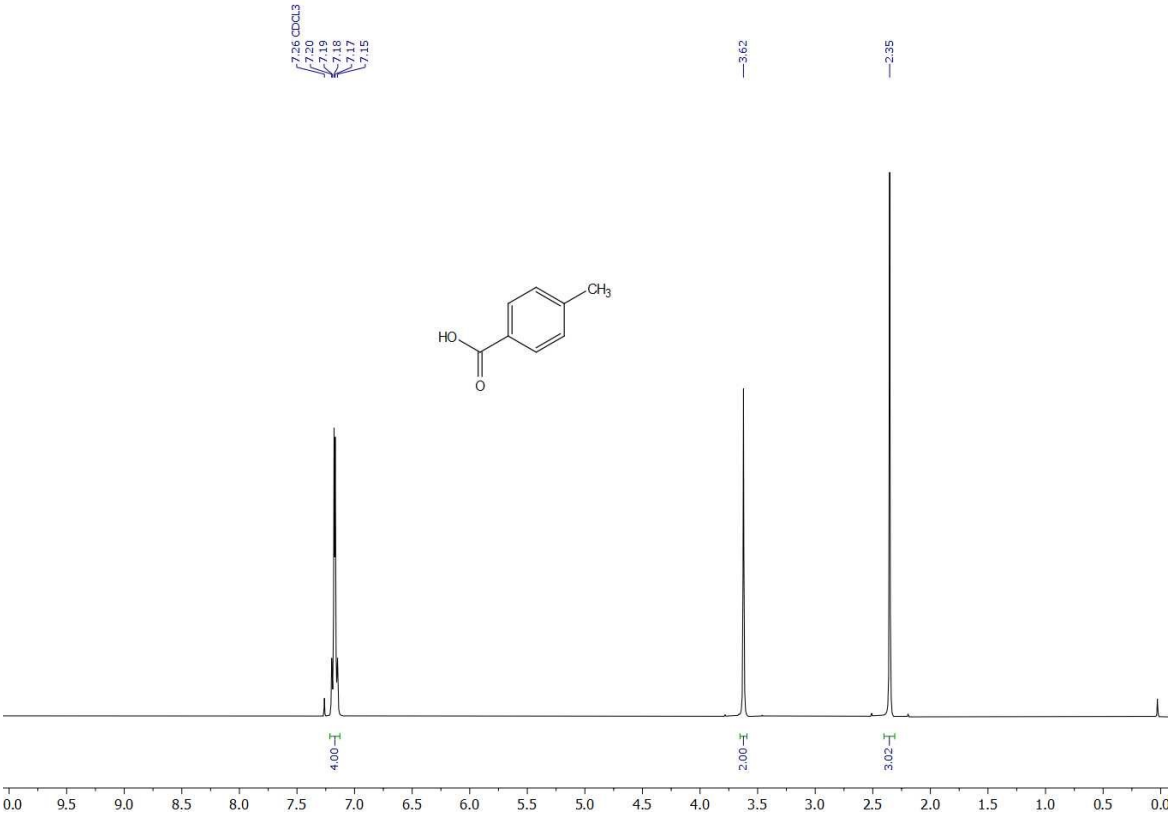
7.26 CDCl3
7.20
7.19
7.18
7.17
7.15
3.62
2.35
HO
O
CH3
4.00
2.00
3.02
0.0
9.5
9.0
8.5
8.0
7.5
7.0
6.5
6.0
5.5
5.0
4.5
4.0
3.5
3.0
2.5
2.0
1.5
1.0
0.5
0.0

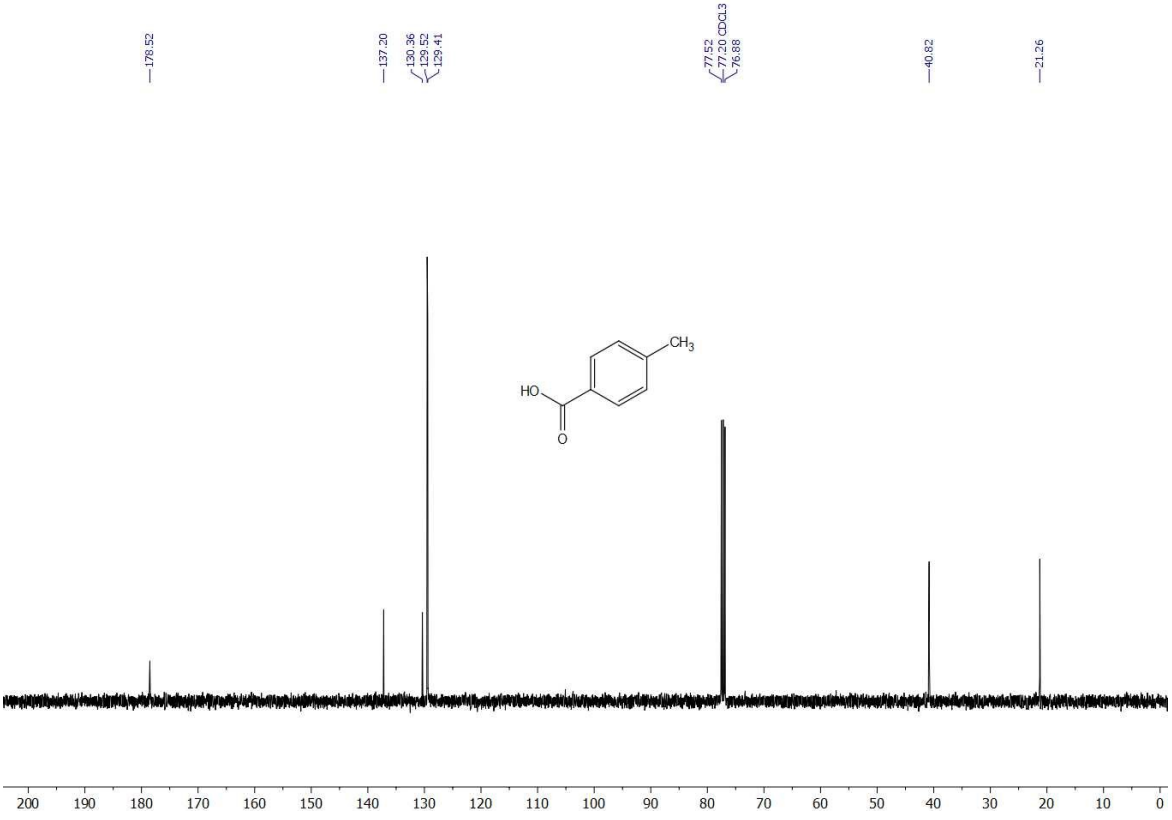
178.52
137.20
130.36
129.52
129.41
77.52
77.20 CDCl3
76.88
40.82
21.26
HO
O
CH3
200
190
180
170
160
150
140
130
120
110
100
90
80
70
60
50
40
30
20
10
0

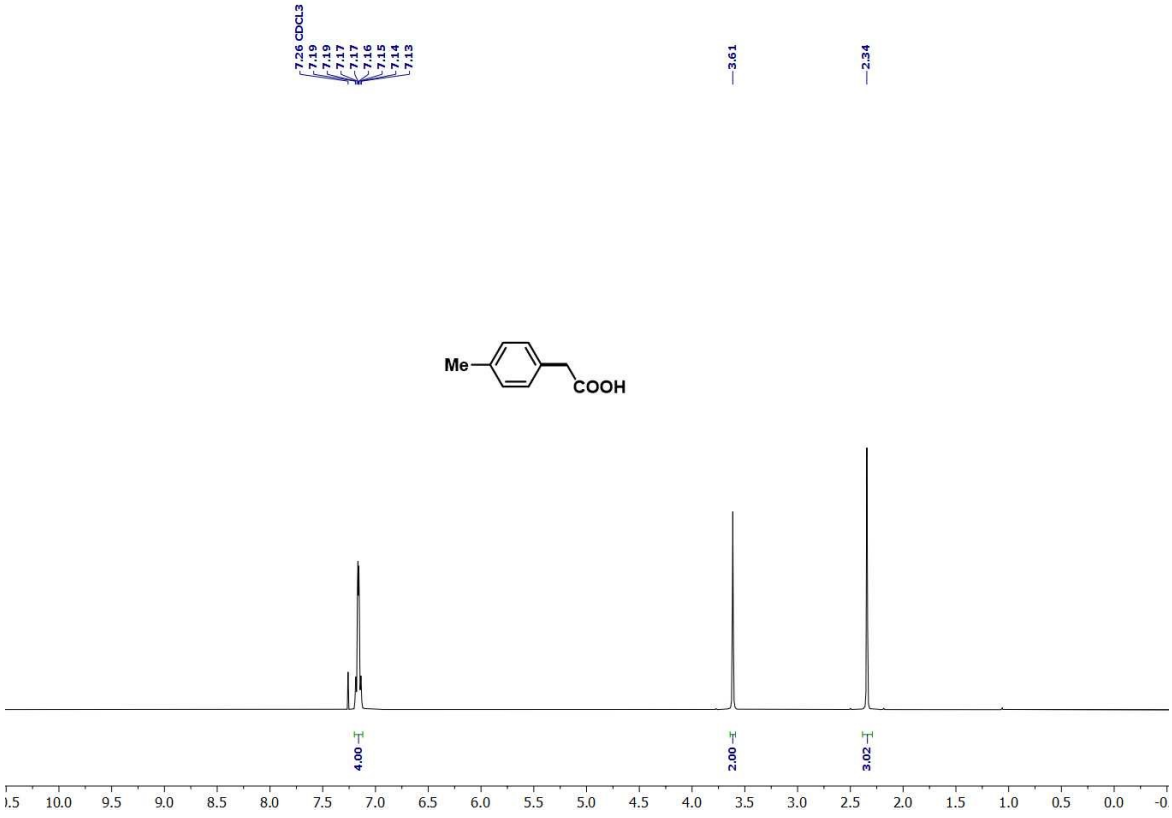
7.26 CDCL3
7.19
7.19
7.17
7.17
7.16
7.15
7.14
7.13
3.61
2.34
Me
COOH
4.00
2.00
3.02

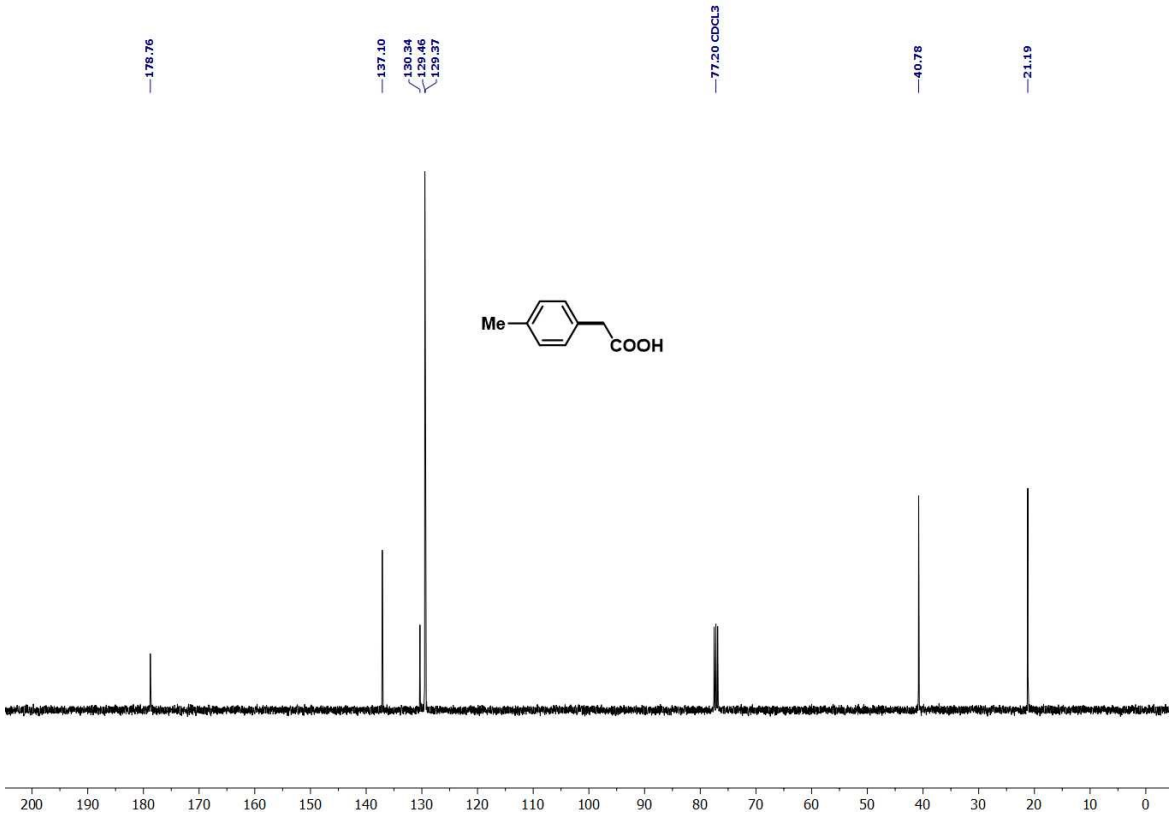
178.76
137.10
130.34
129.46
129.37
77.20 CDCL3
40.78
21.19
Me
COOH

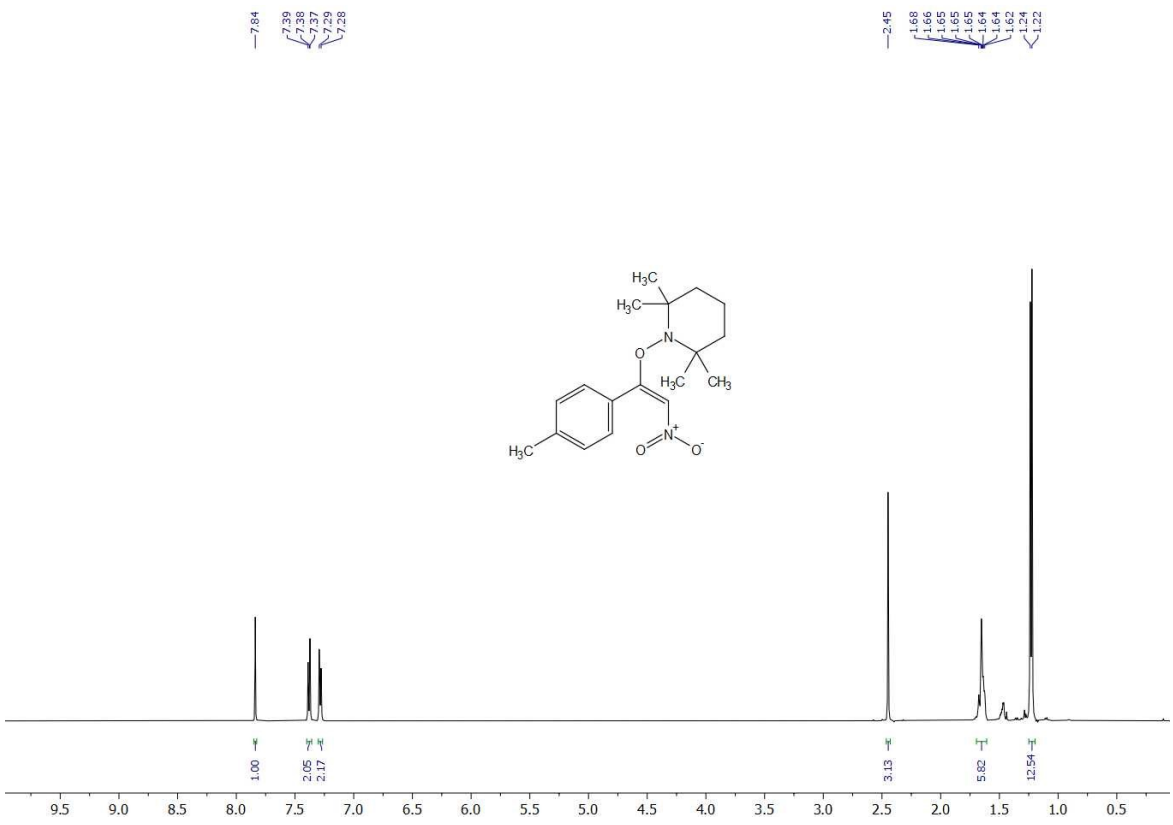
7.84
7.39
7.38
7.37
7.29
7.28
2.45
1.68
1.66
1.65
1.65
1.65
1.64
1.64
1.62
1.24
1.22
1.00
2.05
2.17
3.13
5.82
12.54
9.5
9.0
8.5
8.0
7.5
7.0
6.5
6.0
5.5
5.0
4.5
4.0
3.5
3.0
2.5
2.0
1.5
1.0
0.5

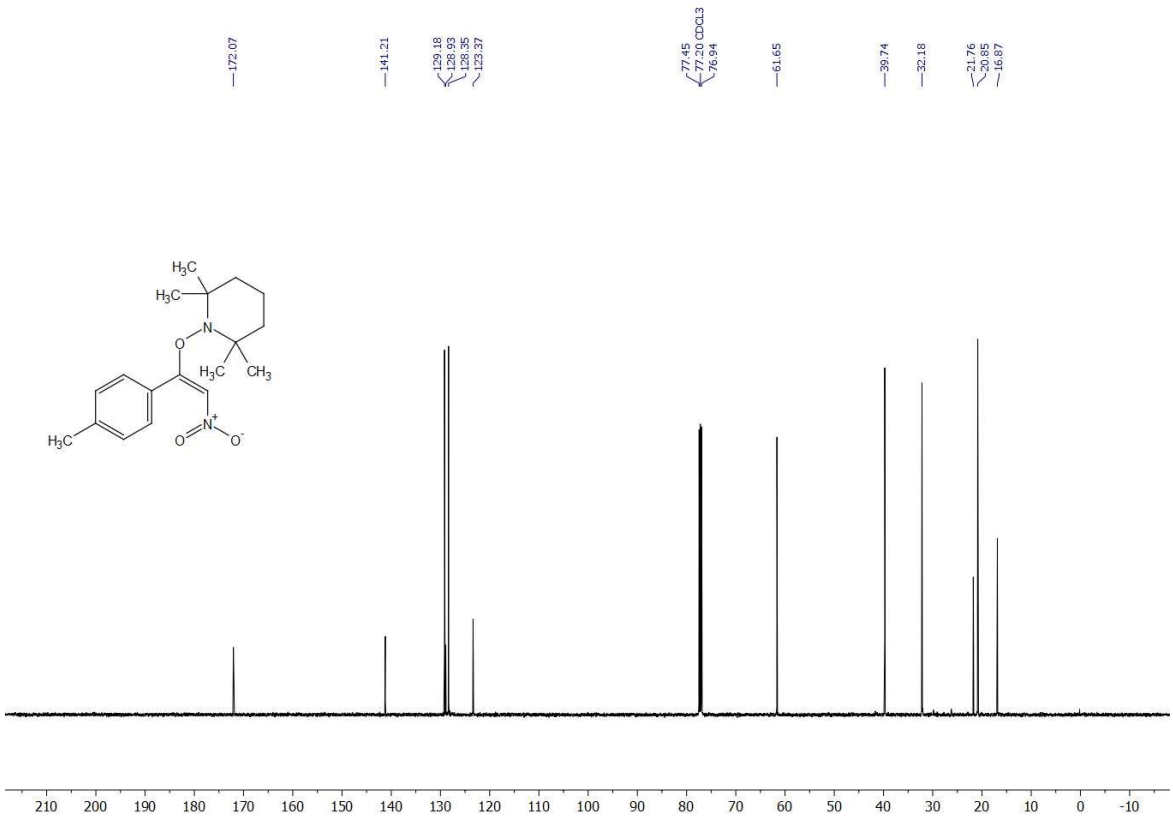
172.07
141.21
129.18
128.93
128.35
123.37
77.45
77.20 CDCl3
76.94
61.65
39.74
32.18
21.76
20.85
16.87
210
200
190
180
170
160
150
140
130
120
110
100
90
80
70
60
50
40
30
20
10
0
-10

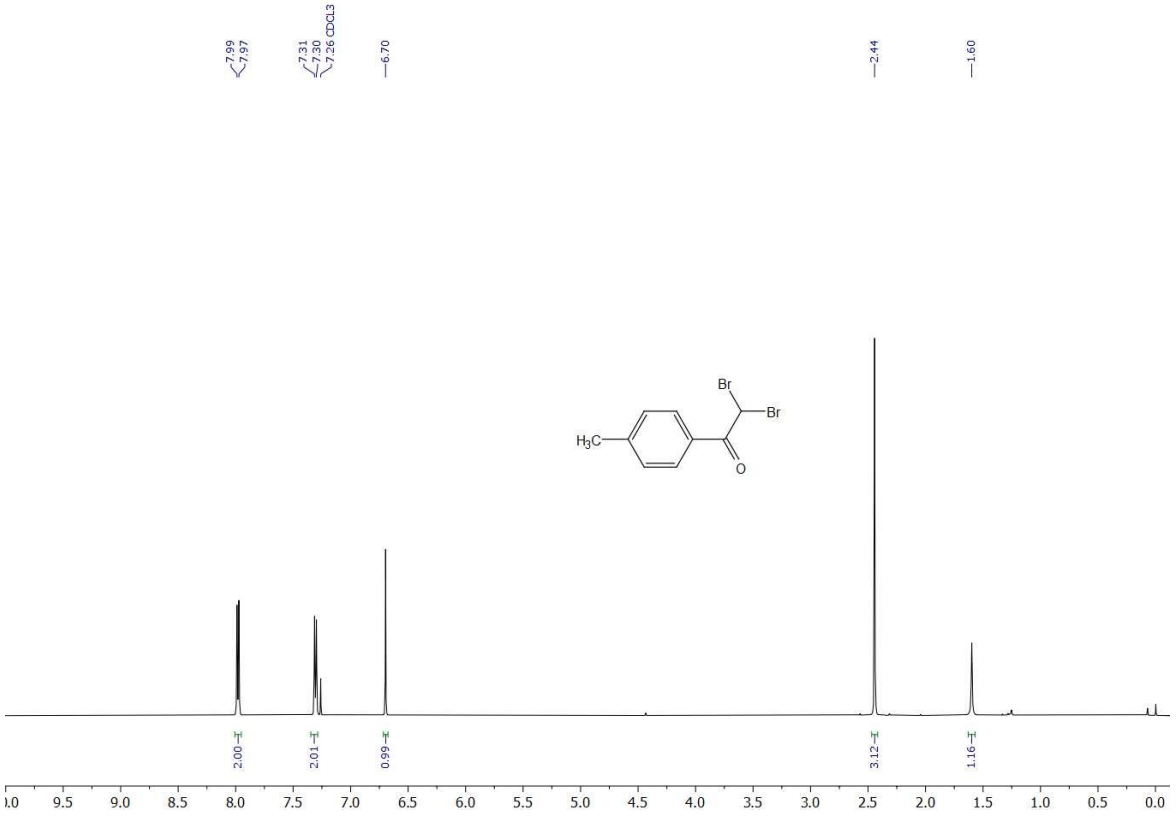
7.99
7.97
7.31
7.30
7.26 CDCl3
6.70
2.44
1.60
Br
Br
H3C
O
2.00
2.01
0.99
3.12
1.16
9.5
9.0
8.5
8.0
7.5
7.0
6.5
6.0
5.5
5.0
4.5
4.0
3.5
3.0
2.5
2.0
1.5
1.0
0.5
0.0

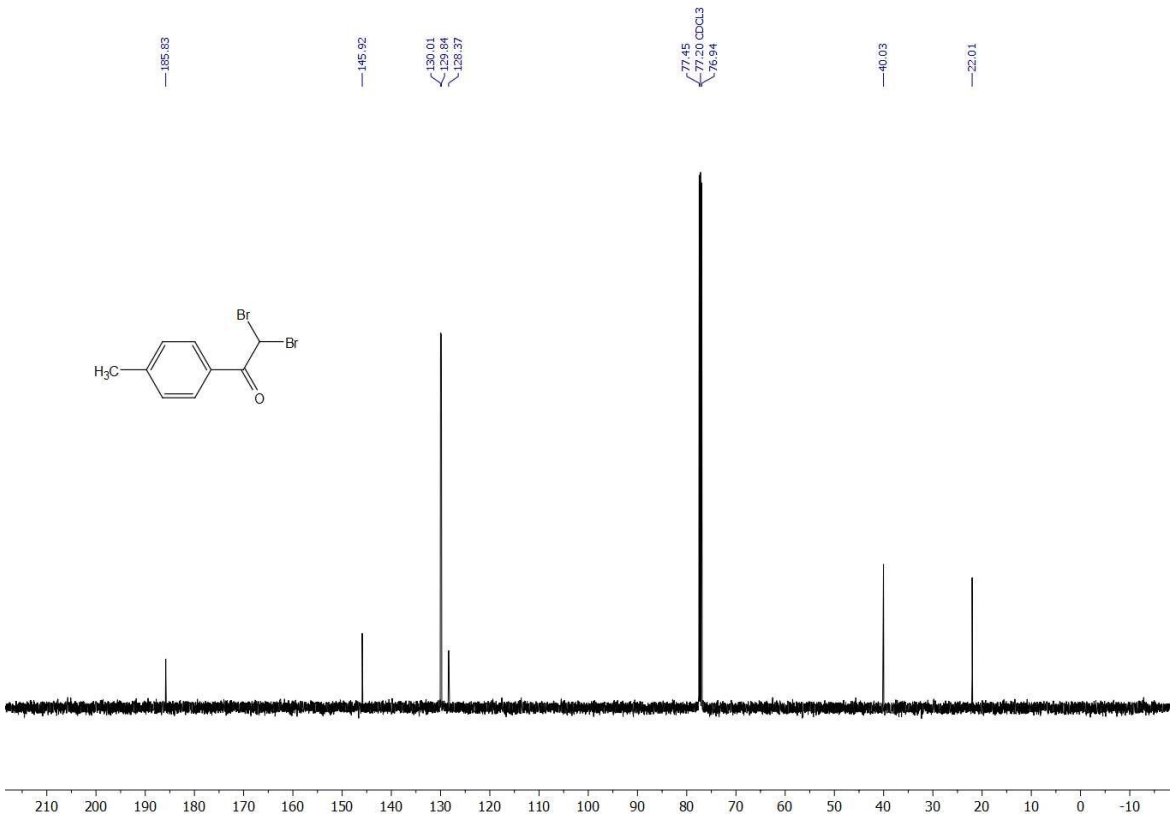
185.83
145.92
130.01
129.84
128.37
77.45
77.20 CDCl3
76.94
40.03
22.01
Br
Br
H3C
O
210
200
190
180
170
160
150
140
130
120
110
100
90
80
70
60
50
40
30
20
10
0
-10

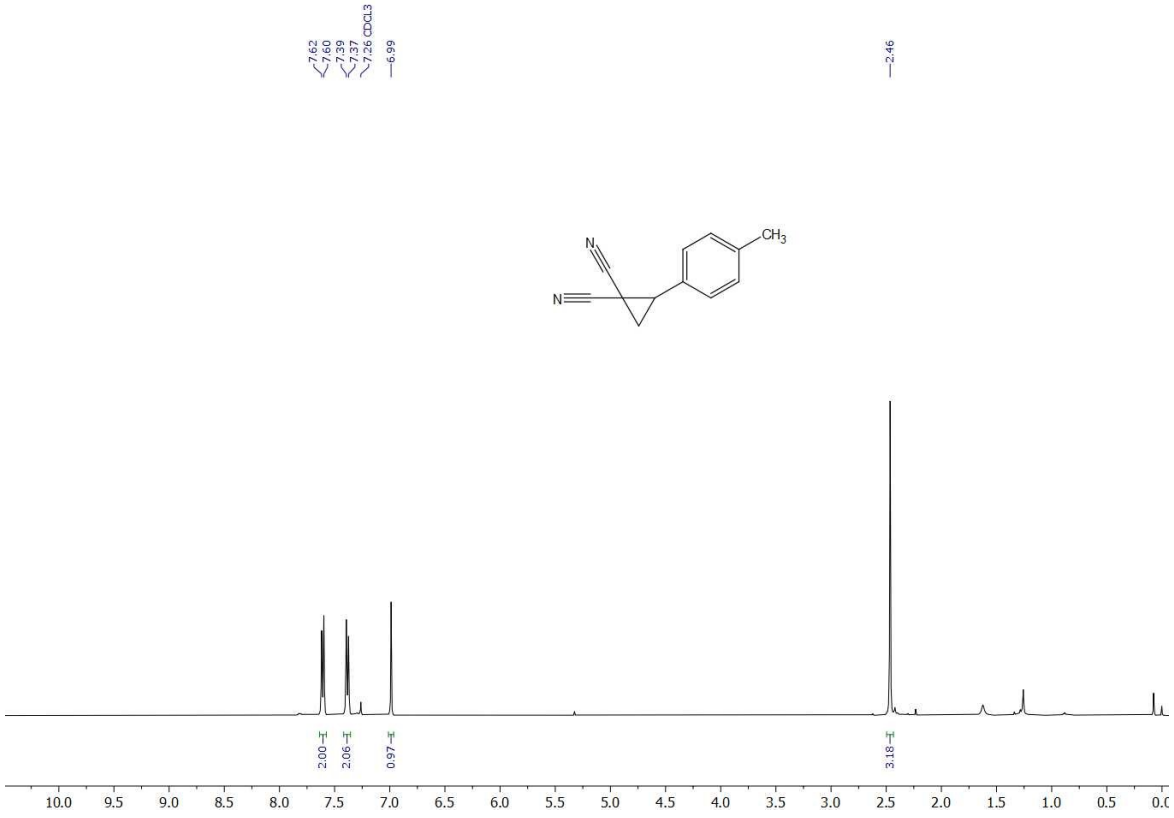
7.62
7.60
7.39
7.37
7.26 CDCl3
6.99
2.46
N
N
CH3
2.00
2.06
0.97
3.18
10.0
9.5
9.0
8.5
8.0
7.5
7.0
6.5
6.0
5.5
5.0
4.5
4.0
3.5
3.0
2.5
2.0
1.5
1.0
0.5

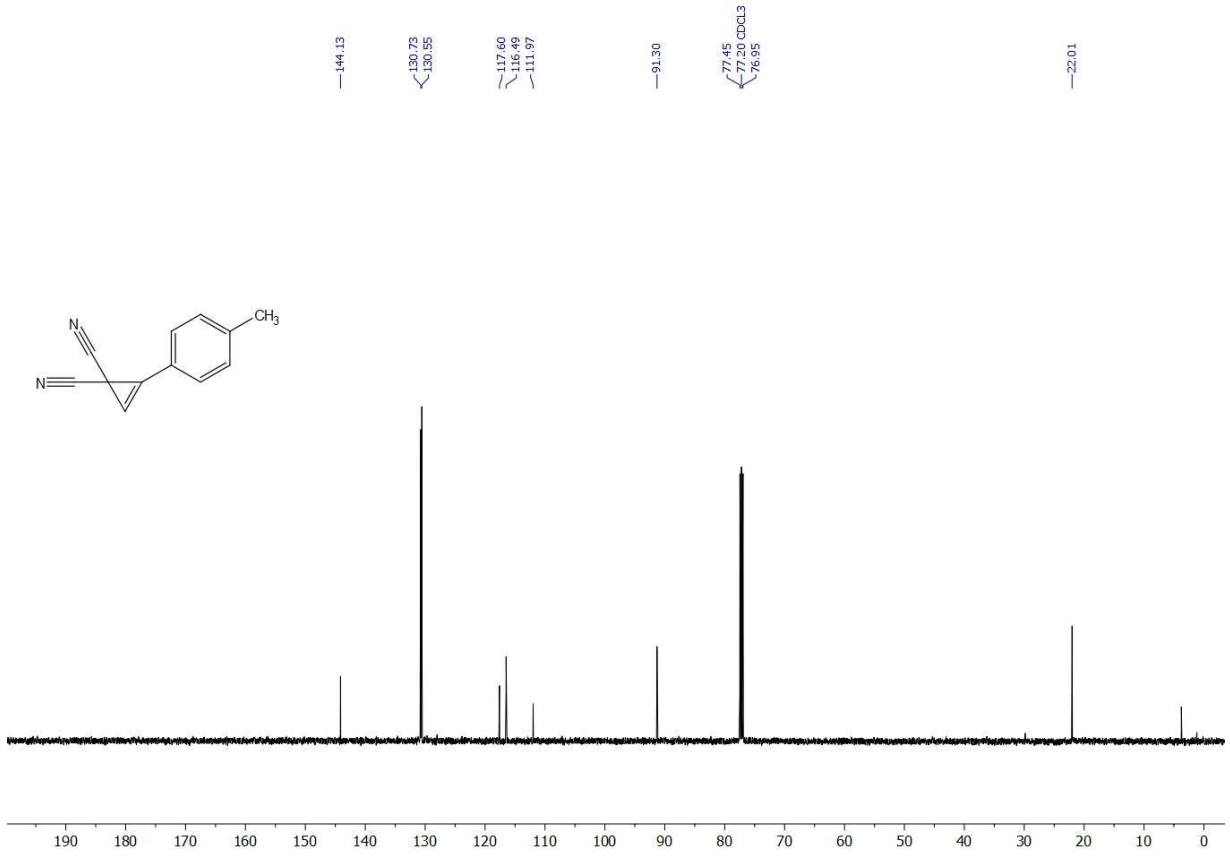
144.13
130.73
130.55
117.60
116.49
111.97
91.30
77.45
77.20 CDCl3
76.95
22.01
N
N
CH3
190
180
170
160
150
140
130
120
110
100
90
80
70
60
50
40
30
20
10
0